

(unpublished manuscript – Version 1 July 28, 2004 – updated several times with latest update – 7/31/09 comments are welcome)

EEG and Brain Connectivity: A Tutorial

Robert W. Thatcher, Ph.D., Carl J. Biver, Ph.D. and Duane M. North,
MA.

University of South Florida College of Medicine and Applied
Neuroscience Laboratories

Contact Robert W. Thatcher, Ph.D.
For comments or questions at:

rwthatcher@yahoo.com

Table of Contents

- 1 – Introduction
- 2- EEG Amplitude
- 3- What is Volume Conduction and Connectivity?
- 4- How is network zero phase lag different from volume conduction?
- 5- Pearson product correlation coefficient (“co-modulation” & Lexicor)
- 6- What is Coherence?
- 7- How Does One Compute Coherence?
- 8- First Compute the auto-spectra of channels X and Y based on the “atoms” of the spectrum
- 9- Second Compute the cross-spectra of X and Y from the “atoms” of the spectrum
- 10- How to Compute the cospectrum and quadspectrum
- 11- Third Compute Coherence as the ratio of the auto-spectra and cross-spectra
- 12- Some Statistical Properties of Coherence
- 13- How large should coherence be before it can be regarded as significantly larger than zero?
- 14- Is there an inherent time limit for EEG Coherence Biofeedback?
- 15- What is “Phase Delay” or Phase Angle?
- 16 – What is Phase Resetting?
- 17- How large should coherence be before Phase Difference can be regarded as stable?
- 18- Why the average reference and Laplacian fail to produce valid coherence and phase measures.
- 19- What is “Inflation” of Coherence and Correlation
- 20- What are the limits of EEG Coherence, Correlation and Phase Difference Biofeedback
- 20a - 19 Channel EEG Biofeedback
- 21 – Coherence, Phase and Circular Statistics
- 22 – Phase Straightening
- 23 - EEG Spindles and Burst Activity
- 24- The Bi-Spectrum
- 25 - What is the physiological meaning of EEG Bi-Coherence and Bi-Phase?
- 26- How to compute Auto Channel Cross-Frequency Coherence (ACC)
- 27- How to compute Cross Channel Cross-Frequency Coherence (CCC)
- 28- Definition of Auto Channel Cross-Frequency Coherence

- 29- Definition of the Cross Channel Cross-Frequency Coherence**
- 30- Generic Bi-Spectral Phase**
- 31- Definition of the Auto Channel Cross-Frequency Phase Difference**
- 32- Definition of the Cross Channel Cross-Frequency Phase Difference**
- 33- Coherence of Coherences**
- 34 – Phase Difference of Coherences**
- 35 – Coherence of Phase Differences**
- 36 – Coherence of Phase Resets**
- 37 – Phase Difference of Phase Differences**
- 38 – Phase Difference of Phase Resets**
- 39- Bi-Spectrum Cross-Frequency Power Correlations**
- 40- Bi-Spectrum Cross-Frequency Phase Synchrony & Phase Reset**
- 41 – References**
- 42 – Appendix A – General Time & Frequency Issues**
- 43- Appendix B – Instantaneous Coherence, Phase and Bi-Spectra**
- 44- Appendix C – Listing of Equations**

1 - Introduction

Measurements of real-time and off-line electrodynamics of the human brain have evolved over the years and one purpose of this paper is to provide simple hand calculator equations to facilitate standardization and the implementation of standardized methods. We begin with the fact that the brain weighs approximately 2.5 pounds and consumes approximately 60% of blood glucose (Tryer, 1988) and consumes as much oxygen as our muscles consume during active contraction, 24 hours a day. How is this disproportionate amount of energy used? The answer is that it is used to produce electricity including synchronized and collective actions of small and large groups of neurons linked by axonal and dendritic connections. Each neuron is like a dynamically oscillating battery that is continually being recharged (Steriade, 1995). Locally connected neurons recruit neighboring neurons with a sequential build up of electrical potential referred to as the recruiting response and the augmenting response also called EEG “burst activity” and “spindles” (Thatcher and John, 1977; Steriade, 1995). EEG burst activity is recognized by spindle shaped waves that wax and wane (i.e., augmenting by sequential build up, then asymptote and then decline to repeat as a waxing and waning pattern) are universal and are present in delta (1 – 4 Hz) theta (4-7.5Hz), alpha (8 to 12 Hz), beta (12.5 Hz to 30 Hz) and gamma (30 Hz – 100 Hz) frequency bands during waking in normal functioning people. Another fundamental fact is that only

synchronized cortical neurons produce the electricity called the electroencephalogram and the generators are largely located near to the electrode location with approximately 50% of the amplitude produced directly beneath the recording electrode and approximately 95% within a 6 cm radius (Nunez, 1981; 1995). Unrelated distant sources produce lower amplitude potentials by volume conduction that add or subtract at a zero phase difference between the source and the surface sensors. Locally synchronized neurons are connected to distant groups of neurons (3 cm to 21 cm) via cortico-cortical connections (Braitenberg, 1978; Schulz and Braitenberg, 2002) and are connected to localized clusters or populations of neurons that exhibit significant phase differences or delays due to axonal conduction velocities, synaptic rise times, synaptic locations and other neurophysiological delays that can not be produced by volume conduction which is defined at Phase Difference = 0. Connectivity is defined as the magnitude of coupling between neurons, independent of volume conduction. This is because in this paper we are interested in the synchronous coupling and de-coupling of local and long distance populations of neurons that add together and give rise to the rhythmic patterns of the EEG seen at the scalp surface (i.e., dynamic connectivity). Much has been learned about brain function in the last few decades and EEG biofeedback to control robotic limbs coupled with PET and fMRI cross-validation of the location of the sources of the EEG shows that the future of quantitative EEG or QEEG is very bright and positive because of the reality of the neurophysics of the brain and high speed computers. 3-dimensional EEG source localization methods have proliferated with ever increased spatial resolution and cross-validation by fMRI, PET and SPECT. Understanding measurements of coupling between populations of neurons in 3-dimensions using 3-Dimensional Source analysis such as by Michael Scherg, Richard Greenblatt, Mark Pflieger, Fuchs, Roberto Marqui-Pascual and others in the last 20 years. An easily applied “Low Resolution Electromagnetic Tomography” is one of the better localization methods although it does offer resolutions of only 3 – 6 cm, but nonetheless, much better than the alternative of zero 3-dimensional resolution that conventional EEG provides (Pascual-Marqui, 1999; Pascual-Marqui et al, 2001; Thatcher et al, 1994; 2005a; 2005b; 2006; Gomes and Thatcher, 2001). As emphasized by many, it is critical to understand how widely distant regions of the brain communicate before one can understand how the brain works. It is in recognition of the importance of understanding brain connectivity especially using explicit and step by step methods that the present paper was undertaken. We attempt to use hand calculator simplicity when ever

possible and this is why the cospectrum and quadspectrum are in simple notation such as $a(x)$ or $u(y)$ to represent different values that are added or multiplied. The hand calculator equations in section 9 are important as a reference for a programmer or a systems analyst to implement in a digital computer and thereby provide testable standards and simplicity.

2- EEG Amplitude

Nunez (1994) estimated that 50% of the amplitude arises from directly beneath the scalp electrode and approximately 95% is within a 6 cm diameter. Cooper et al (1965) estimated that the minimal dipole surface area necessary to generate a potential measurable from the scalp surface is 6 cm^2 which is a circle with a diameter = 2.76 cm. However, the amplitude of the EEG is not a simple matter of the total number of active neurons and synapses near to the recording electrode. For example, volume conduction and synchrony of generators are superimposed and mixed in the waves of the EEG. Volume conduction approximates a gaussian spatial distribution for a given point source and volume conduction of the electrical field occurs at phase delay = 0 between any two recording points (limit speed of light) (Feinmann, 1963). If there is a consistent and significant phase delay between distant synchronous populations of neurons or sources, for example, a consistent 30 degree phase at 6 to 28 cm, then this phase difference can not be explained by volume conduction. Network properties are necessary to explain the EEG findings. This emphasizes the importance of phase differences between different EEG channels that are located at different positions on the human scalp. A large phase difference can not be explained by volume conduction and the stability of phase differences influences the amplitude of the EEG as well. Mathematically, phase can only be measured using complex numbers, however, we try with our hand calculator equations to both explain this and make available simple equations that use the cospectrum and quadspectrum (see page 23 section 10). However, it is important to note that complex numbers are necessary at a fundamental level of physics in which the electrical field and quantum mechanics both rely upon complex numbers and nature itself obeys the algebra of complex numbers. One wonders if the physical laws of the universe dictate the evolution of human mathematical invention? The human mind tends to find and extend the laws of the universe by a recurrent loop back on itself?

The importance of the synchrony of a small percentage of the synaptic sources of EEG generators is far greater than the total number of generators. For example, Nunez (1981; 1994) and Lopes da Silva (1994) have shown

that the total population of synaptic generators of the EEG are the summation of : 1- a synchronous generator (M) compartment and, 2- an asynchronous generator (N) compartment in which the relative contribution to the amplitude of the EEG is $A = M \sqrt{N}$. This means that synchronous generators contribute much more to the amplitude of EEG than asynchronous generators. For example, assume 10^5 total generators in which 10% of the generators are synchronous or $M = 1 \times 10^4$ and $N = 9 \times 10^4$ then EEG amplitude = $10^4 \sqrt{9 \times 10^4}$, or in other words, a 10% change in the number of synchronous generators results in a 33 fold increase in EEG amplitude (Lopez da Silva, 1994). Blood flow studies of intelligence often report less blood flow changes in high I.Q. groups compared to lower I.Q. subjects (Haier et al, 1992; Haier and Benbow, 1995; Jausovec and Jausovec, 2003). Cerebral blood flow is generally related to the total number of active neurons integrated over time, e.g., 1 – 20 minutes (Yarowsky et al, 1983: 1985; Herscovitch, 1994). In contrast, EEG amplitude as described above is influenced by the number of synchronous generators much more than by the total number of generators and this may be why high I.Q. subjects while generating more synchronous source current than low I.Q. subjects often fail to show greater cerebral blood flow (Thatcher et al, 2006).

3- What is Volume Conduction and Connectivity?

The EEG has a dual personality. One personality are the electrical fields of the brain which operate at the speed of light where dipoles distributed in space turn on and off and oscillate at different amplitudes and frequencies. Paul Nunez's book "Electrical Fields of the Brain", Oxford Univ. Press, 1981 is an excellent text especially in regard to the electrical personality of the EEG. The other personality of the EEG is the source of the electrical activity which is an excitable medium, much like a forest fire in which the fuel at the leading edge of the fire results in a traveling wave with ashes left behind representing a long duration refractory period. Hodgkin and Huxley wrote the fundamental excitable medium equations of the brain in 1952 for which they later received the Nobel prize. The excitable medium of the brain are the axons, synapses, dendritic membranes and ionic channels that behave like "kindling" at the leading edge of a confluence of different fuels and excitations. As mentioned previously, the majority of the cortex about 80% is excitatory with recurrent loop connections yet there is no epilepsy in a healthy brain. How is such stability possible with such an abundance of positive feedback? The answer

is because there are relatively long refractory periods (after action potentials and after potentials) and this single property is responsible for the self-organizational stability of the neocortex. Given this introduction, “EEG Connectivity” is a property of the “excitable medium” of axons, synaptic rise and fall times and burst durations of neurons and is defined by the magnitude of coupling between neurons. Magnitude is typically defined by the strength, duration and time delays as measured by electrical recording of the electrical fields of the brain produced by the excitable medium. Connectivity does not occur at the speed of light and is best measured when there are time delays, in fact, volume conduction of electricity is not a property of the excitable medium and it occurs at zero time delay. This important property of the excitable medium sources of the EEG versus the electrical properties means that time delays determine whether or not and to the extent that an excitable medium is responsible for the electrical potentials measured at the scalp surface. Volume conduction defined at zero phase lag is the electrical personality and lagged correlations is the excitable medium personality of EEG.

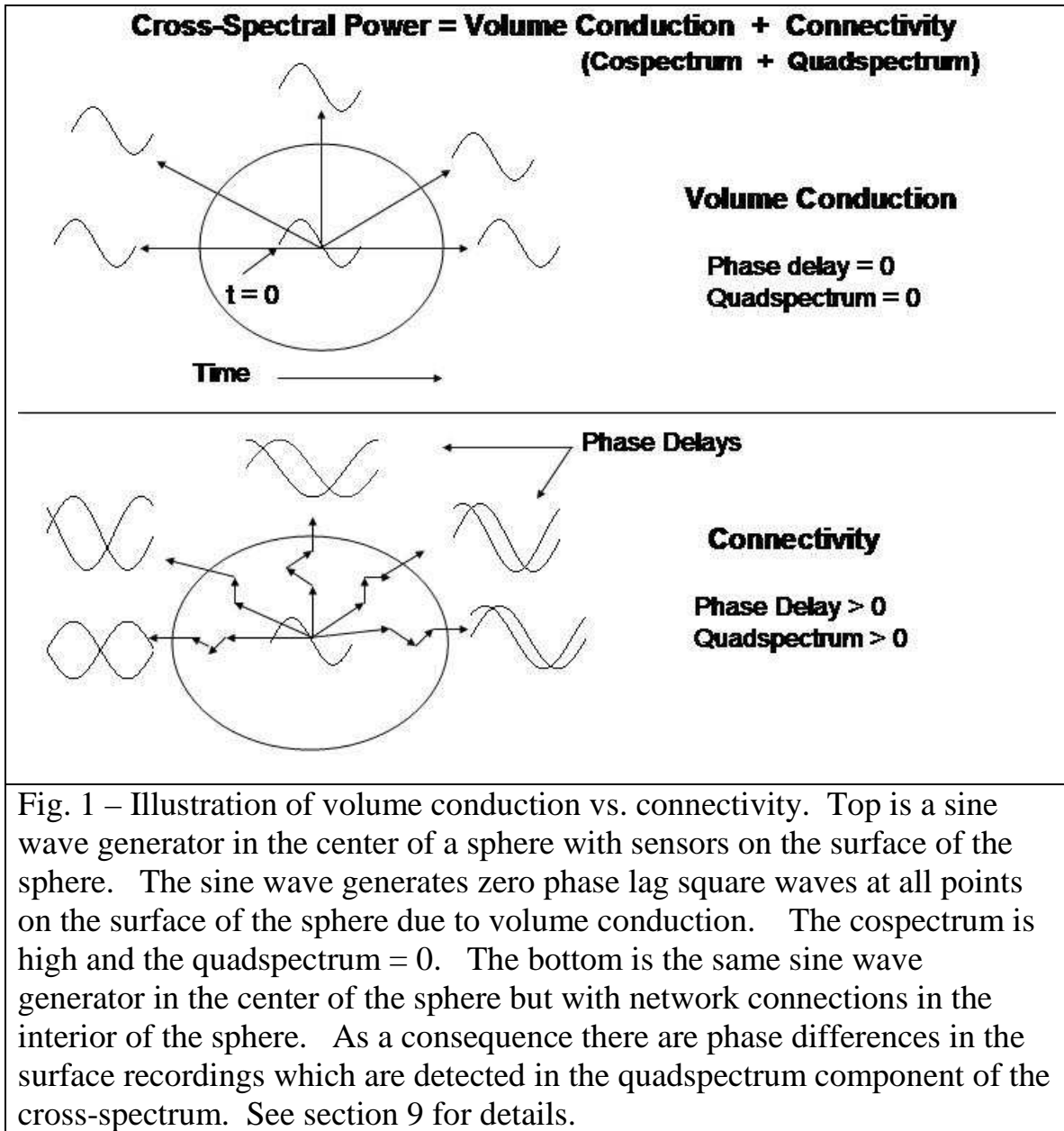
Coupled oscillators in an excitable medium are the topic of this paper starting with the genesis of the electrical potentials being ionic fluxes across polarized membranes of neurons with intrinsic rhythms and driven rhythms (self-sustained oscillations) as described by Steriade (1995) and Nunez (1981; 1994).

Electrical events occur inside of the human body which is made up of 3-dimensional structures like membranes, skin and tissues that have volume. Electrical currents spread nearly instantaneously throughout any volume. Because of the physics of conservation there is a balance between negative and positive potentials at each moment of time with slight delays near to the speed of light (Feynmann, 1963). Sudden synchronous synaptic potentials on the dendrites of a cortical pyramidal cell result in a change in the amplitude of the local electrical potential referred to as an “Equivalent Dipole”. Depending on the solid angle between the source and the sensor (i.e., electrode) the polarity and shape of the electrical potential is different. Volume conduction involves near zero phase delays between any two points within the electrical field as collections of dipoles oscillate in time (Nunez, 1981). As mentioned previously, zero phase delay is one of the important properties of volume conduction and it is for this reason that measures such as the cross-spectrum, coherence, bi-coherence and coherence of phase delays are so critical in measuring brain connectivity independent of volume conduction.

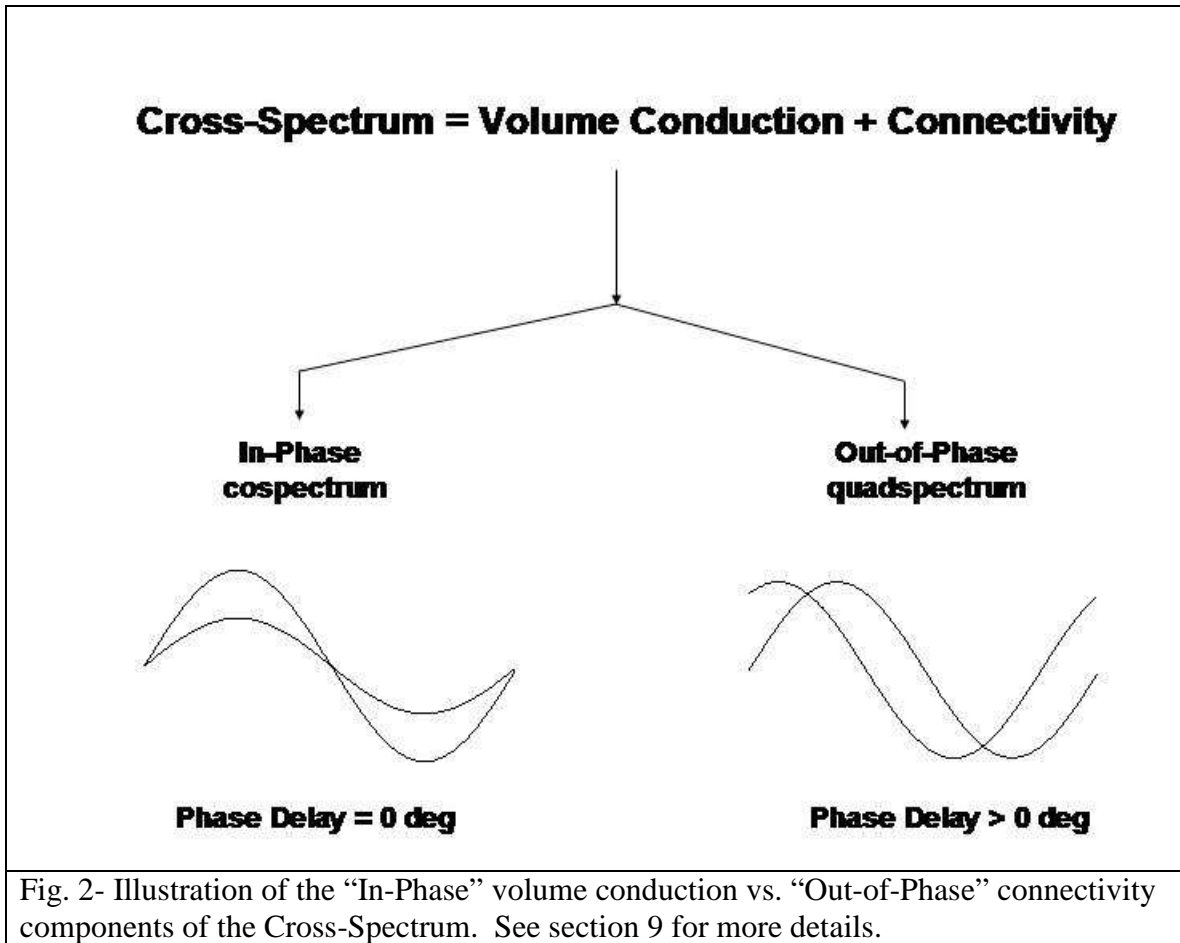
When separated generators exhibit a stable phase difference of, for example, 30 degrees then this can not be explained by volume conduction.¹ As will be explained in later sections correlation coefficient methods such as the Pearson product correlation (e.g., “co-modulation” and “Lexicor correlation”) do not compute phase and are therefore incapable of controlling for volume conduction. The use of complex numbers and the cross-spectrum is essential for studies of brain connectivity not only because of the ability to control volume conduction but also because of the need to measure the fine temporal details and temporal history of coupling or “connectivity” within and between different regions of the brain.

Figure 1 is an illustration of the cross-spectrum of volume conduction vs. connectivity in which a sine wave is generated inside a sphere with sensors on the surface. The top shows the zero phase lag recordings of a sine wave and illustrates volume conduction in which the solid angle from the source to the surface is equal in all directions. The bottom shows recordings with significant phase differences which can not be accounted for by volume conduction and must be due to “connections” in the interior of the sphere. As discussed in more detail in section 9, the cross-spectrum is the sum of the in-phase potentials (i.e., cospectrum) and out-of-phase potentials (i.e., quadspectrum). The in-phase component contains volume conduction and the synchronous activation of local neural generators. The out-of-phase component contains the network or connectivity contributions from locations distant to a given source. In other words, the cospectrum = volume conduction and the quadspectrum = non-volume conduction which can be separated and analyzed by independently evaluating the cospectrum and quadspectrum (see section 9).

¹ Theoretically, large phase differences can be produced by volume conduction when there is a deep and temporally stable tangential dipole that has a positive and negative pole with an inverse electrical field at opposite ends of the human skull. In this instance, phase difference is maximal at the spatial extremes and approximates zero half way between the two ends of the standing dipole. However, this is a special situation that is sometimes present in evoked potential studies but is absent in spontaneous EEG studies. In the case of spontaneous EEG there is no time locked event by which to synchronize potentials that result in a standing dipole, instead, there is an instantaneous summation of millions of ongoing rhythmic pyramidal cell dipoles with different orientations averaged over time.



Another illustration of the relationship between “In-Phase” and volume conduction vs. “Out-of Phase” and connectivity is in figure 2.



In NeuroGuide it is simple to test the “In-Phase” vs “Out-of-Phase” analyses by using sine waves and shifting one sine wave with respect to a second sine wave and then computing the cospectrum and quadspectrum. To test the cospectrum and quadspectrum download NeuroGuide from <http://www.appliedneuroscience.com/Contact%20Download1.htm> and after launching NeuroGuide click File > Open > Signal Generation and then enter sine waves at different phase shifts for a given frequency and then compute the cospectrum and quadspectrum. Figure 3 shows an example of the

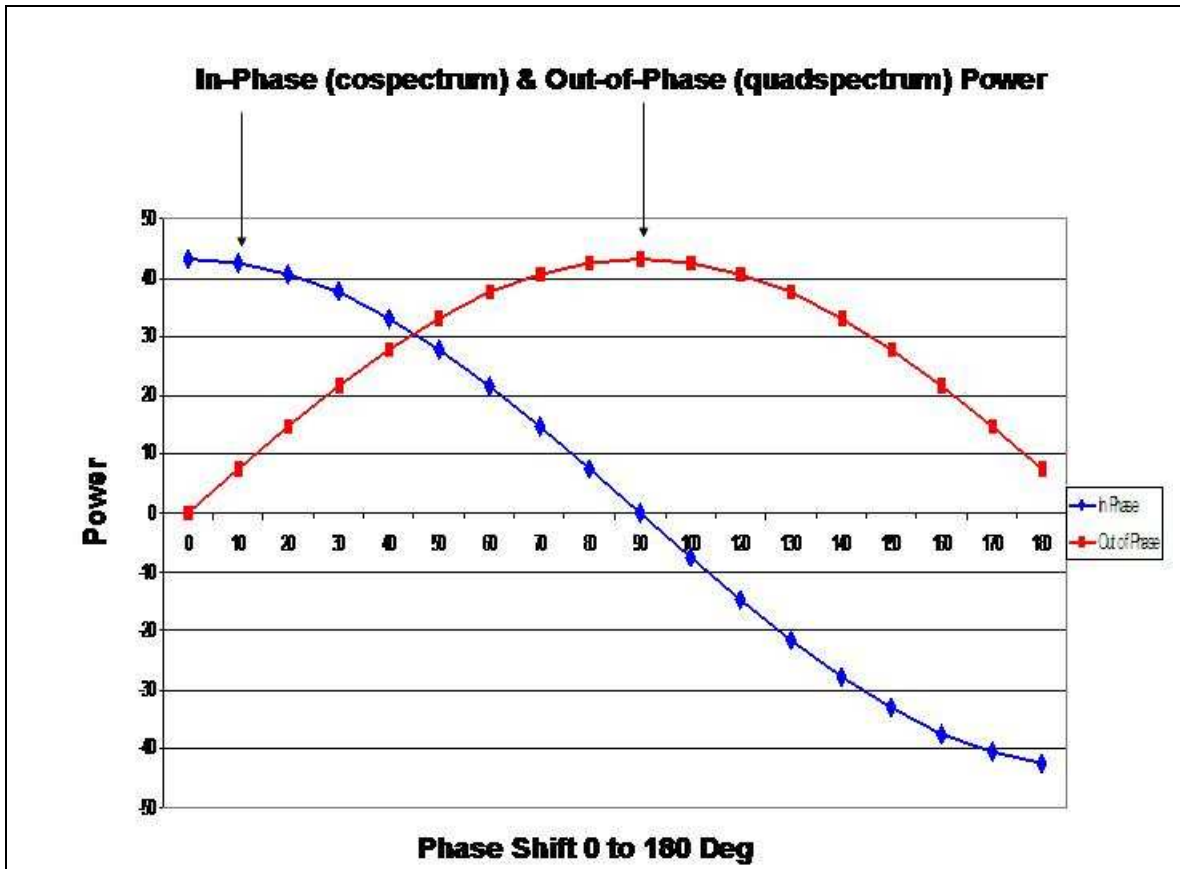


Fig. 3- Example of cospectrum (in-phase) and quadspectrum (out-of-phase) power using two 5 Hz sine waves shifted by 10 degrees from 0 to 180 degrees. Blue diamonds are the in-phase cospectrum values and the red squares are the out-of-phase quadspectrum power values.

The use of the quadspectrum or “Out-of-Phase” computation is a method to remove zero phase lag from the computation of coherence and thus is volume conduction corrected coherence also referred to as Zero-phase lag removed coherence (Nolte et al, 2004; Pascual-Marqui, 2007).

4- How is network zero phase lag different from volume conduction?

Spatially distributed neurons exhibit near zero phase difference, referred to as a “binding” or “synchrony” within a network of neurons, which is independent of volume conduction (Ekhorn et al, 1988; Gray et al, 1989, John, 2005; Thatcher et al, 1994). The thalamus is the master synchronizer of the EEG and “binding” at zero phase lag can easily be produced by the centrally located thalamus (see Steriade, 1995). Multiple unit recordings and Magnetic electroencephalography (MEG) which is invisible to volume conduction have firmly established the scientific validity of network zero phase lag independent of volume conduction (Rogers,

1994). The thalamus and septo-hippocampal systems are centrally located inside of the brain and contains “pacemaker” neurons and neural circuits that regularly synchronize widely disparate groups of cortical neurons (Steriade, 1995). As illustrated in Figure 4, a centrally synchronizing structure “C” can produce zero phase lag and simultaneously synchronize neural populations “A” and “B” without any direct connection between “A” and “B”. As shown in figure 3 the cross-spectrum of coherence and phase difference can distinguish between volume conduction and network zero phase differences such as produced by the thalamus or the septal-hippocampus-entorhinal cortex, etc. For example, if the phase difference is uniformly zero in the space between “A” and “B” then this is volume conduction. On the other hand if the phase difference is not zero at points spatially intermediate between “A” and “B” then this is an example of zero phase difference independent of volume conduction. This is why a larger numbers of electrodes is important and why dipole source reconstruction can help resolve thalamic synchronization of cortical sources. The study by Thatcher et al, 1994 is an example of significant phase differences at intermediate short distances in contrast to zero phase difference between more distant locations which can not be explained by volume conduction.

In the chapters below we begin with a discussion of correlation, then coherence and phase difference and then bi-spectra. We show that there is a commonality shared by all of these measures – the commonality is the statistical “degrees of freedom”. Each measure of cortical network dynamics involves the detection of a “signal” within “noise” and each measure shares the same statistical properties, namely, increased sample sizes are proportional to increased sensitivity and increased accuracy of the estimates of coupling.

5- Pearson product correlation (“comodulation” and Lexicor “spectral correlation coefficient”)

The Pearson product correlation coefficient is often used to estimate the degree of association between amplitudes or magnitudes of the EEG over intervals of time and frequency (Adey et al, 1961). The Pearson product correlation coefficient does not calculate a cross-spectrum and therefore does not calculate phase nor does it involve the measurement of the consistency of phase relationships such as with coherence and the bi-spectrum. However, coherence and the Pearson product correlation coefficient are statistical measures and both depend on the same number of degrees of freedom for determining the accuracy of the measure as well as the same levels of statistical significance. The Pearson product correlation

coefficient is a valid and important measure of coupling and it is normalized and independent of absolute values.

The Pearson product correlation coefficient (PCC) has been applied to the analysis of EEG spectra for over 40 years, for example, some of the earliest studies were by Adey et al (1961); Jindra (1976) Paigacheva, I.V. and Korinevskii (1977). The general method is to compute the auto power spectrum for a given epoch and then to compute the correlation of power or magnitude over successive epochs, i.e., over time. The number of degrees of freedom is determined by the number of epochs. Neuroscan, Inc. offered this method of EEG analysis in the 1980s. Recently, the application of the Pearson product correlation coefficient (PCC) for magnitude has been called “comodulation” (Serman and Kaiser, 2001). Below is the general equation for the computation of “spectral correlation” or “spectral amplitude correlation” and the recent term “comodulation” which is a limited term because it fails to refer to the condition of a 3rd source affecting two other sources without the two sources being directly connected. It is also limited because comodulation can not correct for volume conduction. The term “comodulation” has a different meaning than “synchronization” (Pikovsky et al, 2003) and in order to reduce confusion it is best to simply refer to the correlation itself. In other words, it is best to use the term “Correlation” or “Pearson product correlation coefficient” (PCC) unless additional path analyses or partial correlation analyses were used to show that “comodulation” and not a 3rd modulator “C” is the correct model or that there is no synchrony involved. Figure 3 illustrates the differences in meaning when using the terms “Correlation” vs the term “Comodulation”. Coherence has the same problem as the correlation in distinguishing a 3rd source. However the term coherence, like correlation, does not wrongly assume comodulation.

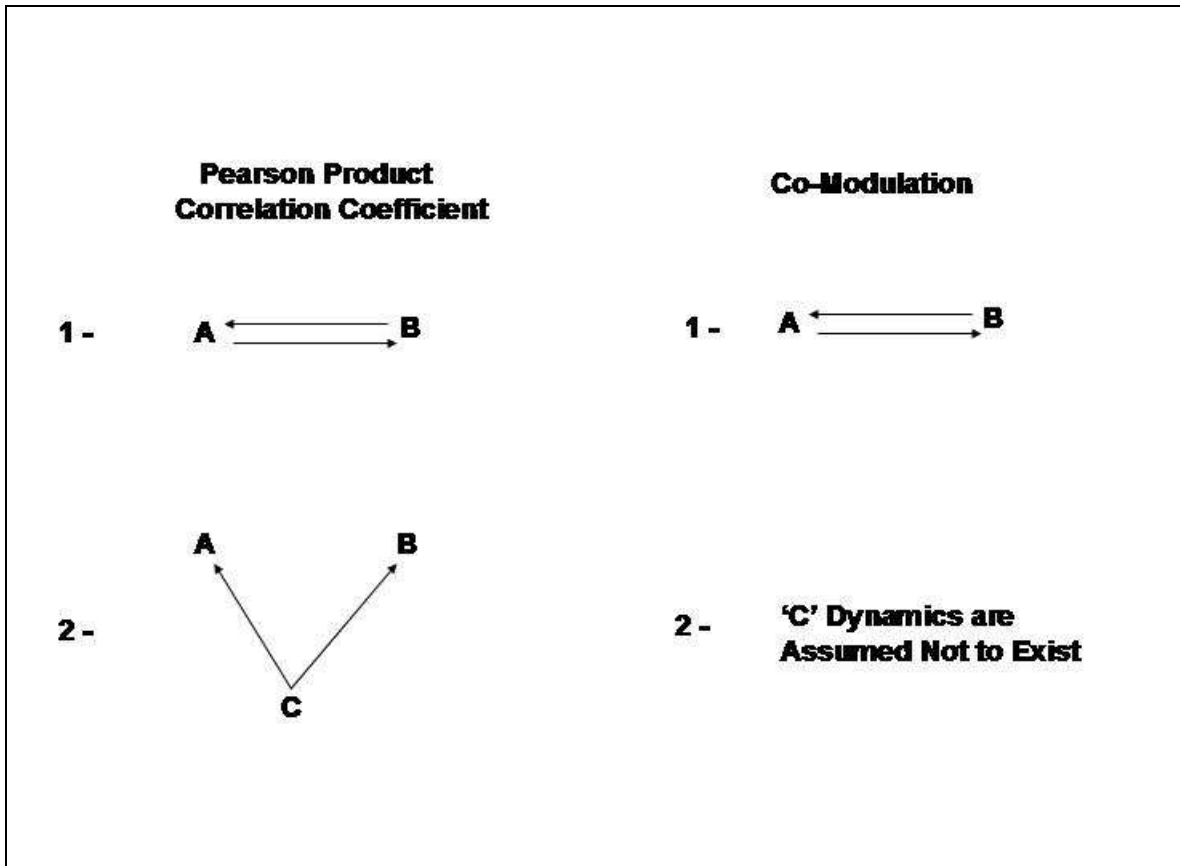


Fig. 4 – The correlation coefficient (and coherence) includes at least two possible couplings and mixtures of these two types of coupling: 1- where neuron A influences neuron B and vice versa and, 2- where a third neuron ‘C’ influences neuron A and neuron B and there is no connection between A and B. Co-modulation omits the standard ‘C’ possibility and is limited to where neuron A influences neuron B and vice versa. The limitation of the term “comodulation” is that without partial correlation analyses or path analyses it is not possible to omit coupling number 2 which means that the term comodulation can be misleading unless these additional analyses are conducted.

As discussed by Pikovsky et al (2003) the term modulation is complicated and it is possible for there to be modulation without synchronization and synchronization without modulation. As stated by Pikovsky et al (2003, p. 77) “Generally, modulation without synchronization is observed when a force affects oscillations, but cannot adjust their frequency.” Without further analyses to determine this distinction it is best to simply refer to amplitude or power correlation.

The distinguishing characteristic of the application of the Pearson product correlation coefficient is the computation of the time course of the normalized covariance of spectra over an interval of time:

Eq. 1-

$$r = \frac{\sum_N (X - \bar{X})(Y - \bar{Y})}{\sqrt{\sum_N (X - \bar{X})^2 \sum_N (Y - \bar{Y})^2}}$$

or the computationally simpler equation that one can compute more easily using a hand calculator:

Eq. 2 -

$$r = \frac{N \sum XY - \sum X \sum Y}{\sqrt{(N \sum X^2 - (\sum X)^2)(N \sum Y^2 - (\sum Y)^2)}}$$

For example, if one computes the FFT over 1 second epochs for a 60 second recording period, i.e., $N = 60$, then the number of degrees of freedom in the spectral correlation coefficient (SCC) for channels X and $Y = 60 - 1 = 59$. For 59 degrees of freedom then a correlation of 0.258 or higher is statistically significant at $P < .05$. This is a valid and commonly used connectivity measure, however, it is important to remember that the correlation coefficient includes volume conduction + network connectivity, i.e., they are inextricably confounded. This is because the correlation coefficient omits phase difference and involves the “in-phase” or autospectral values and therefore volume conduction can not be separated and eliminated. This makes it more difficult to know if factors such as the number and strength of connections are what are changing due to experimental control or is it the “volume conduction” that is changing? As explained in section 8, coherence using complex numbers and phase differences separate volume conduction from network dynamics and automatically solve this problem.

Another method of applying the Pearson Product correlation was developed by Lexicor, Inc. in the 1990s. This method computes the correlation between EEG spectra measured from two different locations and uses the individual spectral bin values within a frequency band. For example, if there are five frequency bins in the alpha frequency band (i.e., 8Hz, 9Hz, 10Hz, 11Hz and 12Hz), then $N = 5$ and the number of degrees of freedom = $N - 1 = 4$. When the degrees of freedom = 4 then a correlation coefficient of 0.961 or higher is necessary in order to achieve statistical significance at $P < .05$. Equations 1 and 2 are used to calculate the Pearson product correlation in both instances.

Dr. Thomas Collura recently evaluated the commonalities and differences between “comodulation” and the Lexicor application of the Pearson product correlation (Collura, 2006). It was shown that the difference between the “co-modulation” and Lexicor methods is primarily in terms of the number of degrees of freedom as well as the evaluation of covariance of spectral energies over time in the former application of the Pearson Product correlation versus within frequency band covariation across channels in the Lexicor method of applying the Pearson product correlation.

Below is a hand calculator example of a Lexicor application of the Pearson product correlation coefficient for the alpha frequency band (8 – 12 Hz column on the left) between channel X and channel Y using easy numbers for a hand calculator using equation 2 with N = 5 (i.e., number of spectral bins within a band and the number of degrees of freedom = 4).

Table I

	X (uV)	Y (uV)	X ² (uV ²)	Y ² (uV ²)	XY
8Hz	1	2	1	4	2
9Hz	2	1	4	1	2
10Hz	3	2	9	4	6
11Hz	3	1	9	1	3
12Hz	4	2	16	4	8
	ΣX = 13	ΣY = 8	ΣX ² = 39	ΣY ² = 18	ΣXY = 21

$$r = \frac{N \sum XY - \sum X \sum Y}{\sqrt{(N \sum X^2 - (\sum X)^2)(N \sum Y^2 - (\sum Y)^2)}}$$

$$r = \frac{5 \times 21 - 13 \times 8}{\sqrt{(5 \times 39 - 13^2)(5 \times 18 - 8^2)}}$$

$$r = \frac{1}{\sqrt{26 \times 26}} = +0.001479$$

Figure 5 shows the results of the BrainMaster implementation of the Lexicor spectral correlation method in which very high correlation values are present because of the low number of degrees of freedom and especially the divergent differences at higher frequencies because of slight differences in filtering. This figure emphasizes that extreme caution should be used when computing a correlation coefficient using the Lexicor method with low degrees of freedom.

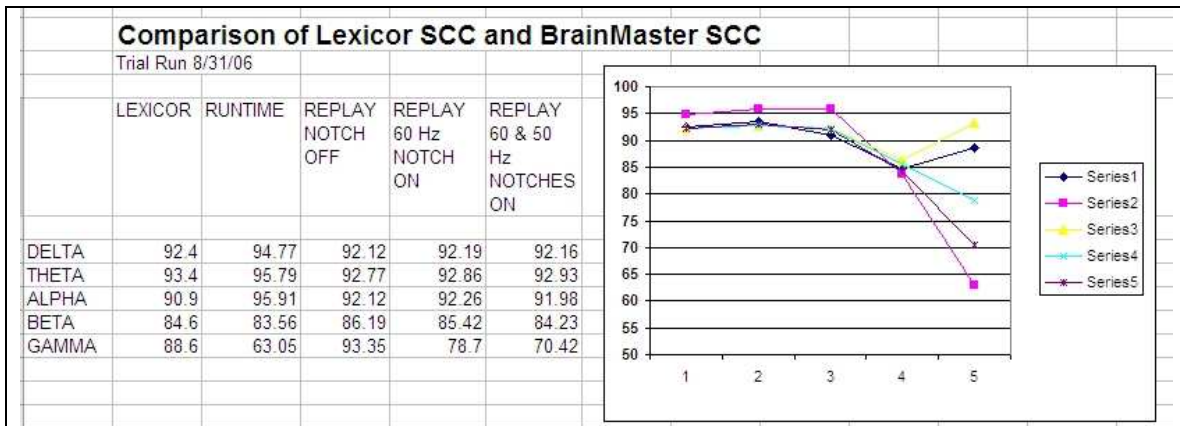
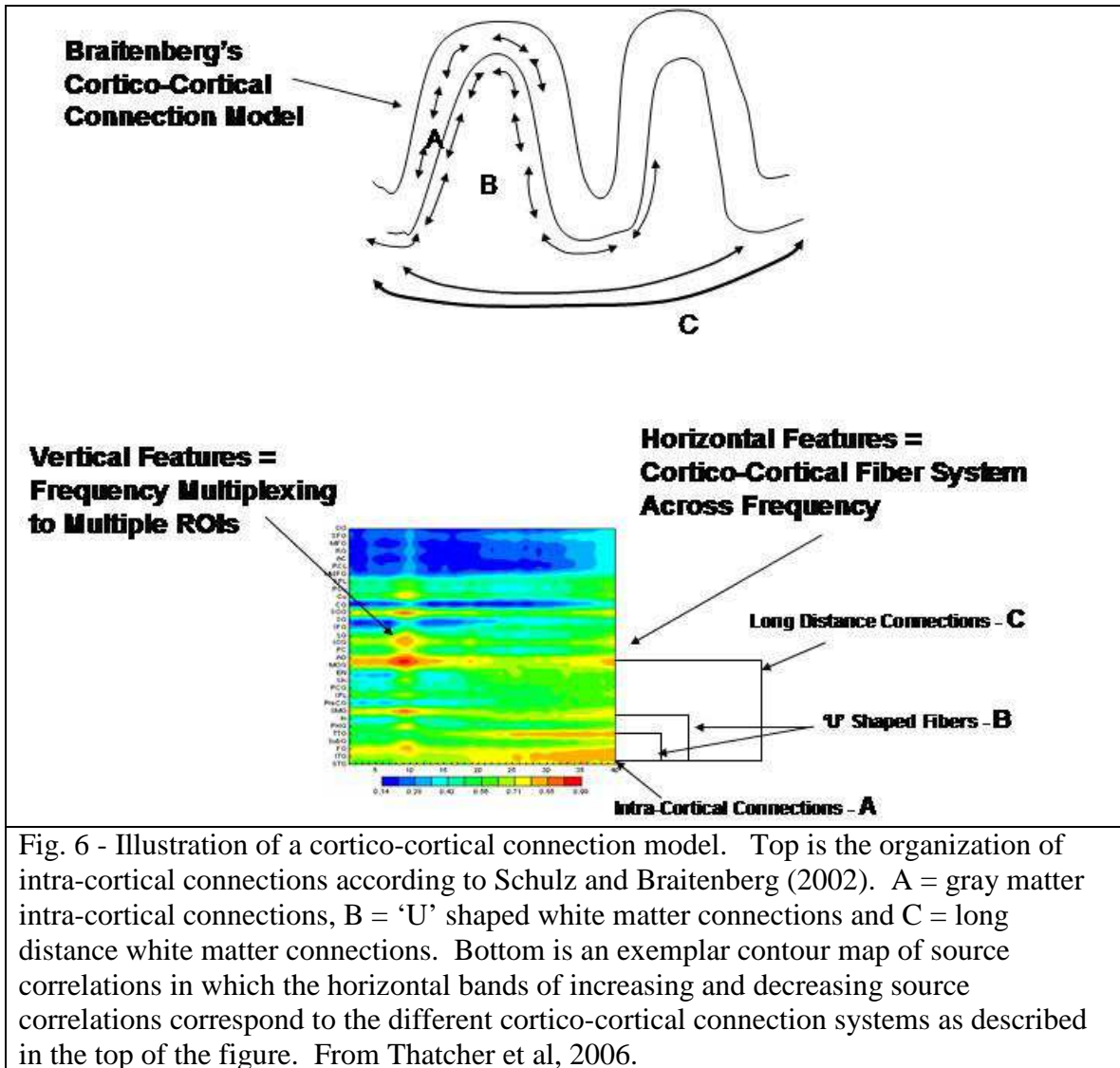


Fig. 5 - Comparisons between the BrainMaster and Lexicor implementation of the spectral correlation method. The correlation values are all very high due to the low degrees of freedom and miss-match of calculation occurs at the higher frequencies depending on the filter parameters (From Collura, 2006).

LORETA source correlations are another example of the application of the Pearson product correlation coefficient (Thatcher et al, 2006). Below are examples of the relationship between cortico-cortical connectivity and distance from a point source using LORETA current sources and the Pearson product correlation coefficient (PCC) as applied to sequential epochs of time. The degrees of freedom ranged from 29 to 60 in which a correlation of 0.367 to 0.254 is necessary for $P < .05$. This analysis is a cross-frequency correlation as well as a cross-region of interest correlation. The time series analyses of cross-channel and cross-frequency coherence and phase synchrony is discussed in sections 25 to 39.



6- What is Coherence?

Coherence is a measure of the amount of phase stability or phase jitter between two different time series. Coherence combines something analogous to the "Pearson product-moment correlation" to the phase angles between two signals. When the phase difference between two signals is constant then coherence = 1, when the phase difference between signals is random then coherence = 0. It is possible for there to be a constant phase angle difference at two different frequencies. In the later case the terminology is cross-frequency coherence or bi-spectral coherence or n:m phase synchrony (Schack et al, 2002; 2005). If the measures are within the same frequency band, then the terminology is simply "coherence" which assumes auto-frequency coherence. Coherence is mathematically analogous

to a Pearson product-moment correlation and therefore is amplitude normalized, however, coherence is a statistic of phase differences and yields a much finer measure of shared energy between mixtures of periodic signals than can be achieved using the Pearson product-moment correlation coefficient of amplitudes. In fact, coherence is essential because the degree of relationship or coupling between any two living systems cannot be fully understood without knowledge of its frequency structure over a relative long period of time. Another advantage of Coherence, as mentioned previously, is its dependence on the consistency of the average phase difference between two time series, whereas the Pearson product-moment correlation coefficient is independent of phase differences. The fine details of the temporal relationship between coupled systems is immediately and sensitively revealed by coherence.

In this paper we will first describe the mathematics of the autospectrum and power spectrum as they apply to EEG coherence by using simple hand calculator instructions so that one can step through the mathematics and understand coherence and phase at a basic level (some of the deeper mathematical detail is in the Appendix). We will step the reader through simple examples that can be solved with a hand calculator (scientific calculator is recommended) to further illustrate how coherence is computed and to demonstrate by simulation of EEG signals and noise. We will also address the statistical properties of the power spectrum, coherence and phase synchrony using calibration sine waves and the FFT in order to illustrate the nature of coherence and phase angle (i.e., phase difference and direction) and finally, a statistical standard by which the signal-to-noise ratio and degrees of freedom in the computation of EEG coherence are measured using a hand calculator and by computer simulation of the EEG. Computer signal generators not only verify but most importantly also explore a rich universe of coherence and phase angles with a few mouse clicks (download a free EEG simulator at: <http://www.appliedneuroscience.com> and download the NeuroGuide demo program. Click File > Open > Signal Generation to simulate the EEG, including “Spindles” and inter-spindle intervals, etc. Another free EEG simulation program is at: http://www.besa.de/index_home.htm, a third free EEG simulation program (purchase of MatLab required) is at: <http://www.sccn.ucsd.edu/eeglab/index.html> and a fourth simulation program for the mathematics of the Fourier series is: <http://www.univie.ac.at/future.media/moe/galerie/fourier/fourier.html#fourier>

Mathematical and statistical standardization of EEG coherence are best understood using a hand held calculator and then by simulation of the EEG.

Coherence arises from Joseph Fourier's 1805 fundamental inequality where by the ratio of the cross-spectrum/product of auto-spectrum < 1 . Coherence is inherently a statistical estimate of coupling or association between two time series and is in essence the correlation over trials or repeated measures. As mentioned previously, the critical concept is "phase consistency", i.e., when the phase relationship between two time series is constant over trials than coherence = 1.

7- How Does One Compute Coherence?

The first step in the calculation of the coherence spectrum is to describe the activity of each raw time-series in the frequency domain by the "auto-spectrum" which is a measure of the amount of energy or "activity" at different frequencies. The second step is to compute the "cross-spectrum" which is the energy in a frequency band that is in common to the two different raw data time-series. The third step is to compute coherence which is a normalization of the cross-spectrum as the ratio of the auto-spectra and cross-spectra. To summarize:

- 1- Compute the auto-spectra of channels X and Y based on the "atoms" of the spectrum
- 2- Compute the cross-spectra of X and Y from the "atoms" of the spectrum
- 3- Compute Coherence as the ratio of the auto-spectra and cross-spectra

8- First Compute the auto-spectra of channels X and Y based on the "atoms" of the spectrum

Joseph Fourier in his thesis of 1805, benefiting from almost a century of failed attempts, finally correctly showed that any complex time-series can be decomposed into elemental "atoms" of individual frequencies (sine and cosine and linear operations). Fourier defined the autospectrum as the amount of energy present at a specific frequency band. He showed that the autospectrum can be computed by multiplying each point of the raw data by a series of cosines, and independently again by a series of sines, for the frequency of interest. The average product of the raw-data and cosine is known as the cosine coefficient of the finite discrete Fourier transform, and that for the sine and the raw data as a sine coefficient. The relative contributions of each frequency are expressed by these cosine and sine (finite discrete Fourier) coefficients. The cosine and sine coefficients

constitute the basis for all spectrum calculations, including the cross-spectrum and coherence. Tick (1967) referred to the sine and cosine coefficients as the “atoms” of spectrum analysis. For a real sequence $\{x_i, i = 0, \dots, N-1\}$ and $\Delta t =$ the sample interval and $f =$ frequency, then the cosine and sine transforms are:

$$\text{Eq.3 - The cosine coefficient} = a(n) = \Delta t \sum_{i=1}^N X(i) \cos 2\pi f i \Delta t$$

$$\text{Eq.4 - The sine coefficient} = b(n) = \Delta t \sum_{i=1}^N X(i) \sin 2\pi f i \Delta t$$

A numerical example of the computation of the Fourier Transform is shown in Table II. The data is from Walter (1969) which served as a numeric calibration and tutorial of EEG coherence in the 1960s (see also Jenkins and Watts, 1969 and Orr and Naitoh, 1976). This 1960s dataset is still useful for explaining the concept of spectral analysis as it applies to the Electroencephalogram as QEEG was developed in the 1950’s and used at UCLA and other universities giving rise to a large number of publications and the development of the BMDP Biomedical statistical programs in the 1960s. The Walter (1969) data are 8 digital time points that were sampled at 100 millisecond intervals (0.1 sec. intervals) with 3 separate measurements (i.e., repetitions). The highest frequency resolution of this data set is defined as $1/T = 1/0.8 \text{ sec.} = 1.25 \text{ Hz}$. The highest discernable frequency is 5 Hz (Nyquist limit) and thus the data are bounded by 1.25 Hz and 5 Hz, with values at every 1.25 Hz. We will use the same historic examples that pioneers used in the early development of quantitative EEG used in the 1950s - 1970s. The analyses below are based on the careful step by step evaluation of the Walter (1969) paper by Orr, W.C. and Naitoh, P. in 1967 which we follow.

The Walter (1969) cosine and sine coefficients in Table II will be used for the purpose of this discussion. The focus will be on the use of a hand calculator to compute coherence using the values in Table II and not on the computation of the coefficients themselves.² The reader is encouraged to

² A Matlab computation of the sine and cosine coefficients using the raw data in Table II produced the following coefficients 2.5355- 2.9497i, 17.0000- 1.0000i, -4.5355- 6.9497i using the complex notation $a + ib$. Even though different coefficients may be produced than those published (Walter (1969; Orr and Naitoh, 1976) let us continue to use the Walter (1969) coefficients because the procedures to compute coherence and not the coefficients are what are of interest in this paper. We will produce an updated table and set of numbers in a future revision.

either write intermediate values on a piece of paper or to store temporary variable values using the memory keys of their hand calculator.

Table II
Example of Raw Data

Table of Observation (seconds)	Channel X								Table of Observation (seconds)	Channel Y							
	0.0	0.1	0.2	0.3	0.4	0.5	0.6	0.7		0.0	0.1	0.2	0.3	0.4	0.5	0.6	0.7
Record 1	3	5	-6	2	4	-1	-4	1	Record 1	-1	4	-2	2	0	-0	2	-1
Record 2	1	1	-4	5	1	-5	-1	4	Record 2	4	3	-9	2	7	0	-5	1
Record 3	-1	7	-3	0	2	1	-1	-2	Record 3	-1	9	-4	-1	2	4	-1	-5

Hand Calculator Example of Cosine and Sine Coefficients

Channel X Cosine Coefficients a(x)					Channel Y Cosine Coefficients b(y)				
f (Hz)	1.25	2.5	3.75	5.0	f (Hz)	1.25	2.5	3.75	5.0
Record 1	0.634	4.25	-1.134	-1.25	Record 1	-0.073	-0.25	-0.427	-0.75
Record 2	0.634	2.0	-1.134	-0.875	Record 2	-0.398	6.5	-1.106	-1.25
Record 3	-0.043	1.75	-1.457	-1.375	Record 3	-0.368	1.5	-0.934	-1.375
Average	0.408	2.667	-1.242	-1.167	Average	-0.272	2.583	-0.822	-1.125

Channel X Sine Coefficients b(x)					Channel Y Sine Coefficients b(y)				
f (Hz)	1.25	2.5	3.75	5.0	f (Hz)	1.25	2.5	3.75	5.0
Record 1	0.737	0.25	1.737	0.000	Record 1	0.237	0.75	2.237	0.000
Record 2	0.487	-3.25	1.987	0.000	Record 2	-0.043	0.00	1.457	0.000
Record 3	0.414	2.5	2.414	0.000	Record 3	0.641	4.75	2.341	0.000
Average	0.546	-1.67	2.048	0.000	Average	0.345	1.833	2.012	0.000

Autospectrum X					Autospectrum Y				
f (Hz)	1.25	2.5	3.75	5.0	f (Hz)	1.25	2.5	3.75	5.0
Record 1	0.945	18.125	4.303	1.563	Record 1	0.061	0.625	3.186	0.561
Record 2	0.639	14.563	5.234	0.766	Record 2	0.159	42.25	3.342	1.563
Record 3	0.173	9.313	7.95	1.891	Record 3	1.036	24.813	6.353	1.891
Average	0.586	14.00	5.838	1.407	Average	0.419	22.561	4.96	1.339

The frequency analysis of a time series of finite duration “at” a chosen frequency does not really show the activity precisely at that frequency alone. The spectral estimate reflects the activities within a frequency band whose width is approximately $1/T$ around the chosen frequency. For example, the activity “at” 1.25 Hz in the example in Table II represents in fact the activities from 0.625 Hz to 1.875 Hz (or equivalently, $1.25 \text{ Hz} \pm 0.625 \text{ Hz}$).

The autospectrum is a “real” valued measure of the amount of activity present at a specific frequency band. The autospectrum is computed by multiplying the raw data by the cosine, and independently, by the sine for the frequency of interest in a specific channel. The average product of the raw-data and cosine is referred to as the “cosine coefficient” of the finite discrete Fourier transform, and the average product of the sine and the raw-data is referred to as the sine coefficient. Let N , f and $a(x)$ represent the number of observed values for a time series $x(i)$, the frequency of interest, and a cosine coefficient n , then the summation or necessary “smoothing” is defined as:

$$\text{Eq. 5 - The average cosine coefficient} = a(n) = \frac{1}{N} \sum_{i=1}^N X(i) \cos\left(\frac{2\pi i f}{N}\right)$$

$$\text{Eq.6 - The average sine coefficient} = b(n) = \frac{1}{N} \sum_{i=1}^N X(i) \sin\left(\frac{2\pi i f}{N}\right)$$

Each frequency component has a sine and cosine numerical value. The actual autospectrum value is arrived at by squaring and adding the respective sine and cosine coefficients for each time series. The power spectral value for any frequency intensity is:

$$\text{Eq. 7 - } F(x) = (a^2(x) + b^2(x)),$$

That is, the power spectrum is the sum of the squares of the sine and cosine coefficients at frequency f as shown in Table II.

9- Second Compute the cross-spectra of X and Y from the “atoms” of the spectrum

To calculate the cross-spectrum, it is necessary to consider the “in-phase” and “out-of-phase” components of the signals in channels X and Y. The former is referred to as the co(incident) spectrum or cospectrum and the

latter is referred to as the quadrature spectrum or quadspectrum. The “in-phase” component is computed by considering the sine coefficients as well as the cosine coefficients of X and Y. The “out-of-phase” component concerns relating the cosine coefficient of time series X to the sine coefficient of times series Y, and similarly the sine coefficient of times series X to the cosine coefficient of time series Y.

A simple hand calculator test will show that the quadspectrum = 0 for any two in-phase sine waves (i.e., phase difference = 0). This simple test is important when eliminating or separating the “volume conduction” contribution to the cross-spectra generated by the brain network or brain “Connectivity” aspects of EEG as discussed in section 2. For example, non-volume conduction measures where there are statistically significant phase differences of less than 1 degree have been published (Ekhorn et al, 1988; Barth, 2003). Long electrical phase differences of 5⁰ to 30⁰ simply can not be explained by volume conduction as a matter of physics.

10- How to Compute the cospectrum and quadspectrum

Below is a hand calculator example of how to compute the coherence spectrum. Step 1 is to calculate the cospectrum and quadspectrum:

a(x) = cosine coefficient for the frequency (f) for channel X
 b(x) = sine coefficient for the frequency (f) for channel X
 u(y) = cosine coefficient for the frequency (f) for channel Y
 v(y) = sine coefficient for the frequency (f) for channel Y

The cospectrum and quadspectrum then are defined as:

$$\text{Eq. 8 - Cospectrum (f) = } a(x) u(y) + b(x) v(y)$$

$$\text{Eq. 9 - Quadspectrum (f) = } a(x) v(y) - b(x) u(y)$$

The cross-spectrum **power** is real valued and defined as:

$$\text{Eq. 10 - (f) = } \sqrt{(\text{cos pectrum}(f)^2 + \text{quadspectrum}(f)^2)}$$

$$\text{Eq. 11- } = \sqrt{((a(x)u(y) + b(x)v(y))^2 + (a(x)v(y) - b(x)u(y))^2)}$$

That is, the cross-spectrum **power** is the absolute value of the complex-valued cross-spectrum. The cross-spectrum **power** is a measure of connectivity based on the total shared energy between two locations at a specific frequency and it is a mixture of in-phase and out-of-phase activity (i.e., local and distant). The cross-spectrum power is a real number because a complex number times the complex conjugate is a real number. **Coherence** is a normalization of the cross-spectral power by dividing by the autospectra or the in-phase component and, therefore, coherence is independent of autospectral amplitude or power and varies from 0 to 1.

Table III is an illustration of the computational details of coherence based on the FFT auto and cross-spectra in Table II:

Table III
Hand Calculator Example
Cospectrum, Quaspectrum and Ensemble Smoothing

F (Hz)	Cospectrum				Quaspectrum			
	1.25	2.50	3.75	5.00	1.25	2.50	3.75	5.00
Record 1	0.128	-0.875	4.375	0.938	0.204	3.25	-1.795	0.000
Record 2	-0.272	13.00	4.147	1.094	-0.22	-21.125	0.541	0.000
Record 3	0.363	14.50	7.012	1.891	0.108	4.563	-1.156	0.000
Average	0.073	8.875	5.176	1.307	0.031	-4.438	-0.803	0.000

$$\text{Cospectrum (1.25 Hz)} = 0.634(-0.073) + 0.737(0.237) = 0.128$$

$$\text{Quadspectrum (1.25 Hz)} = 0.634(0.237) - 0.737(-0.073) = 0.204$$

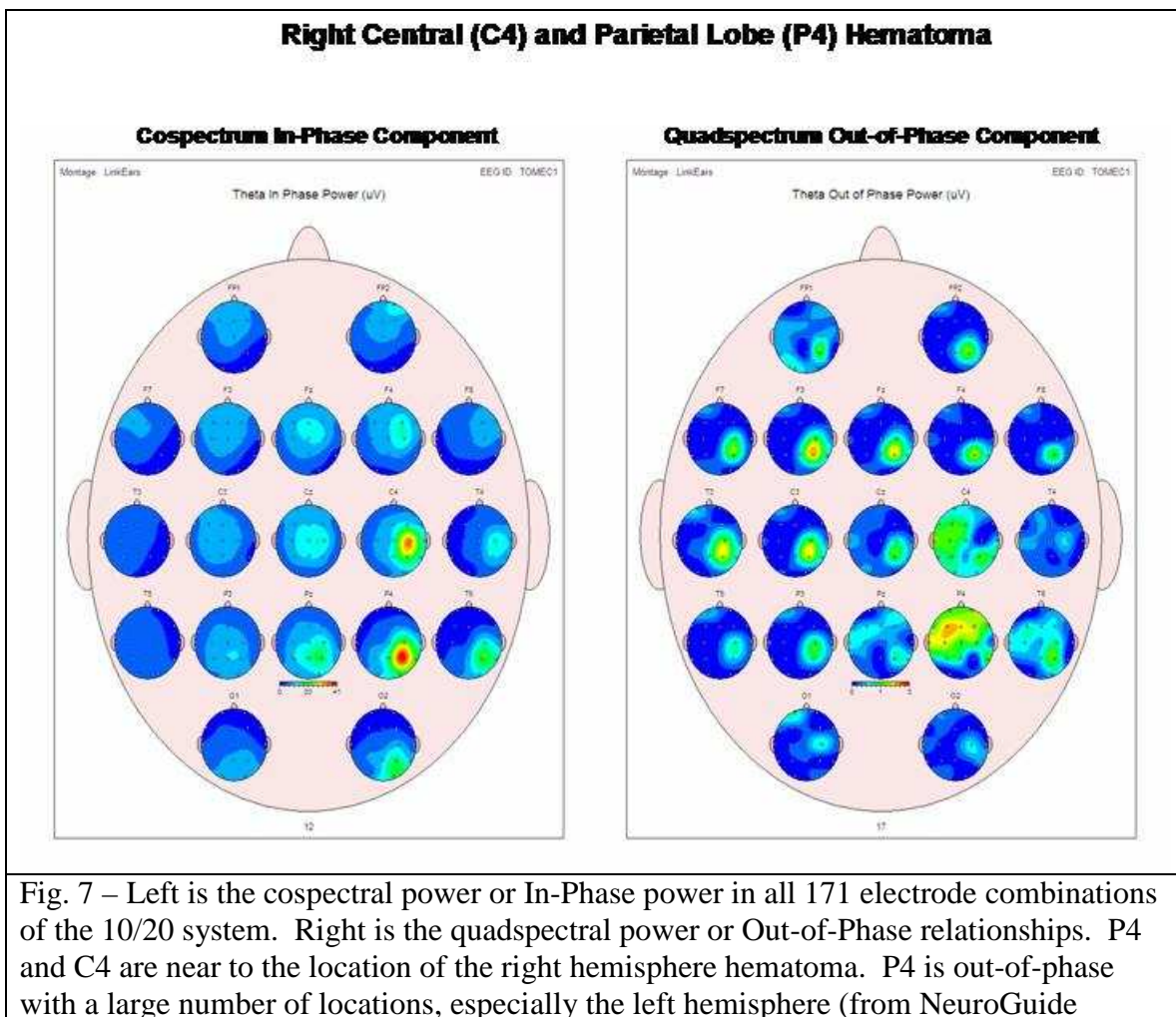
$$\text{Cross-spectrum (1.25 Hz)} = 0.128 + \text{sq. root } -1 (0.204) \text{ and}$$

$$\text{Cross-spectrum power (1.25 Hz)} = (0.128^2 + 0.204^2)^{1/2} = 0.241$$

This computation is repeated for each frequency component to yield the complete cross-spectrum.

As mentioned previously in section 3, the cross-spectrum is the sum of the in-phase potentials (i.e., cospectrum) and out-of-phase potentials (i.e.,

quadspectrum). The in-phase component contains volume conduction and the synchronous activation of local neural generators. The out-of-phase component contains the network or connectivity contributions from locations distant to a given source. In other words, the cospectrum = volume conduction and the quadspectrum = non-volume conduction which can be separated and analyzed by independently evaluating the cospectrum and quadspectrum. Figure 7 is an example of the differences between the in-phase and out-of-phase components of the cross-spectrum in a right hemisphere hematoma patient. The cospectrum shows high focal sources and little distant zero phase lag relations. This is indicative of a source near to the surface of the scalp at P4 and C4. The quadspectrum shows high out-of-phase power or network connections between P4 and the distant left hemisphere and especially F3 that are highly out-of-phase. In general the right parietal lobe is out of phase with respect to the spatially distant left hemisphere.



11- Third Compute Coherence as the ratio of the auto-spectra and cross-spectra

Coherence is usually defined as:

$$\text{Eq. 12 - Coherence (f)} = \frac{|Cross - Spectrum(f)XY|^2}{(Autospectrum(f)(X))(Autospectrum(f)(Y))}$$

However, this standard mathematical definition of coherence hides some of the essential statistical nature and structure of coherence. To illustrate the fundamental statistics of coherence let us return to our simple algebraic notation:

Eq. 13 -

$$\text{Coherence (f)} = \frac{(\sum_N (a(x)u(y) + b(x)v(y)))^2 + (\sum_N (a(x)v(y) - b(x)u(y)))^2}{\sum_N (a(x)^2 + b(x)^2) \sum_N (u(y)^2 + v(y)^2)}$$

Where N and the summation sign represents averaging over frequencies in the raw spectrogram or averaging replications of a given frequency or both. The numerator and denominator of coherence always refers to smoothed or averaged values, and, when there are N replications or N frequencies then each coherence value has 2N degrees of freedom. Note that if spectrum estimates were used which were not smoothed or averaged over frequencies nor over replications, then coherence = 1 (Bendat and Piersol, 1980; Benignus, 1968; Otnes and Enochson, 1972). In order to compute coherence, averaged cospectrum and quadspectrum smoothed values with degrees of freedom > 2 and error bias = 1/N is used.

The numerical example of coherence used the average cospectrum and quadspectrum across replications in Table III. For example from Table III the coherence at 1.25 Hz is:

$$\text{Eq. 14 - Hand Calculator Coherence (1.25 Hz)} = \frac{0.073^2 + 0.031^2}{0.586(0.419)} = 0.026$$

This computation is repeated for each frequency component to yield the complete coherence spectrum, a typical plot of coherence is frequency on the horizontal axis (abscissa) and coherence on the vertical axis (ordinate). Coherence is sometimes defined and computed as the positive square-root and this is referred to as “coherency”.

12- Some Statistical Properties of Coherence

How large should coherence values be before they can be considered reliable? The answer is it depends on the true coherence relationship and the degrees of freedom used in the averaging computation in equation 13. In general the degrees of freedom increase as a square root of N (i.e., the amount of smoothing) and the more the degrees of freedom the better (i.e., averaging across frequency and/or across repetitions or “smoothing”). The trade off is between frequency resolution and reliability, the longer the interval of time over which averaging occurs or the larger the number of repetitions then the greater are the degrees of freedom. Short time intervals of low frequencies by their nature have low degrees of freedom. For this reason the NeuroGuide uses the default of a 1 minute sample, e.g., the theta frequency band 4 – 7 Hz NeuroGuide EEG coherence for a 1 minute sample = 7 (0.5 Hz bins) + 117 FFTs = 124 x 2 = 248 degrees of freedom. To test the statistical properties of coherence select shorter segments of simulated EEG and systematically change the signal-to-noise ratio in the NeuroGuide demo signal generator at www.appliedneuroscience.com. After launching the NeuroGuide demo click Open > Signal Generation.

13- How large should coherence be before it can be regarded as significantly larger than zero?

Low degrees of freedom always involve “Inflation” of the true signal-to-noise relationship between two channels when a Pearson product correlation coefficient is computed. EEG coherence is no exception and this explains why coherence is highly inflated when the degrees of freedom are low and the bandwidth is small. For example, figure 8 shows the inflation of coherence (y-axis) when a signal in one channel (4 Hz – 19 Hz sine wave) is compared to random noise in a second channel with increasing degrees of freedom (x-axis) and different bandwidths. The ideal is coherence = 0.

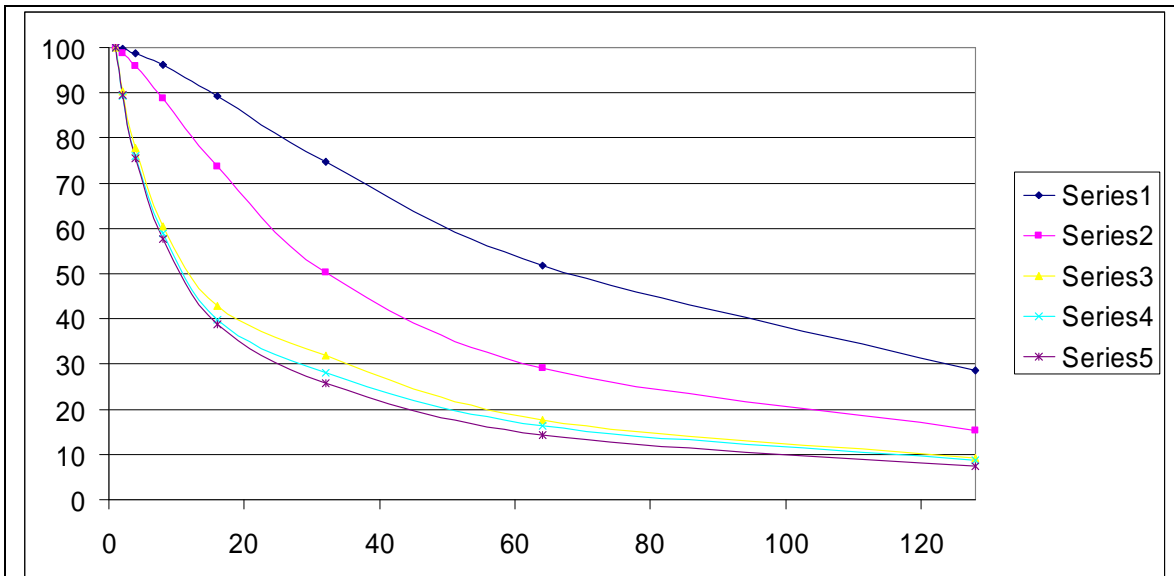


Figure 8 – Coherence (y-axis) vs. number of time samples (y-axis). Sample rate = 128 Hz. The five curves are for different band widths. Series 1 = 4 Hz, series 2 = 6 Hz, series 3 = 8 Hz, series 4 = 10 Hz and series 5 = 12 Hz bandwidths. The wider the band width the more stable and accurate is coherence.

The digital reality of low degrees of freedom using a 2 Hz bandwidth are also shown in figure 8. The y-axis is coherence (x100). The x-axis are the number of time samples at a sample rate of 128 Hz using a digital filter (complex demodulation) to compute coherence. The five curves represent different bandwidths (4 Hz, 6 Hz, 8 Hz, 10 Hz & 12 Hz). The ideal coherence value = 0 at infinity and series 5 with a 12 Hz band width is approximately 9% at 128 time samples. Mathematically coherence inflation is defined as:

Eq. 15 – Inflation of Coherence (IF) = coherence of signal (S) divided by the coherence of white noise (N) = $IF = S/N$

The curves in Figure 8 show that after 1 second of averaging the EEG coherence inflation values ranged from 1 to 0.10 (or 10%). Figure 8 also shows that the wider the band width then the larger the number of degrees of freedom. The equation to compute the degrees of freedom when using complex demodulation is:

Eq. 16 - $Df = 2BT$

Where B = bandwidth and T = time samples (Otnes and Enochson, 1972 and Appendix-B).

Bendat and Piersol (1980) as elaborated by Nunez et al (1997) provide another measure of the 95% interval for coherence which is expressed as:

$$\text{Eq. 17 - } \frac{F(i)}{1+2e} \leq F(i) \leq \frac{F(i)}{1-2e}$$

Where $F(i)$ applies to the auto or cross spectral density or coherence. The confidence interval depends on the error term e defined as the RMS error (i.e., root mean square error). In general, the error may be estimated by:

$$\text{Eq. 18 - } e_f = \frac{1}{\sqrt{N}}$$

14- Is there an inherent time limit for EEG Coherence Biofeedback?

The answer is yes, because coherence is unique in EEG biofeedback because it depends upon averaging the phase angles or phase differences. The lower the variance or the more constant the phase differences (or the greater the phase synchrony or phase locking) then the higher the coherence. Similarly, as a property of statistics the greater the degrees of freedom then the less the statistical inflation of the real coherence value. Based on operant conditioning studies the feedback interval or feedback delay is crucial for the ability of the brain to link together two past events. Too short an interval or too long an interval reduces the likelihood of a person making a “connection” between the biofeedback display/sound or signal and the brain’s electrical state at a previous moment in time. In the case of amplitude and phase difference the calculation does not depend upon an average as it does when computing coherence. Thus, coherence EEG biofeedback inherently requires a longer feedback delay than does the nearly instantaneous computations of power, ratios of power, relative power, amplitude, amplitude asymmetries, phase difference (or phase angle), etc. To the best of our knowledge the minimum amount of inflation that leads to the greatest efficacy of biofeedback training using EEG coherence has not yet been published. The minimal interval is a function of at least two factors: 1- the stability of the signal being fed back, i.e., a noisy and jumpy signal has no connection formation value and, 2- the interval of time between the brain event and the feedback. Both are critical and seconds and milliseconds are the domain. The interval from 0 to about 80 – 100 milliseconds is a neurophysiological “blank period” during the integration interval where simultaneity is resolved as a single “quanta” or “perceptual

frame” of consciousness (Thatcher and John, 1977; John, 2005). At about 300 – 500 msec the match miss-match resolution of expectation and received inputs is completed. Associations and connections in time occur from about 200 msec to minutes of time. Thus, operant conditioning of EEG biofeedback is likely to work best when the interval of time between an “EEG Event” is greater than 100 msec and around 1 – 2 seconds, with a operating curve yet to be produced. When accurate measurements are made of the optimal interval of time between a brain event and the feedback signal and not active stimulation, then one can expect that 500 msec to 1 sec would be a good interval of time for associations to occur using operant conditioning EEG biofeedback. For active stimulation EEG biofeedback then phase reset can occur and many other phenomena that can easily be measured can occur. However, modern EEG science easily handles event related potentials (ERPs) if one knows the instant in time when the stimulus was delivered or the instant in time when the movement of the subject occurred. Spontaneous EEG and ERPs are related in that the background EEG is the “mother” of the ERP (electrical field) at a given moment of time. The powerful and rhythmic background EEG are the summation of millions of excitatory EPSPs oscillating in loops but only firing on the rising phase of the oscillation. This results in a “quantization” of neuron excitability as reflected by the rhythms of the EEG. The idea of “quantization” of neural action potentials time locked to the rising phase of the EEG is old and is well supported by recent evidence (Buzsaki, 2006).

15- What is Phase Difference?

Coherence and phase difference (measured in angles) are linked by the fact that the average temporal consistency of the phase difference between two EEG time series (i.e., phase synchrony) is directly proportional to coherence. For example, when coherence is computed with a reasonable number of degrees of freedom (or smoothing) then the phase difference between the two time-series becomes meaningful because the confidence interval of phase difference is a function of the magnitude of the coherence and the degrees of freedom. If the phase angle is random between two time series then coherence = 0. Another way to view the relationship between phase consistency (phase synchrony) and coherence is to consider that if Coherence = 1, then once the phase angle relation is known the variance in one channel can be completely accounted for by the other. The phase relation is also critical in understanding which time-series lags or leads the other or, in other words the direction and magnitude of the difference.

However, when using circular statistics the mean phase angle or phase difference is relative to an arbitrary reference or starting point which is difficult to define with spontaneous EEG. Spontaneous EEG is perfectly useful because subjects are alert and holding themselves still or with no motion as a reference and the magnitude and direction of a shift in phase angle is all that is relevant (see section 15).

The phase difference is defined as:

$$\text{Eq. 19 - Phase difference (f)} = \text{Arctan} \frac{(\text{Smoothedquad spectrum}(f))}{(\text{Smoothed cos pectrum}(f))}$$

In the numerical example in Table II,

$$\text{Phase difference (or angle at 1.25 Hz)} = \text{Arctan } 0.031/0.073 = 22.7^\circ$$

Two oscillators are *frequency locked* when the first derivative of the phase difference has a stable periodic orbit even if there is a difference in phase between the two oscillators. Two oscillators are *entrained* when they are frequency locked in a 1:1 fashion with no phase difference. Two oscillators are phase locked where there is a stable phase difference that is not 1:1 (e.g., 2:3). Two oscillators are *synchronized* when they are phase locked independent of the absolute value of the phase difference, e.g., when the 1st derivative of the time series of phase ≈ 0 . Synchronization is *in-phase* when the phase difference = 0 and *out-of-phase* is when the phase difference $\neq 0$. Two oscillators are said to be synchronized in *anti-phase* when the phase difference = 180° . Frequency locking without phase locking is called *phase trapping*. The relationship between all of these definitions is depicted in figure 9.

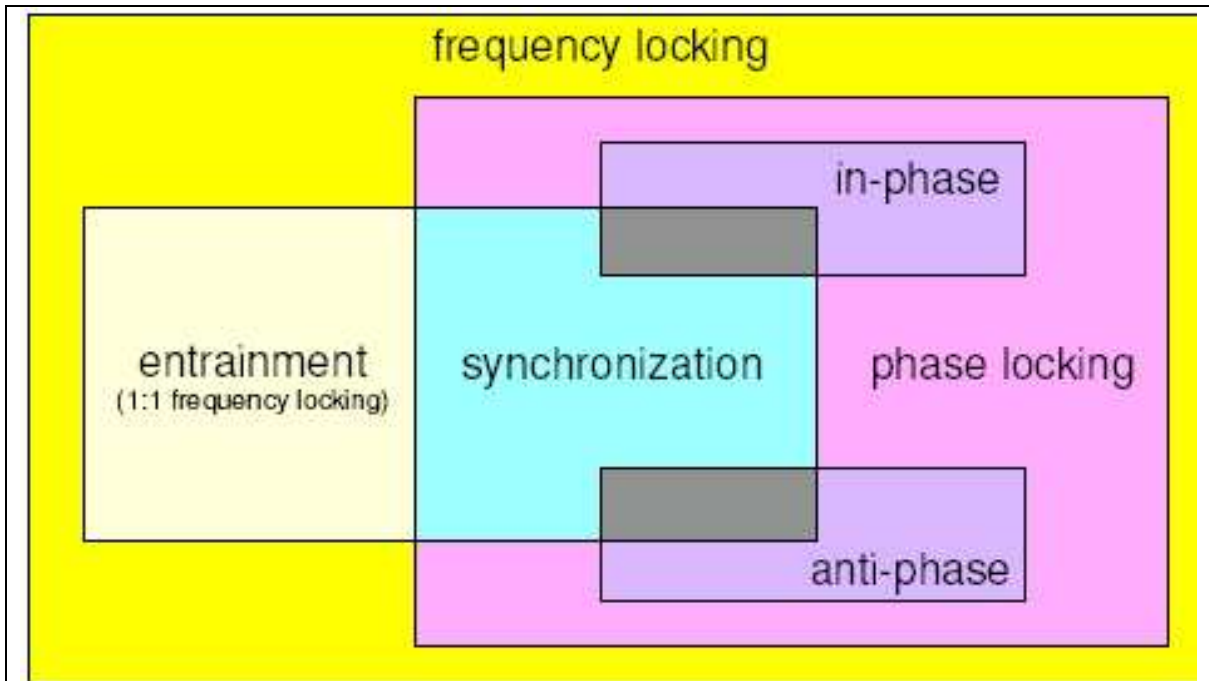


Fig. 9 – Various degrees and types of locking of oscillators. From Izhikevich and Kuramoto, 2005).

16 – What is Phase Resetting?

Coupled oscillators often drift apart in their phase relationship and a synchronizing pulse can shift the phase of one or both of the oscillations so that they are again in phase or phase locked for a period of time (Pikovsky et al, 2003). Synchrony is defined as “an adjustment of rhythms of self-sustaining oscillators due to their weak interactions” (Pikovsky et al, 2003). Phase reset marks the onset of phase locking. Phase locking and the term “entrainment” are synonymous. The amount of phase resetting per unit time is depicted by phase reset curves or $PRC = (\text{new phase} - \text{old phase})$. Positive values of the PRC correspond to phase angle advances, negative values correspond to phase angle reductions. Weak coupling typically exhibits a slow and smooth PRC whereas strong coupling between oscillators often results in abrupt or a discontinuous PRC. A useful method to measure phase resetting is by computing the first derivative of the time series of phase difference on the y-axis and time on the x-axis. A significant positive or negative first derivative of the time series of phase differences represents the magnitude of phase resetting (the second derivative of the phase shift is also useful in this computation). Phase reset is related to onset of phase synchrony or phase locking and the period of near zero 1st derivatives in time is an example of a homeostatic and stable dynamical system (Pikovsky et al, 2003; John, 2005). Two interesting properties of

phase reset are that minimal energy is required to reset phase between weakly coupled oscillators and phase reset occurs independent of amplitude. In weakly coupled chaotic systems amplitude can vary randomly while phase locking is stable.

Phase reset is defined as a significant positive or negative first derivative of the time series of phase difference between two channels, i.e., $d(\varphi_i - \varphi'_i)/t > 0$ or < 0 . Phase locked or phase synchrony is defined as that period of time where there is a stable near zero first derivative of the instantaneous phase difference between $d(\varphi_i - \varphi'_i)/t \approx 0$. A high coherence value is related to extended periods of phase locking. A significant positive first derivative of the time series of coherence marks the onset of phase locking and a significant negative first derivative of the time series of coherence marks the onset of phase dispersion over an interval of time. The significance level can be determined by computing the means and standard deviations of the first derivative for each time series and then computing a Z

score for each time point with alpha at $P < .05$ or $Z = \frac{u - x}{SD}$ where $u = \text{mean}$

and $x = \text{the instantaneous first derivative at } t$ and $SD = \text{standard deviation}$. For example, depending on the method of computation, values near zero st. dev. or < 1 st. dev may define the state of “Phase Locking”. Values > 2 st. dev. may define the state of “Phase Transition” or “Phase Reset” (the alpha threshold is a matter of observation and test).

Figure ten illustrates the concept of phase reset. Coherence is a measure of phase consistency or phase clustering on the unit circle as measured by the length of the unit vector r . The illustration in figure 10 shows that the resultant vector $r_1 = r_2$ and therefore coherence when averaged over time is constant even though there can be a shift in the phase

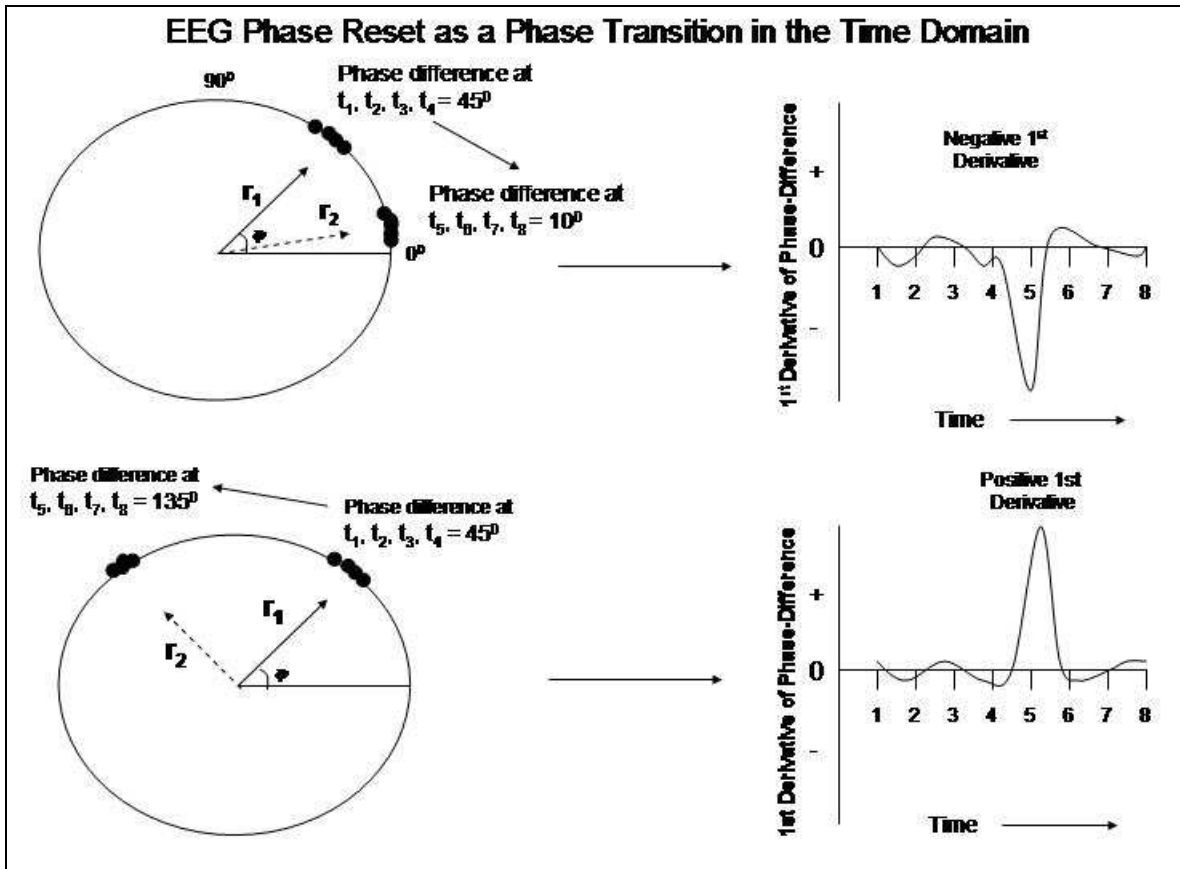


Fig. 10 – Illustrations of phase reset. Left is the unit circle in which there is a clustering of phase angles and thus high coherence as measured by the length of the unit vector r . The vector $r_1 = 45^{\circ}$ occurs first in time and the vector $r_2 = 10^{\circ}$ and 135° occurs later in time. The transition is between time point 4 and 5 where the 1st derivative is a maximum. The right displays are a time series of the approximated 1st derivative of the instantaneous phase differences for the time series t_1, t_2, t_3, t_4 at mean phase angle = 45° and t_5, t_6, t_7, t_8 at mean phase angle = 10° . Phase reset is defined as a significant negative or positive 1st derivative ($y' < 0$ or $y' > 0$). The 1st derivative near zero is when there is phase locking or phase stability and little change over time. The sign or direction of phase reset is arbitrary since two oscillating events are being brought into phase synchrony and represent a stable state as measured by EEG coherence independent of direction. The clustering of stable phase relationships over long periods of time is more common than are the phase transitions. The phase transitions are time markers of the thalamo-cortical-limbic-reticular circuits of the brain (John, 2005; Thatcher and John, 1977).

angle (i.e., phase difference) that occurs during the summation and average of the computation of coherence. This illustrates the advantage of phase differences which are “instantaneous” and not a statistical average like coherence and a correlation coefficient. Details for computing complex demodulation and instantaneous spectra are in Appendix-B.

As mentioned previously, an important property of phase reset is that

it requires essentially zero energy to change the phase relationship between coupled oscillators and by this process rapidly create synchronized clusters of neural activity. In addition to phase reset without any change in frequency or amplitude of the EEG spectrum is that it can also be independent of phase history. That is, phase reset occurs independent of magnitude and direction of the phase difference that existed before the onset of the reset pulse (Kazantsev et al, 2004). What is important in the computation of the first derivative of the time series of phase is the rate of change of phase over time and not the absolute magnitude of phase.

Figure 11 shows the relationship between phase differences using Cz as a reference and phase reset as measured by the 1st derivative of the phase difference time series.

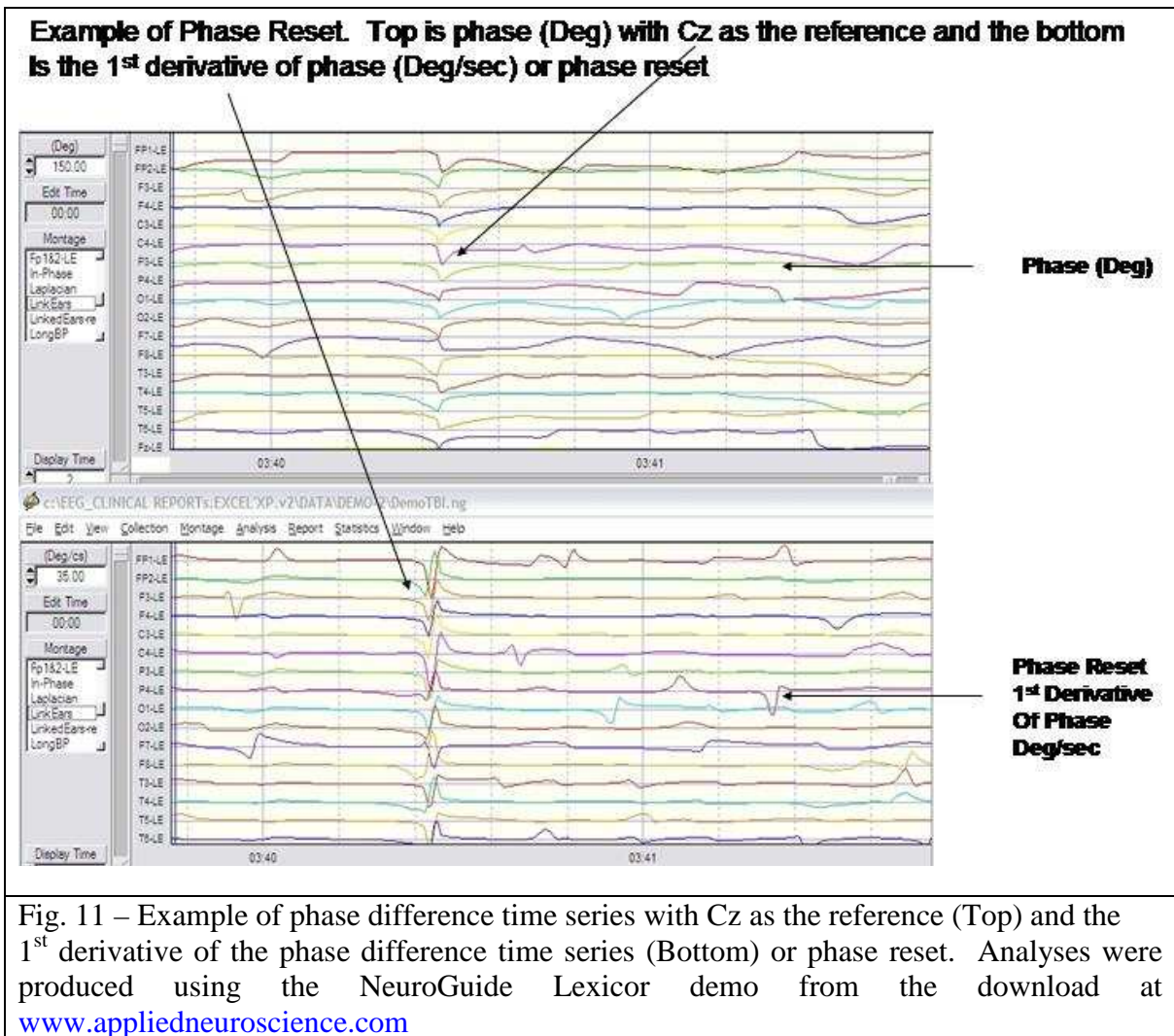


Figure 12 shows examples of phase synchrony or phase locking when the first derivative of the phase difference time series ≈ 0 and phase reset

when the 1st derivative of the phase difference time series $\neq 0$. Global phase reset is defined as $> 90\%$ of the channels exhibiting simultaneous phase reset and local phase reset is defined as 1 or a few channels exhibiting phase reset. The intervals of time between phase reset are periods of phase synchrony.

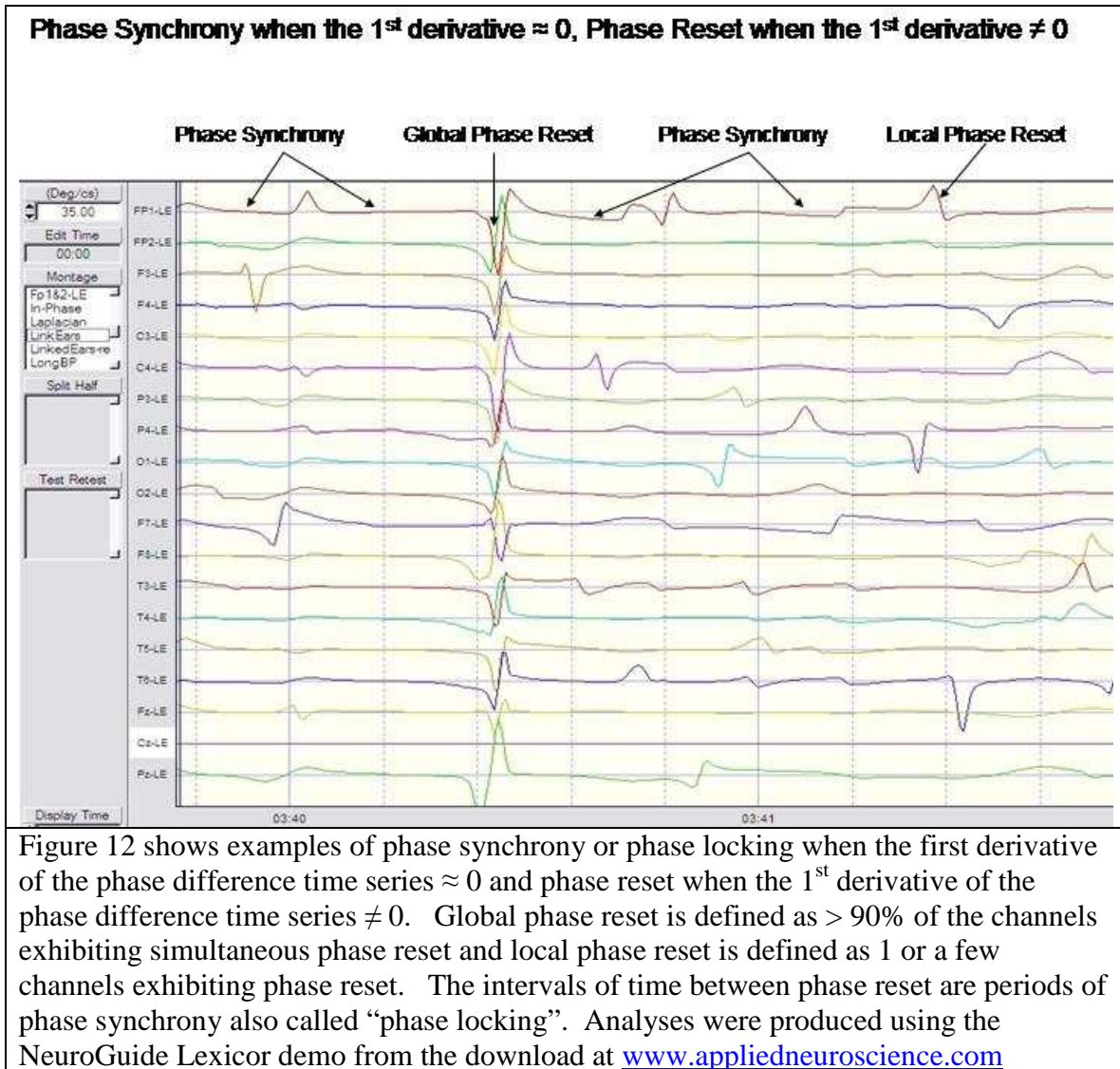


Figure 13 shows how to quantify phase reset by dissecting its two fundamental components, i.e., phase shift followed by phase locking.

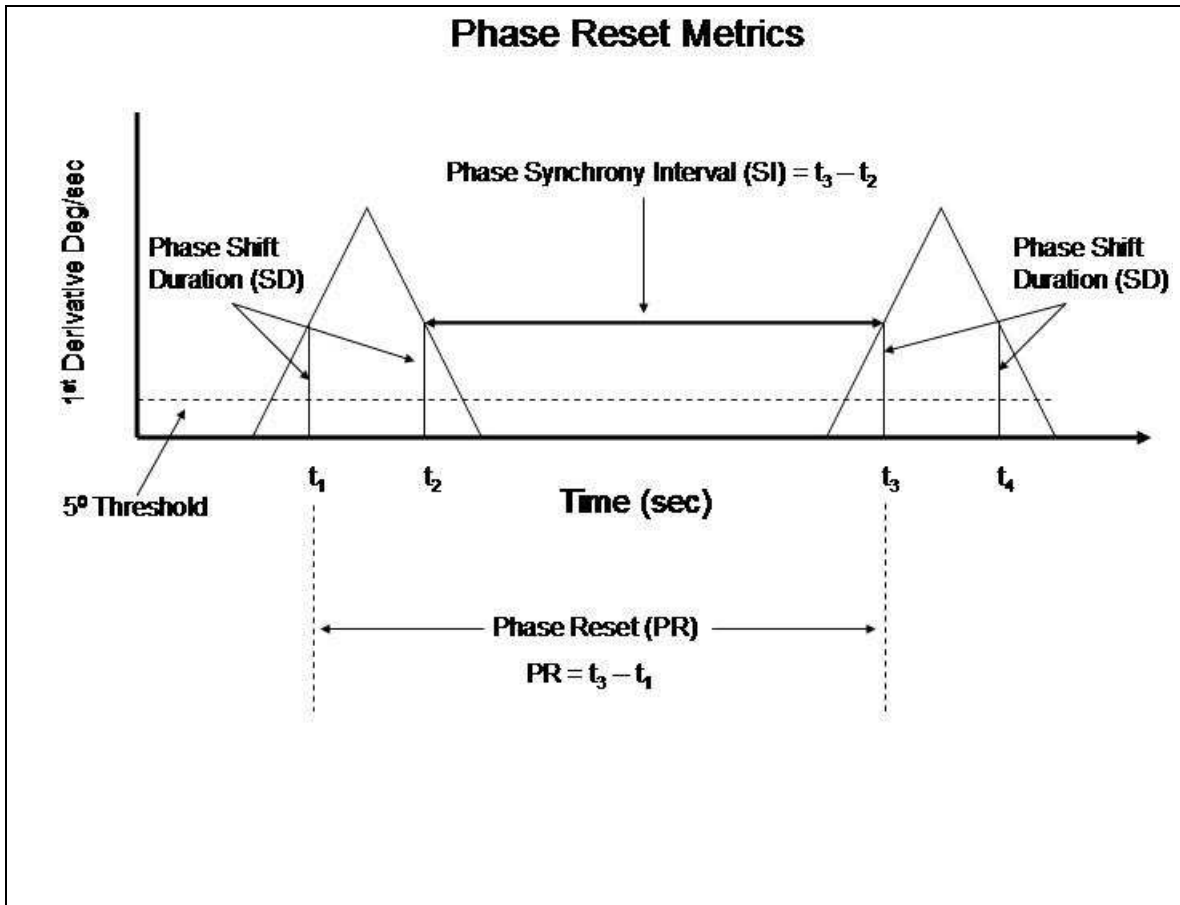


Fig. 13- Diagram of phase reset metrics. Phase shift (PS) onset was defined at the time point when a significant 1st derivative occurred ($\geq 5^\circ$ /centisecond), phase shift duration (SD) was defined as the time from onset to offset of the phase shift and the phase synchrony interval (SI) was defined as the interval of time between the onset of a phase shift and the onset of a subsequent phase shift. Phase reset (PR) is composed of two events: 1- a phase shift and 2- a period of synchrony following the phase shift where the 1st derivative ≈ 0 or $PR = SD + SI$. (from Thatcher et al, 2008a; 2008b)

17- How large should coherence be before Phase Difference can be regarded as stable?

As mentioned previously, the confidence interval for the estimation of the average phase angle between two time series is related to the magnitude of coherence. When coherence is near unity then the oscillators are synchronized and phase and frequency locked. This means that when coherence is too low, e.g., < 0.2 , then the estimate of the average phase angle may not be stable and phase relationships could be non-linear and not synchronized or phase locked. An example of a 30 degree phase angle using the NeuroGuide signal generation program is shown in figure 13:

10 μ V Signal + 30 degree Phase Shift & No Noise

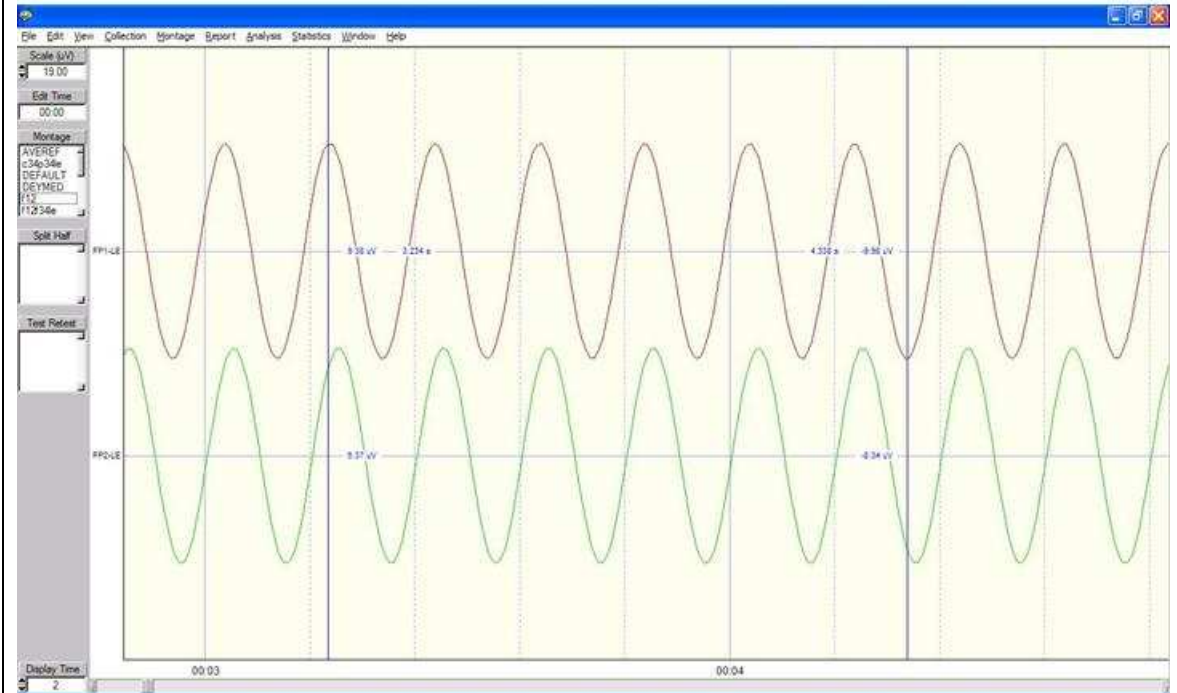


Fig. 13 shows an example of two 10 μ V sine waves with the second sine wave shifted by 30 degrees with increasing amounts of noise added to the signal in one channel (signal-to-noise ratio). The data is 60 seconds sampled at 128 Hz.(from Thatcher et al, 2004). Analyses were produced using the NeuroGuide Lexicor demo from the download at www.appliedneuroscience.com.

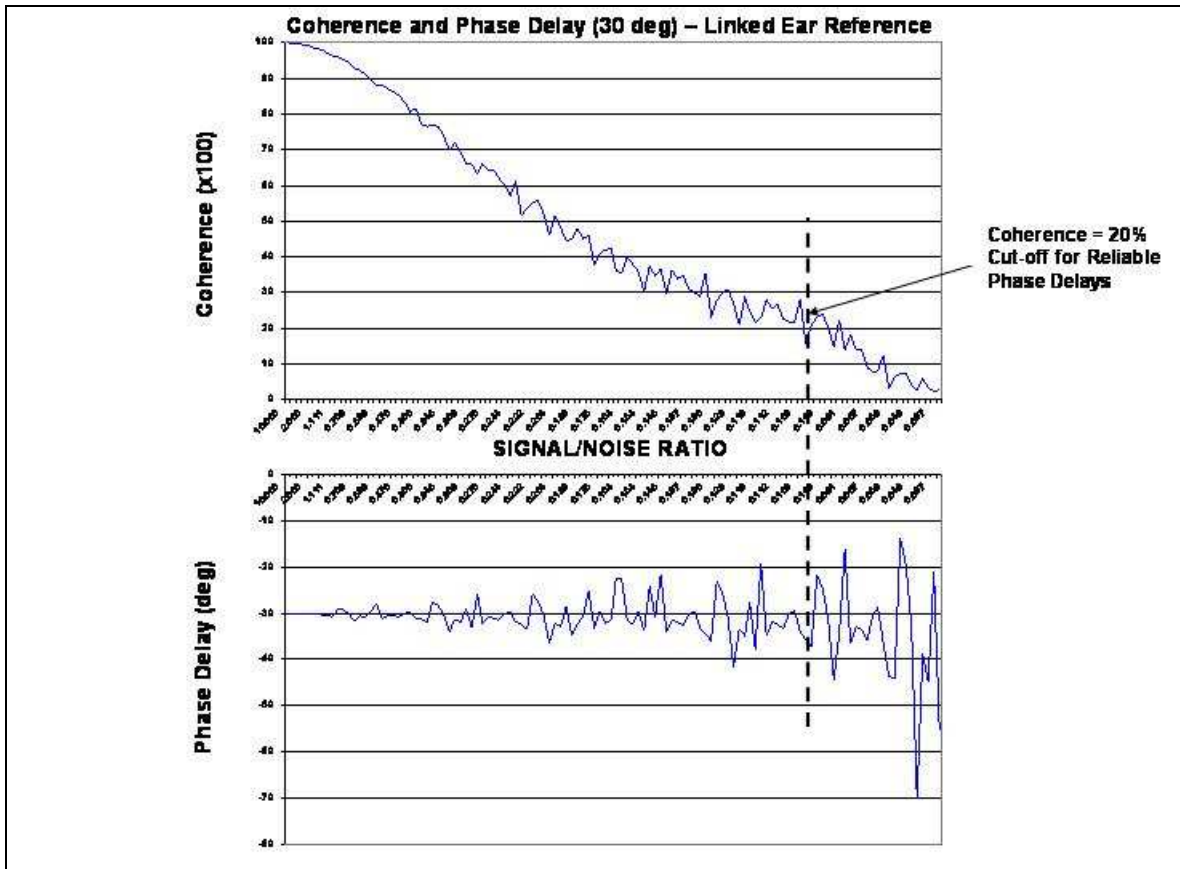


Fig – 14. Top is coherence (y-axis) vs signal-to-noise ratio (x-axis). Bottom is phase angle on the y-axis and signal-to-noise ratio on the x-axis. Phase locking is minimal or absent when coherence is less than approximately 0.2 or 20%.

Figure 14 (from Thatcher et al, 2004) shows increased variability of EEG phase angle or difference as noise is systematically added to the 30 degree shifted sine wave. Note that non-linear dynamical processes are suggested by the fact that the mean = 30 degrees when coherence < 0.2. Chaotic dynamics and reproducible correlations are often embedded in similar time data.

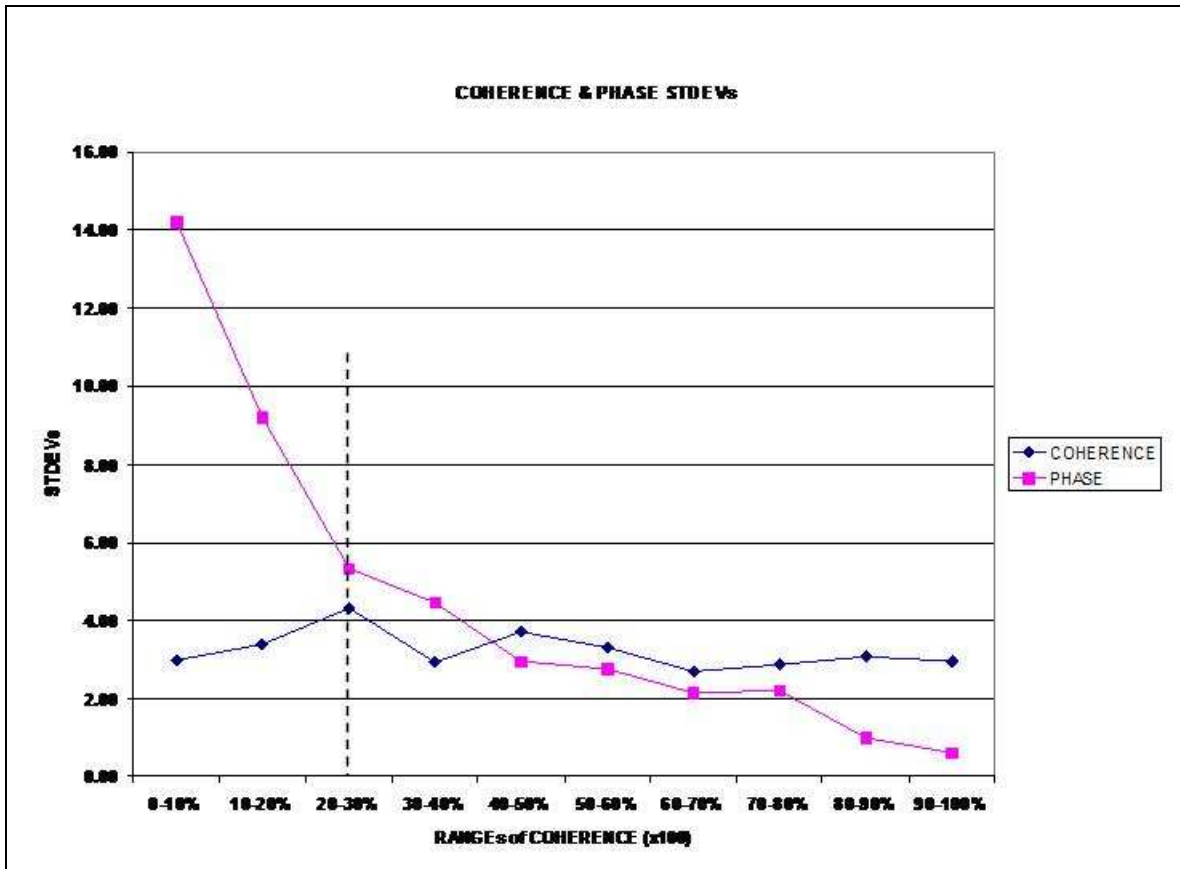


Figure 15 – The x-axis are different ranges of coherence (x100). The y-axis is the standard deviation of coherence (blue circles) and phase angles (pink squares). The dashed vertical line shows the level of coherence (20% or 0.2) when the variance of the phase angle becomes very high. High variance of the phase angle means that there is minimal or no phase locking.

Figure 15 (from Thatcher et al, 2004) shows that EEG coherence linearly decreases as a function of the signal-to-noise ratio. It can be seen that phase angles even with 248 degrees of freedom are unstable and poorly estimated as coherence decreases. EEG coherence at 0.2 or less is used as a cut-off for accepting phase as a valid and stable linear measure. The instability of a non-linear system may be present because the mean phase angle = 30 degrees when coherence is less than 0.2, see Figure 14.

The test signals were computed using the NeuroGuide signal generation program and by systematically increasing the amount of white “noise” added to one of the channels used to compute coherence and phase angle. In general, as the value of coherence decreases below approximately 0.2 or 20% (i.e., coherence x100) then phase angles are extremely variable and unstable even using 248 degrees of freedom.

The calculations exceed what is possible using a hand held calculator, however, computer simulations can produce results much faster than a hand calculator. The understanding of coherence and phase can be explored by any one who downloads the free NeuroGuide demo at: www.appliedneuroscience.com and tests coherence and phase for themselves.

18- Why the average reference and Laplacian fail to produce valid coherence and phase measures.

It is easy to understand why coherence is invalid when using an average reference since the summation of signals from all channels is “subtracted” or ‘added’ to the electrical potentials recorded at each electrode. Figure 16 below shows the results of the average reference where noise and signal from each channel is incorporated into all of the channels by being “subtracted” from the electrical potential recorded from each channel. Thus, signals and noise are mixed and added to the recordings from each channel making coherence and phase differences invalid. A similar situation prevails with source derivation or the Laplacian reference (Figure 17) since spatially weighted signals and noise from other channels are averaged and subtracted from the electrical potential recorded from each electrode site. Coherence when using the average reference or source derivation is especially sensitive to the presence of artifact or noise since the artifact will be mixed with and added to all channels.

Figure 16 are the results of the computation of EEG coherence and EEG phase differences using the average reference EEG simulation. The y-axis in figure 16 (top) is coherence and the x-axis is the signal-to-noise ratio (S/N). The y-axis in figure 16 (bottom) is phase difference (degrees) and the x-axis is the same signal-to-noise ratio (S/N) as in figure 14. It can be seen in Figure 16 that coherence is extremely variable and does not decrease as a linear function of signal-to-noise ratio. It can also be seen in Figure 16 that EEG phase differences never approximate 30 degrees and are extremely variable at all levels of noise.

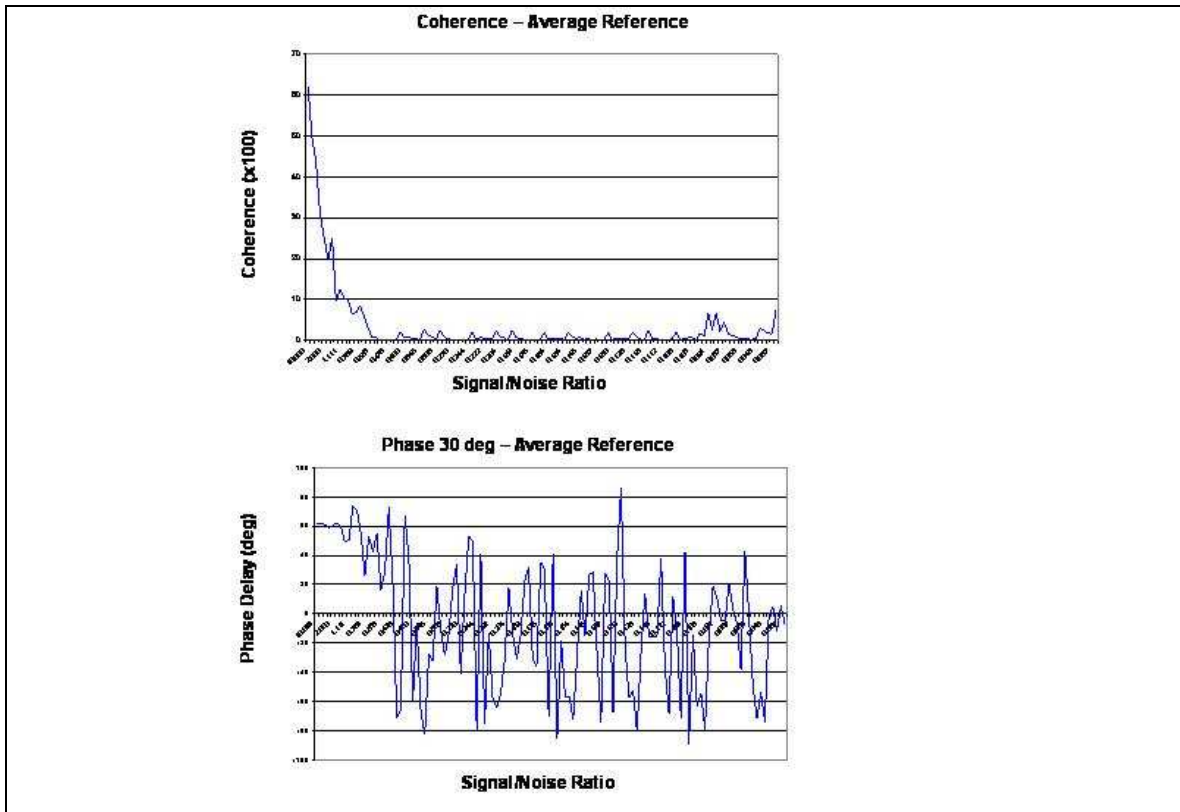
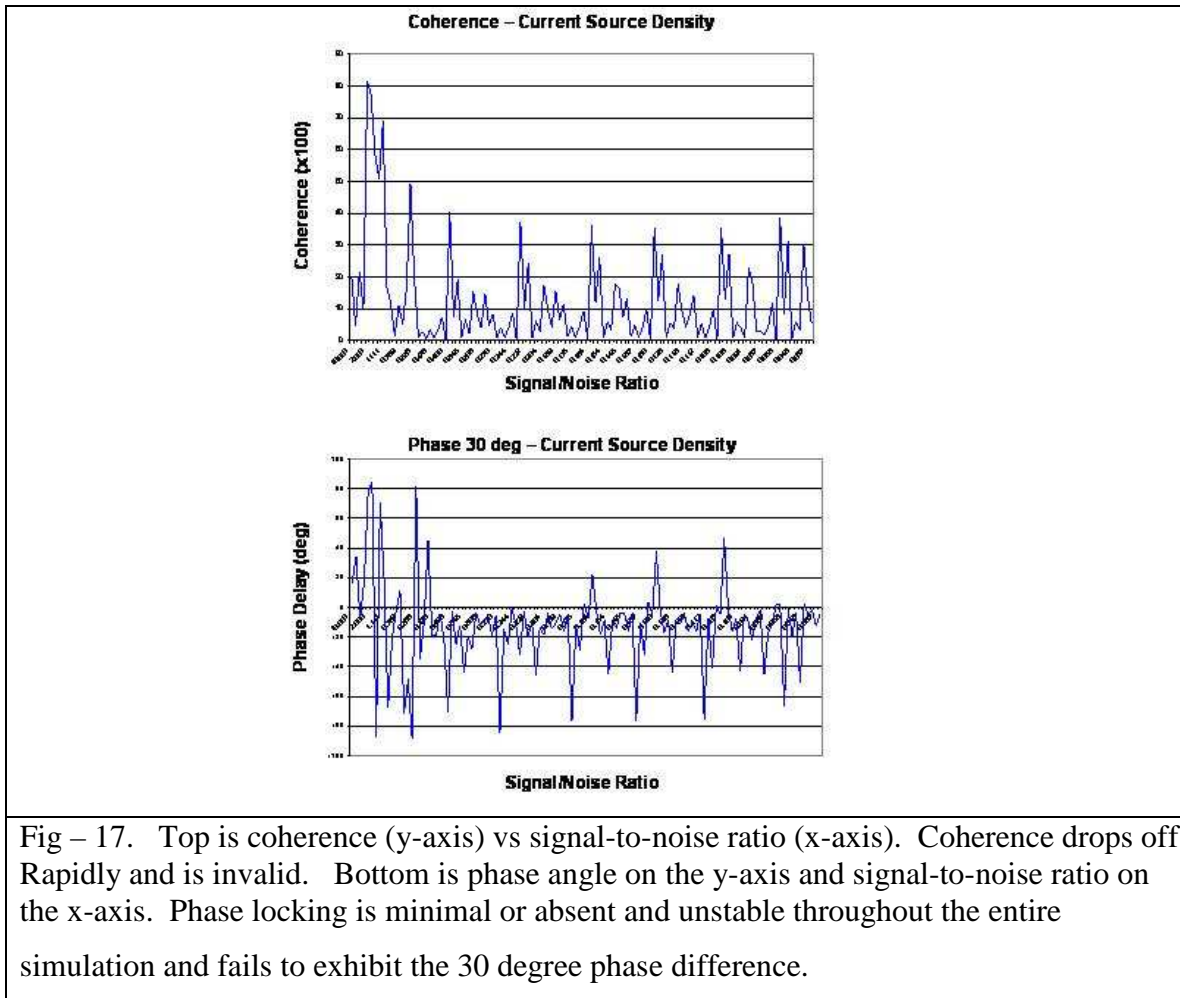


Fig – 16. Top is coherence (y-axis) vs signal-to-noise ratio (x-axis). Coherence drops off rapidly and is invalid. Bottom is phase angle on the y-axis and signal-to-noise ratio on the x-axis. Phase locking is minimal or absent and unstable throughout the entire simulation and fails to exhibit the 30 degree phase difference.

Figure 17 are the results of the computation of EEG coherence and EEG phase differences using the Laplacian reference EEG simulation. The y-axis in figure 17 (top) is coherence and the x-axis is the signal-to-noise ratio (S/N). The y-axis in figure 17 (bottom) is phase difference (degrees) and the x-axis is the same signal-to-noise ratio (S/N) as in figure 14. It can be seen in Figure 17 that coherence is extremely variable and does not decrease as a linear function of signal-to-noise ratio. It can also be seen in Figure 17 that EEG phase differences are invalid and never approximate 30 degrees with high variance at all levels of noise.



The results of these analyses are consistent with those by Rappelsberger, 1989 who emphasized the value and validity of using a single reference and linked ears in estimating the magnitude of shared or coupled activity between two scalp electrodes. The use of re-montage methods such as the average reference and Laplacian source derivation are useful in helping to determine the location of the sources of EEG of different amplitudes at different locations. However, the results of this study which again confirm the findings of Rappelsberger and Petsche, 1988 and Rappelsberger, 1989 which showed that coherence is invalid when using either an average reference or the Laplacian source derivation. This same conclusion was also demonstrated by Korzeniewska, et al (2003).

19- What is “Inflation” of Coherence (and correlation)?

Coherence inflation is defined as any value of coherence (x) greater than zero when coherence (or correlation) is computed using pure Gaussian noise in one of the two channels and a pure sine wave in the other channel.

Eq. 20- Coherence Inflation $\rightarrow x > 0$

This is the error term when one of the channels is pure Gaussian noise and the second channel is signal. Any value of coherence > 0 is due to error attributable to low degrees of freedom, inadequate signal resolution or too short of measurement interval, or improper sample rates within that interval, etc.

Figure 18 below shows an example of a 5 Hz 10uVsine wave in one channel and 100 uV (p-p) gaussian noise in the second channel. The power spectrum of the two channels is shown in the upper right panel. Figure 18 is just one example of the analyses performed by the NeuroGuide Signal Generator that directly test EEG simulated EEG cross-spectra.

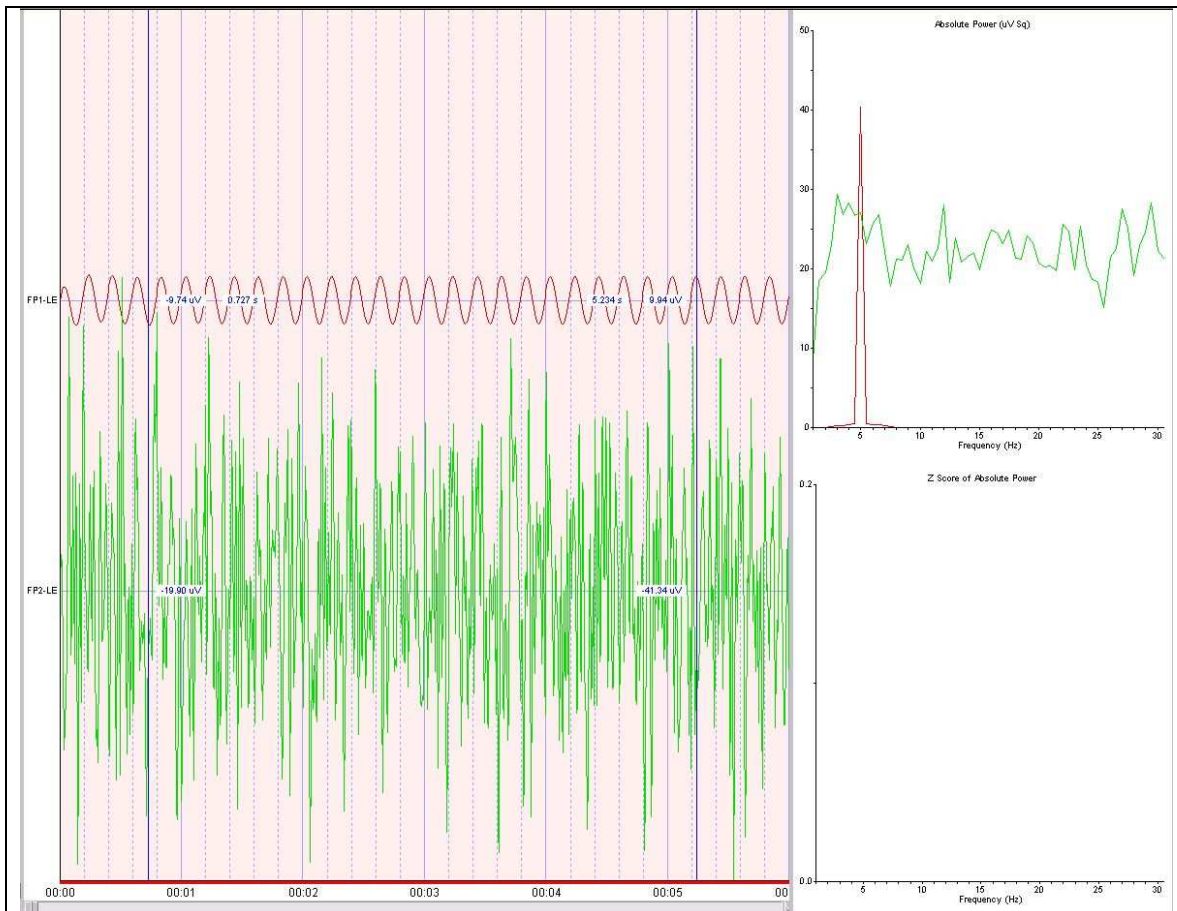


Figure 18. Screen capture of the NeuroGuide signal generation program.

Top trace is a 5 Hz 10 uV sine wave + 0 noise and the bottom trace is the mixture of a 5 Hz 10 uV sine wave + 100 uV Gaussian noise.

20- What are the limits of EEG Correlation, Coherence and Phase Biofeedback

As explained above, correlation and coherence requires averaging of time series data points in order to converge to an accurate estimate of shared activity between two time series. This means that correlation and coherence, unlike absolute power, are not instantaneous and always require time to compute. The most important factors in EEG correlation and coherence biofeedback are: 1- The band width, 2- Sample rate and , 3- Interval of time over which Averaging occurs.

Band width is directly related to the number of degrees of freedom. The wider the band width, the larger the number of degrees of freedom. However, with increased band width then there is reduced frequency resolution. In general, the standard band widths of EEG which are adequate such as theta (4 – 7.5 Hz), Alpha (8 – 12 Hz), Beta (12.5 – 22 Hz) and Gamma (25 – 30 Hz), etc. With narrow bandwidths, for example 0.5 Hz or 1 Hz then coherence will equal unity unless there are sufficient degrees of freedom to resolve true “signals” in the brain, which in the case of the human scalp EEG a 1,000 Hz sample rate is more than adequate.

Figure 19 below shows the results of tests using mixtures of signal and noise as in Figure 11 in which mean coherence is the Y – Axis as a function of sample rate (i.e., 512 Hz top left, 256 top right, 128 bottom left & 64 Hz bottom right). This figure will be replaced with a series of more clearly labeled figures in the next version of this paper. For the moment, accept the fact that the amount of time for averaging on the X - axis (125 msec., 250 msec., 500 msec. and 1,000 msec. results in lower coherence values, i.e., lower coherence inflation. This test involved computing coherence between one channel of pure sine waves (10 uV p-p) at different frequencies (theta, alpha, beta & gamma) and a second channel with pure Gaussian noise (also 10 uV p-p). It can be seen that the most important factor in determining coherence “Inflation” is the length of time for averaging. 1,000 msec. produces coherence = 0.1 (or 10%) inflation. Inflation is defined above as any value > 0 when pure Gaussian noise is in one of the channels. 500 msec produces coherence inflation = 0.2 (or 20%) inflation while 250 msec produces coherence inflation = 0.3 to 0.4 and 125 msec = 0.5 to 0.6 inflation. The coherence inflation is independent of band width, frequency and sample rate. The only critical factor is the interval of

time over which the average is computed, the longer the interval the lower the inflation.

The results of these analyses are that a minimum of a 500 millisecond difference is required when using EEG biofeedback in order to compute an accurate estimate of coherence or coupling between two time series. With a 500 millisecond average then the amount of inflation is relative low (e.g., 0.2 or 20%) and as long as the same interval of time of averaging is used with a normative database, then the Z scores of real-time coherence will be valid and accurate. As seen in Fig. 19 a sample rate of 1,000 produces even lower inflation, however, a 1 second difference between a brain event and the feedback signal may be too long for connection formation in a biofeedback setting.

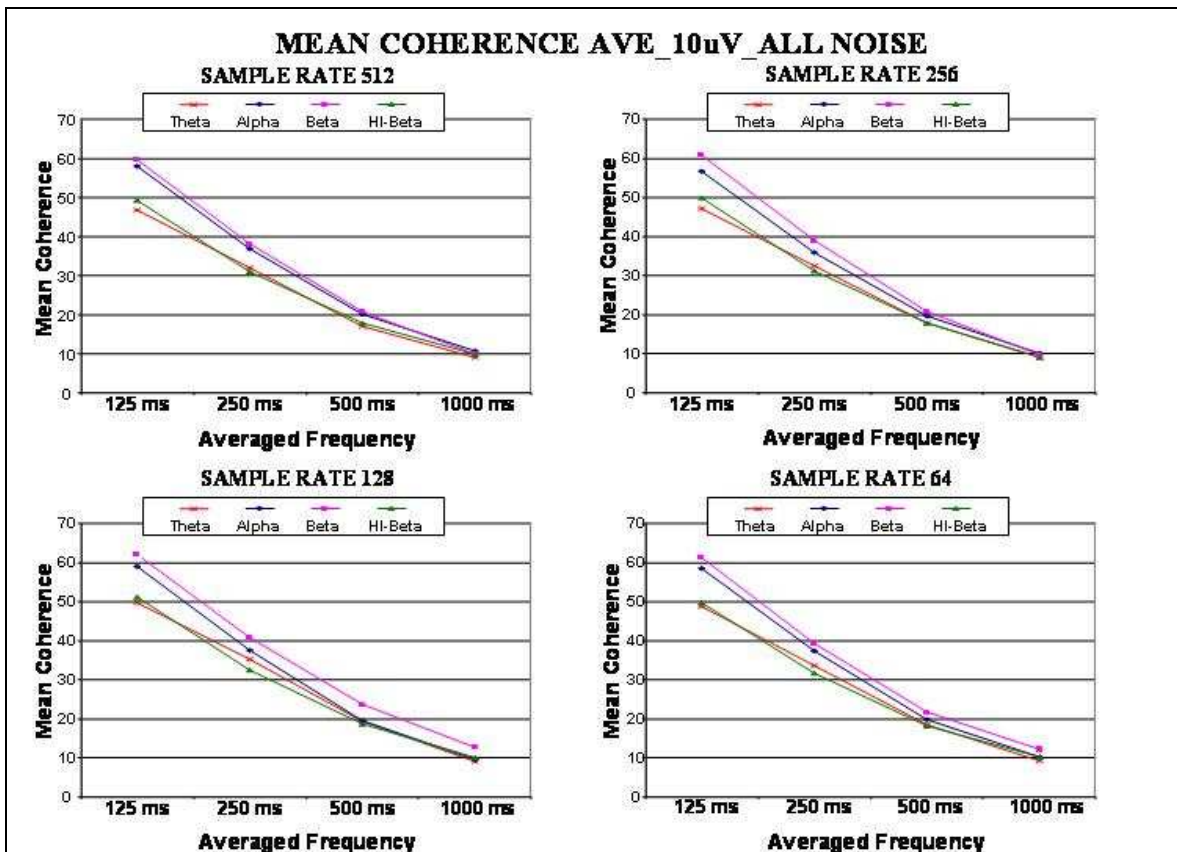


Figure 19. Mean coherence (y-axis) and the integration window size in milliseconds (x-axis). Top left is sample rate = 512 Hz, top right sample rate = 256 Hz, bottom left sample rate = 128 Hz and bottom left sample rate = 64 Hz. The amount of averaging from 125 msec. to 1,000 msec is the critical variable in minimizing “inflation” and not the sample rate.

Figure 20 below is the same as figure 19, but contains the standard deviations. A 500 msec. averaging delay = 0.15 standard deviation while 1,000 msec = 0.1 standard deviation. This figure shows that the choice of a 500 millisecond integration delay yields a reasonably stable estimate of coherence when using EEG biofeedback but that shorter intervals, such as 125 msec or 250 msec produce high inflation and high standard deviations and will not provide a valid “feedback” signal and thus less averaging will likely reduce neurotherapy efficacy.

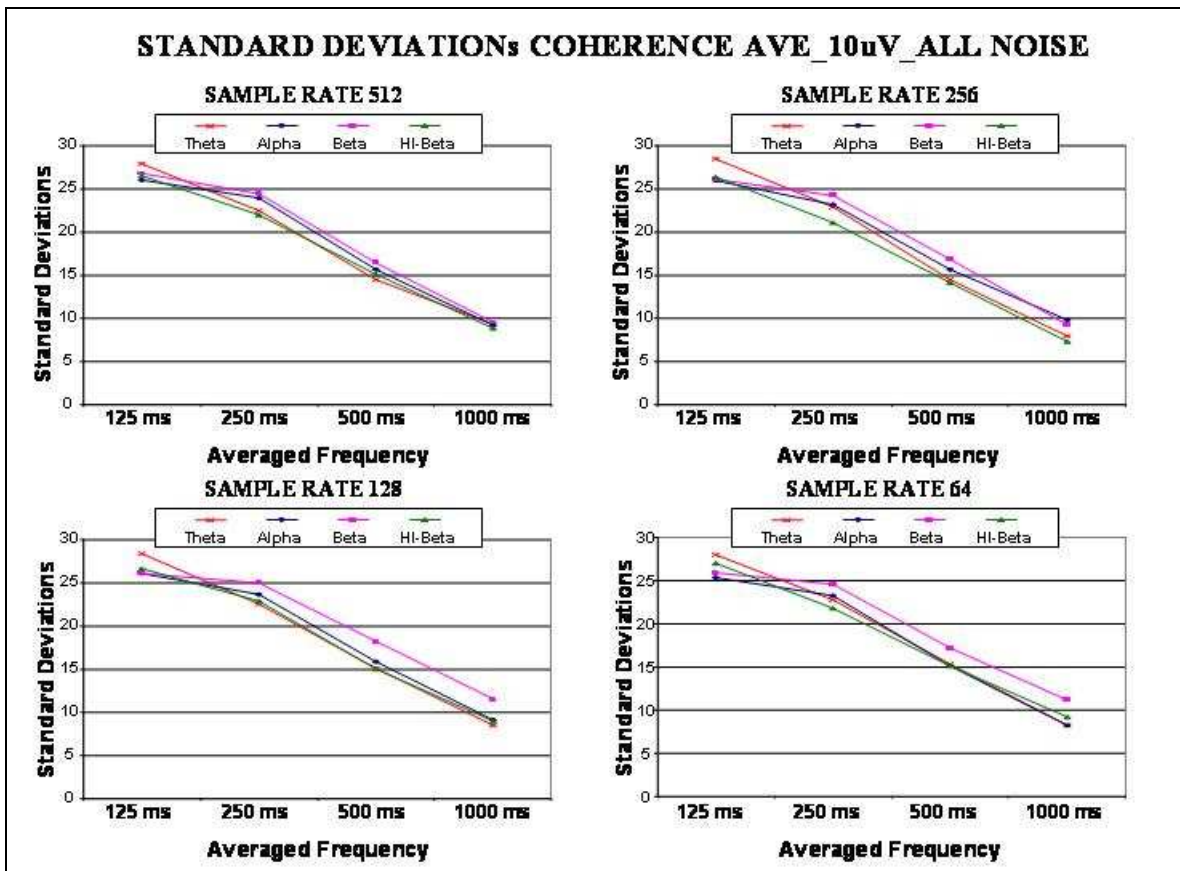


Figure 20. Standard deviations of coherence (y-axis) and the integration window size in milliseconds (x-axis). Top left is sample rate = 512Hz, top right sample rate = 256 Hz, bottom left sample rate = 128 Hz and bottom left sample rate = 64 Hz.

EEG phase is not the same as coherence and it can be computed instantaneously without averaging. Phase reset curves without averaging provide a detailed picture of the phase stability between coupled oscillators.

Nonetheless, “instantaneous” phase is variable and it is advisable to average the phase angles over intervals of time if greater stability is required especially when using Z score biofeedback.

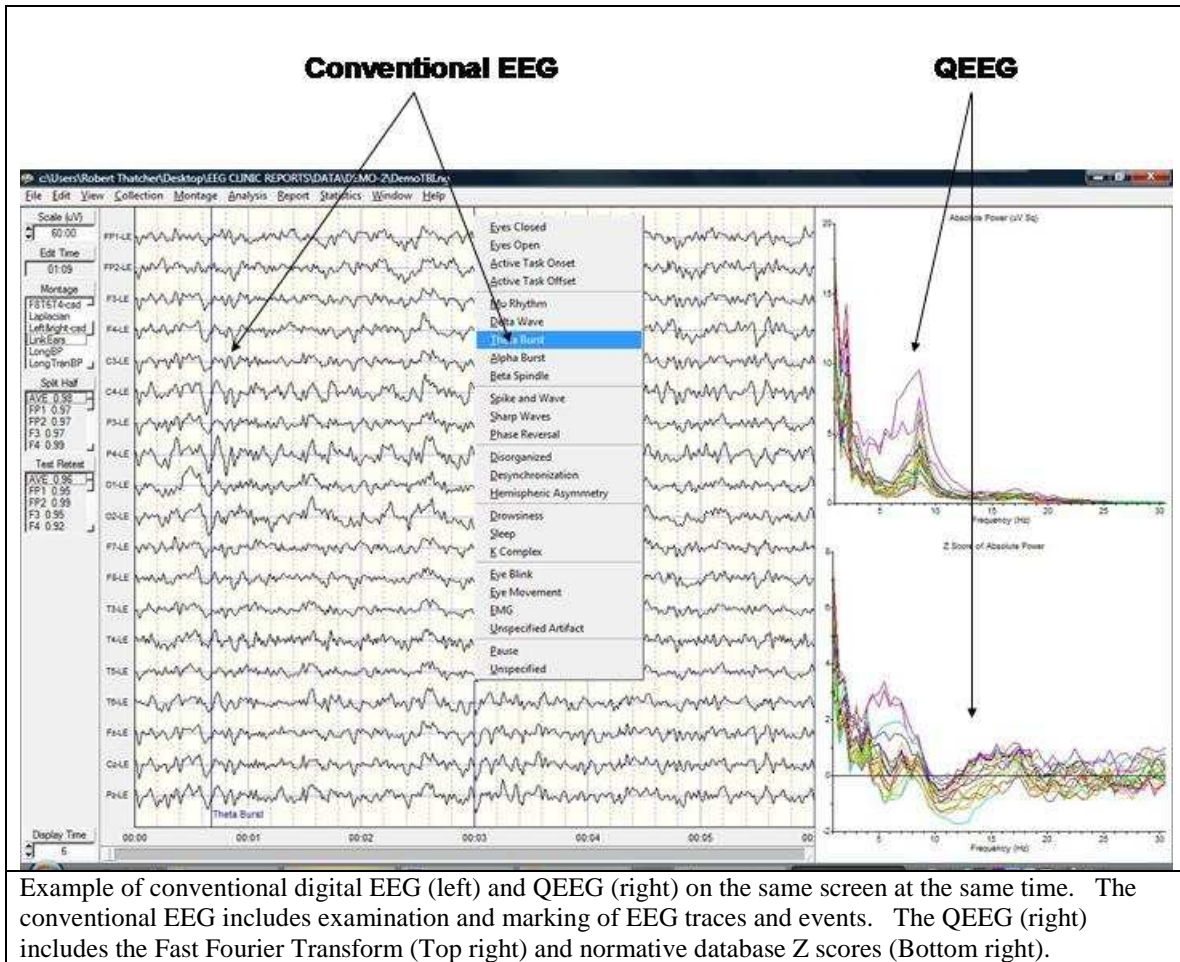
20A - 19 Channel EEG Biofeedback

This use of the EEG changed dramatically in the 1960s when computers were used to modify the EEG thru biofeedback, referred to today as Neurofeedback (NF). Studies by Fox and Rudell (1968); Kamiya (1971) and Serman (1973) were a dramatic departure from the classical use of conventional visual EEG and QEEG in that for the first time clinicians could consider treating a disorder such as epilepsy or attention deficit disorders and other mental disorders by using operant conditioning methods to modify the EEG itself. Thus, QEEG and EEG Biofeedback have a “parent-child” relationship in that EEG Biofeedback necessarily uses computers and thus is a form of QEEG that is focused on treatment based on the science and knowledge of the physiological meaning and genesis of the EEG itself. Ideally, as knowledge about brain function and the accuracy and resolution of the EEG increases, then EEG Biofeedback should change in lock step to better link symptoms and complaints to the brain and in this manner treat the patient based on solid science. To the extent the EEG can be linked to functional systems in the brain and to specific mental disorders then EEG Biofeedback could “move” the brain toward a healthier state (i.e., “normalize” the brain) (Thatcher 1998; 1999). Clearly, the clinical efficacy of EEG Biofeedback is reliant on knowledge about the genesis of the electroencephalogram and specific functions of the human brain. The parent-child relationship and inter-dependencies between QEEG and EEG Biofeedback is active today and represents a bond that when broken results in reduced clinical efficacy and general criticism of the field of EEG biofeedback. The traditional and logical relationship between QEEG and NF is to use QEEG to assess and NF to treat based on a linkage between the patient’s symptoms and complaints and functional systems in the brain. This parent/child linkage requires clinical competence on the one hand and technical competence with computers and the EEG on the other hand. Competence in both is essential and societies such as ISNR, SAN, ABEN, ECNS, BCIA, AAPB and other organization are available to help educate and test the requisite qualifications and competence to use EEG biofeedback. The parent/child link is typically optimized by following three steps: 1- perform a careful and thorough clinical interview and assessment of the patient’s symptoms and complaints (neuropsychological assessments are the most desirable), 2- conduct a QEEG in order to link the patient’s symptoms and complaints to functional systems in the brain as evidenced in fMRI, PET and QEEG/MEG and, 3- devise a EEG biofeedback protocol to address the de-regulations observed in the QEEG

assessment that best match the patient's symptoms and complaints. This approach reinforces the close bond between parent (QEEG) and child (Neurofeedback) and allows for the objective evaluation of the efficacy of treatment in terms of both behavior and brain function.

Figure one illustrates a common modern quantitative EEG analysis where conventional EEG traces are viewed and examined at the same time that quantitative analyses are displayed so as to facilitate and extend the analytical power of the EEG. Seamless integration of QEEG and Neurofeedback involves two basic steps: 1- visual examination of the EEG traces and 2- Spectral analyses of the EEG traces³. Numerous studies have shown a relationship between the time domain and frequency domain of an EEG time series and LORETA 3-dimensional source analyses which provide 7 mm³ maximal spatial resolution in real-time (Pascual-Marqui et al, 1974; Gomez and Thatcher, 2001) (see footnote 6). There is a verifiable correspondence between the time series of the EEG and the power spectrum and LORETA 3-dimensional source localization, for example, visual cortex source localization of hemiretinal visual stimulation, temporal lobe source localization of auditory simulation, theta source localization in the hippocampus in memory tasks, localization of theta in the anterior cingulate gyrus in attention tasks, linkage between depression and rostral and dorsal cingulate gyrus, etc.⁴ The number of clinical QEEG studies cited in the National Library of Medicine attests to the linkage between patient symptoms and functional systems in the brain and protocols for treatment are commonly guided by this scientific literature .

³ Spectral analysis includes space and time sequences that are transformed such as Joint-Time-Frequency-Analysis, FFT and all other methods that decompose EEG energies at different frequencies in space and time.



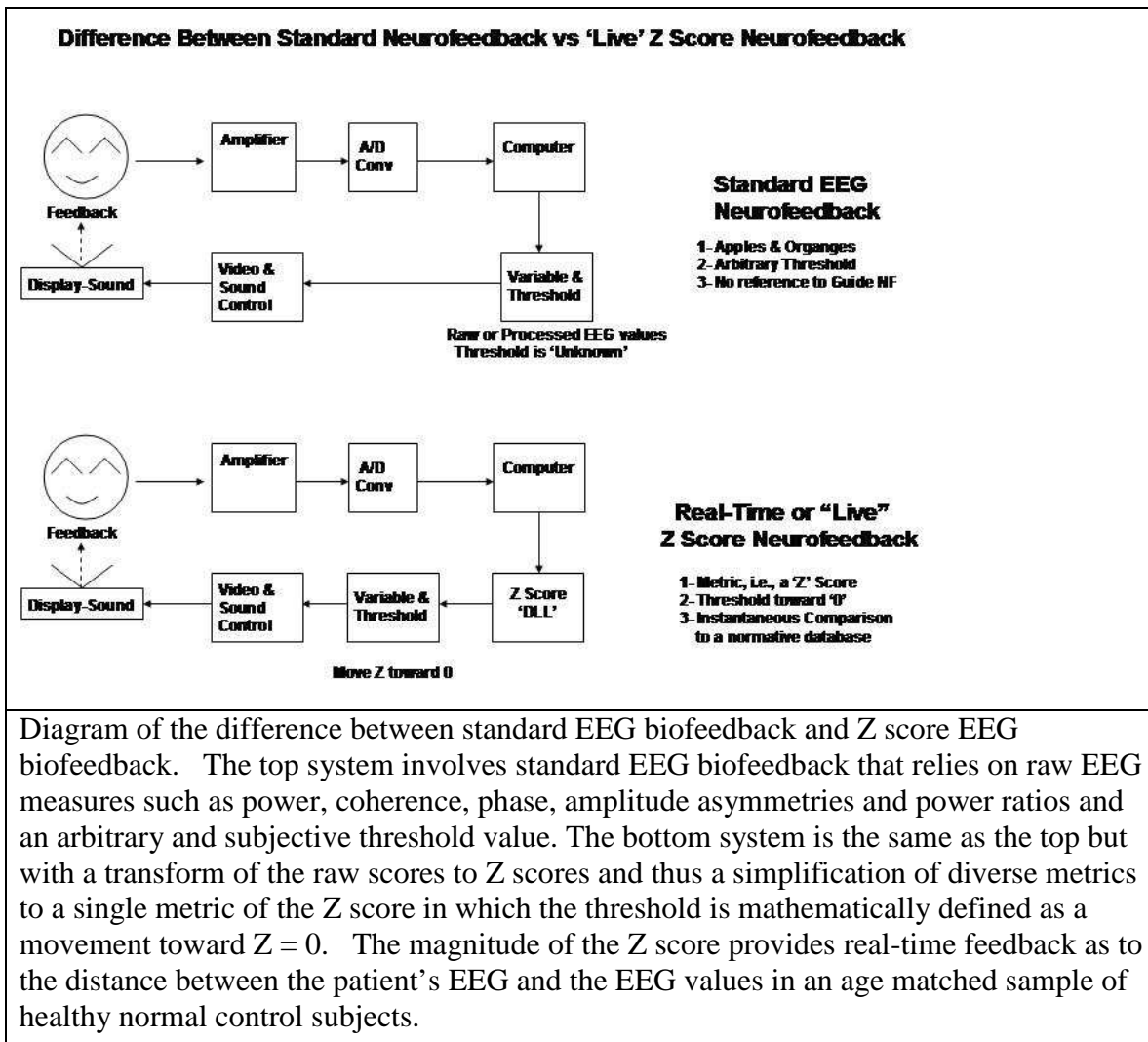
Example of conventional digital EEG (left) and QEEG (right) on the same screen at the same time. The conventional EEG includes examination and marking of EEG traces and events. The QEEG (right) includes the Fast Fourier Transform (Top right) and normative database Z scores (Bottom right).

The Use of 19 Channel Surface QEEG Z Scores and EEG Biofeedback

As described by Thatcher and Lubar (2008), scientists at UCLA in the 1950s (Adey et al, 1961) and later Matousek and Petersen (1973) were the first to compute means and standard deviations in different age groups and then Z scores to compare an individual to a reference normative database of means and standard deviations. The Z statistic is defined as the difference between the value from an individual and the mean of the normal reference population divided by the standard deviation of the population. John and colleagues (John, 1977; John et al, 1977; 1987) expanded on the use of the Z score and reference normal databases for clinical evaluation including the use of multivariate measures such as the Mahalanobis distance metric (John et al, 1987; John et al, 1988). For purposes of assessing deviation from normal, the values of Z above and below the mean, which include 95% to 99% of the area of the Z score distribution is often used as a level of confidence necessary to minimize Type I and Type II errors. The standard-score equation is also used to cross-validate a normative database which

again emphasizes the importance of approximation to a Gaussian for any normative QEEG database (Thatcher et al, 2003).

The standard concepts underlying the Z score statistic and QEEG evaluations were recently combined to give rise to real-time EEG Z score biofeedback, also referred to as “Live Z Score Biofeedback” (Thatcher 1998a; 1998b; 2000a; 2000b; Thatcher and Collura, 2006; Collura et al, 2009). The use of real-time Z score EEG biofeedback is another method to advance the integration of QEEG and Neurofeedback. The figure below illustrates the differences between raw score EEG biofeedback and real-time Z score EEG biofeedback.



There are several advantages of real-time Z score biofeedback including: 1- Simplification by reducing different metrics (power, coherence, phase, asymmetry, etc.) to a single common metric of the Z

score; 2- Simplification by providing a threshold and direction of change i.e., $Z = 0$ to move the EEG toward a normal healthy reference population of subjects,⁴ and 3- improved linkage between patient's complaints and symptoms and localization of functional systems in the brain. The next three figures show examples of how a symptom check list and QEEG evaluation are linked to give rise to a neurofeedback protocol.

Symptom Check List to Create Hypotheses for Neurofeedback

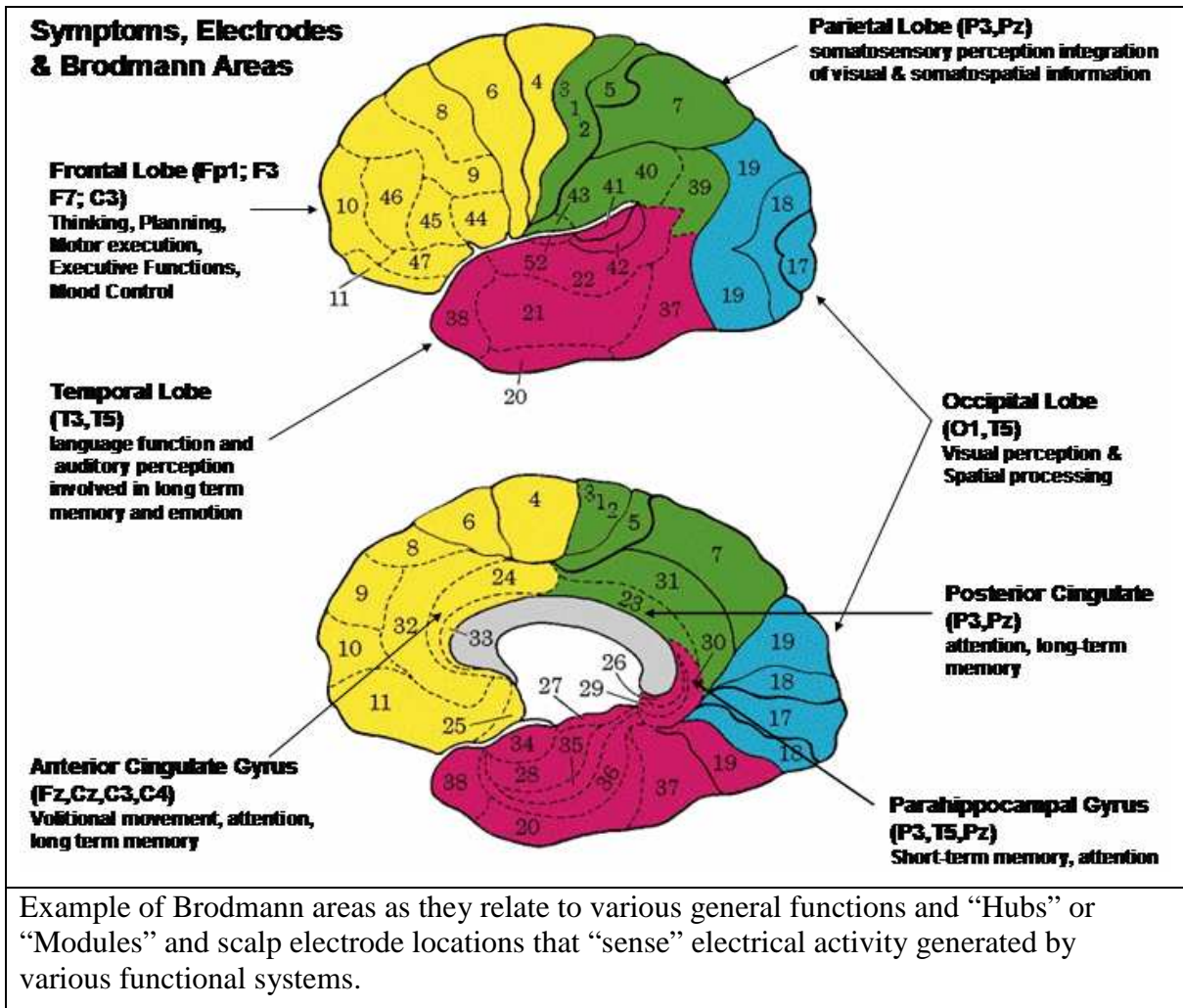
Symptom / Complaint	Severity	Channel	Region of Interest
Perception of Letters Problems	0	FP1	Angular-Super Parietal-Supramarginal Gyrus
Slow Reader	0	FP2	Anterior Cingulate
Problems with Spatial Perception	0	F3	Cingulate Gyrus
Orientation in Space	0	F4	Cuneus
Auditory Sequencing	0	C3	Fusiform Gyrus
Short-Term Memory Problems	0	C4	Inferior Frontal-Extra Nuclear Gyrus
Depression	0	P3	Inferior Parietal Lobule
Word Finding Problems	0	P4	Inferior Temporal Gyrus
Problems Multi-Tasking	0	O1	Inferior-Middle-Superior Occipital Gyrus
Poor Judgement	0	O2	Insula
Attention Deficits	0	F7	Lingual Gyrus
Hyperactive	0	F8	Medial Frontal-Subcallosal Gyrus
Skilled Motor Movements	0	T3	Middle Frontal Gyrus
Obsessive Thoughts	0	T4	Middle Temporal-SubGyral Gyrus

Example of a computer generated Symptom Check list in which the clinician first evaluates the patient's symptoms and complaints using clinical and neuropsychological tools and then enters a score of 0 to 10 based on the severity of the symptoms. Hypotheses as to the most likely scalp locations and brain systems are then formed based on the scientific literature that links symptoms and complaints to the locations of functional specialization. (From NeuroGuide 2.5.7)

Modules or “Hubs” are linked to various basic functional systems that are involved in cognition and perception (Hagmann et al, 2009; Chen et al,

⁴ Simultaneous suppression of excessive theta and reinforcement of deficient beta is achieved by using a absolute Z score threshold, which is a simplification compared to standard raw score EEG biofeedback. For example, if the threshold is set to an absolute value of $Z < 2$, then reduced theta amplitude and elevated beta amplitude will both be rewarded when the instantaneous EEG event exhibits a $Z < 2$ theta and beta power value.

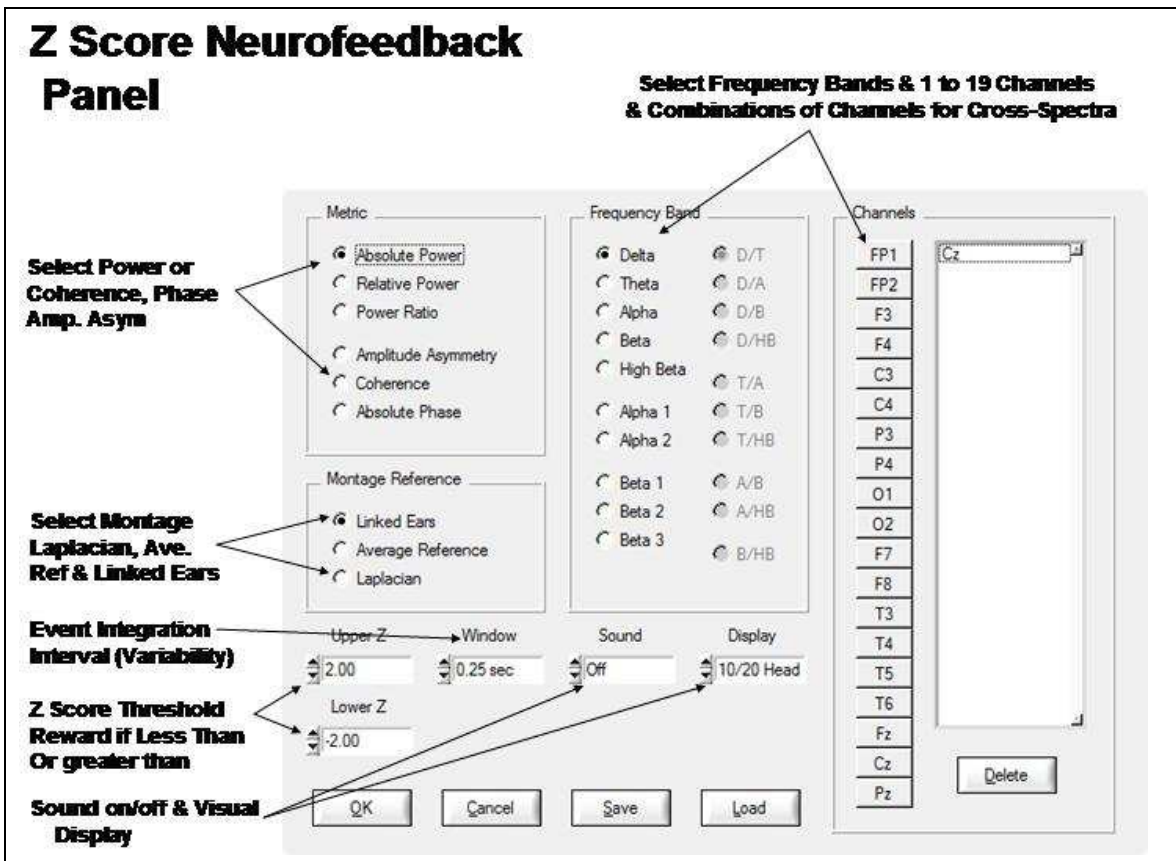
2008; He et al, 2009). Recent neuroimaging studies show that all of the various “modules” are dynamically linked and interactive and that sub-sets of neural groups in different modules “bind” together for brief periods of time to mediate a given function (Sauseng, and Klimesch, 2008, Thatcher et al, 2008a; 2008b). An illustration of Brodmann areas and electrodes as they relate to functional systems is shown in the figure below.



The linkage of a patient’s symptoms and complaints to the localization of functional systems in the brain is based on the accumulated scientific and clinical literature from QEEG, MEG, fMRI, PET and SPECT studies conducted over the last few decades as well as the basic neurological and neuropsychological lesion literature. The Russian neuropsychologist Alexandra Luria (1973) and the American neuropsychologist Hans-Lukas Teuber (1968) are among the leading scientists to make important linkages between symptoms and complaints and localization of functional systems in

matrix are the 19 channels of the 10/20 International electrode sites and the rows are symptoms and QEEG EEG features. Hypotheses are formed as to the most likely electrode site locations associated with a given symptom and complaint based on the scientific literature. The hypotheses are then tested based on QEEG and LORETA Z scores. Weak systems representing “loss of function” are identified when there is a match of QEEG Z scores with the hypothesized scalp locations based on symptoms. Compensatory locations are identified by a mismatch between hypothesized symptoms and complaints and the locations of observed QEEG Z scores. A suggested neurofeedback protocol is then produced based on the locations of the “weak” systems.

Figure below is an example of a 19 channel surface EEG biofeedback setup screen in Neuroguide where users can select a wide variety of measures or metrics all reduced to the single metric of the Z score. This includes, power, coherence, phase differences, amplitude asymmetries, power ratios and the average reference and Laplacian montages. 19 channels is a minimum number of channels in order to compute accurate average references and the Laplacian montage which is an estimate of the current density vectors that course at right angles thru the skull.



Example of 19 channel surface EEG Z score biofeedback setup screen inside of Neuroguide.

Multiple frequencies and multiple metrics may be selected in which a threshold must be reached before a visual and/or auditory reward is given (e.g., $Z < 2.0$). The 19 channel Z score approach provides for seamless integration of QEEG assessment and 19 channel Z score neurofeedback or treatment. Because there are approximately 8,000 possible instantaneous Z scores, it is important to limit and structure the biofeedback protocol in a manner that best links to the patient's symptoms and complaints. The linkage of patient's symptoms and complaints as hypotheses that are confirmed or disconfirmed by QEEG assessment are used to develop a neurofeedback protocol. Blind and random selection of Z score metrics runs the risk of altering "compensatory" systems and not focusing on the weak or "loss of function" systems that are linked to the patient's symptoms and complaints.

The figure below shows an example of a simple 10/20 head display for feedback where the circles turn green when threshold is met (e.g., $Z < 2.0$) and provides feedback about the scalp locations that are meeting threshold.

Neurofeedback Reinforcement Window – Can Be Moved to a 2nd Monitor

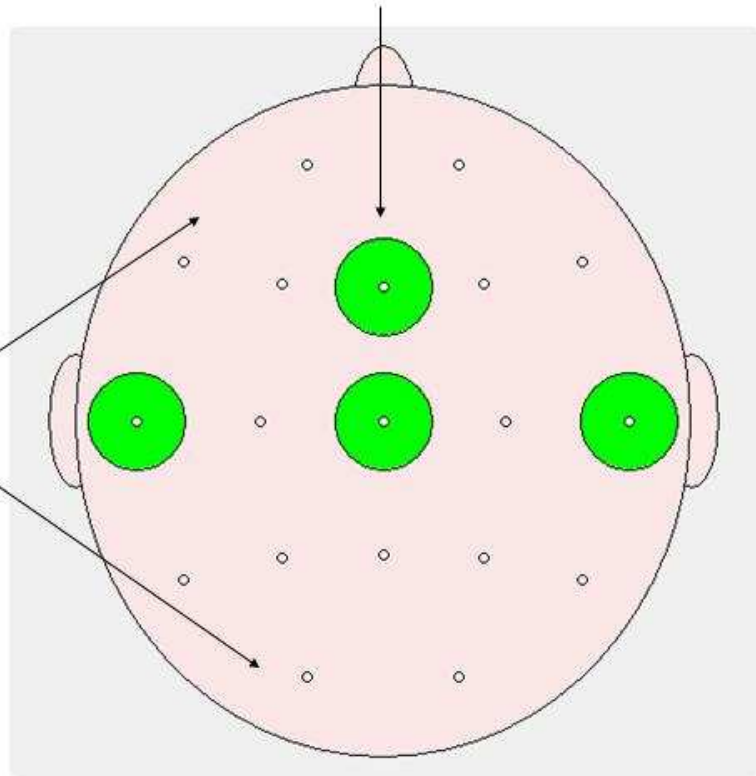
Threshold is < Z value set in the Surface NF Window

Reinforcement requires that 100% of the time points in a 250 msec to 1 sec window are less than the Z threshold

10/20 Scalp Locations

Sound feedback can be used Simultaneous with visual Feedback or alone for eyes Closed conditions

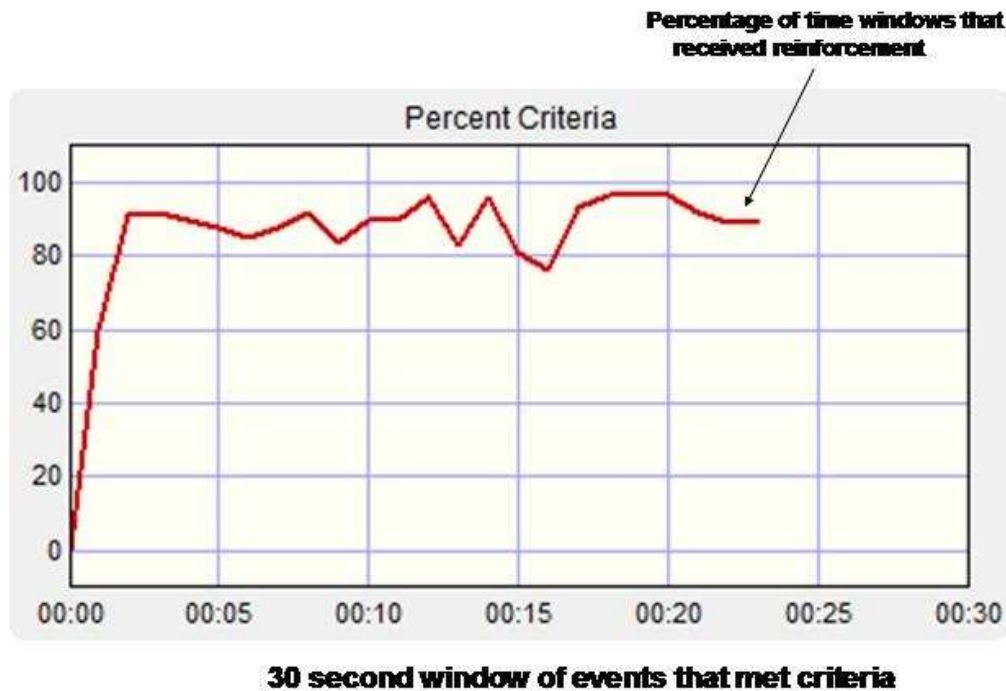
Green = Threshold was reached



Example of 19 channel feedback display. The circles at a particular location turn green when threshold is reached, e.g., $Z < 2.0$

The figure below is an example of a progress monitoring chart that is displayed for the clinician during the course of biofeedback. One strategy is to develop a protocol based on the linkage to the patient's symptoms and complaints as discussed previously and then to set the Z score threshold so that it is easy for the subject to meet threshold and thus produce a high rate of successful 'Hits' or rewards. Step two is to lower the threshold and make the feedback more difficult, e.g., $Z < 1.5$ and as the patient or client gains control and receives a high rate of reinforcement to again the lower the threshold, e.g., $Z < 1.0$ in a "shaping" process in which operant conditioning is used to move the patient's brain metrics toward the center of the normal reference population or $Z = 0$.

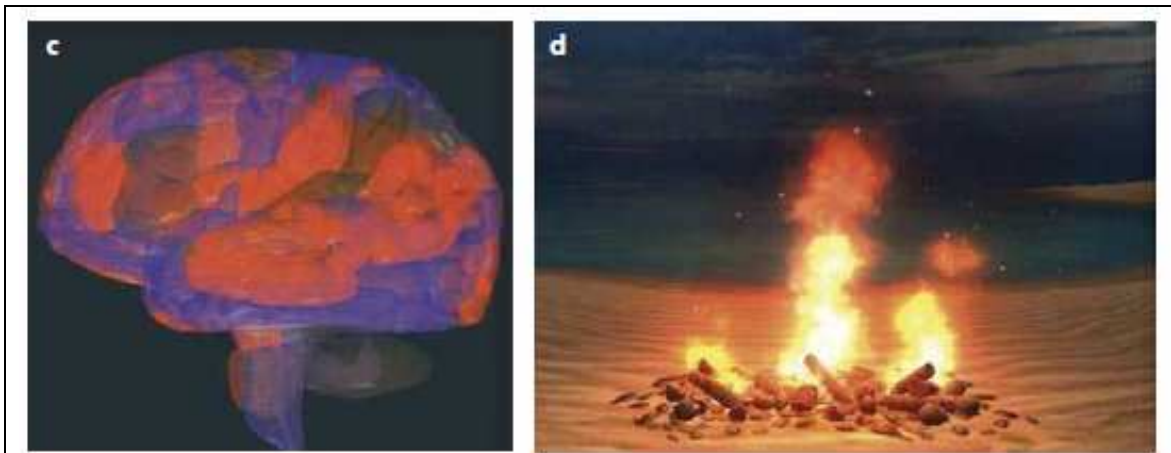
Neurofeedback Progress Window – Monitor the Client/Patient's Progress



Example of one of the progress charts that a clinician views during the course of neurofeedback. The idea is to shape the patient's brain toward the center of the normal healthy reference population where $Z = 0$. Initially the threshold is set so that the patient receives a high rate of reinforcement, e.g., $Z < 2.0$, then to lower the threshold and make it more difficult, e.g., $Z < 1.5$ and then as the patient again receives a high rate of reinforcement to again lower the threshold, e.g., $Z < 1.0$ so as to shape the brain dynamics using a standard operant conditioning procedure.

NeuroImaging Neurofeedback or Real-Time LORETA Z Score Biofeedback

Improved accuracy in the linkage between a patient's symptoms and complaints and the localization of functional systems can be achieved by the biofeedback of real-time 3-dimensional locations or voxels in the brain. This method has been successfully implemented with functional MRI (i.e., fMRI) for chronic pain, obsessive compulsive disorders and anxiety disorders (Apkarian, 1999; Yoo et al, 2006; Weiskopf et al, 2003; Cairia et al, 2006; Bray et al, 2007; de Charms et al, 2004; de Charms, 2008). The figure below shows an example of fMRI biofeedback displays



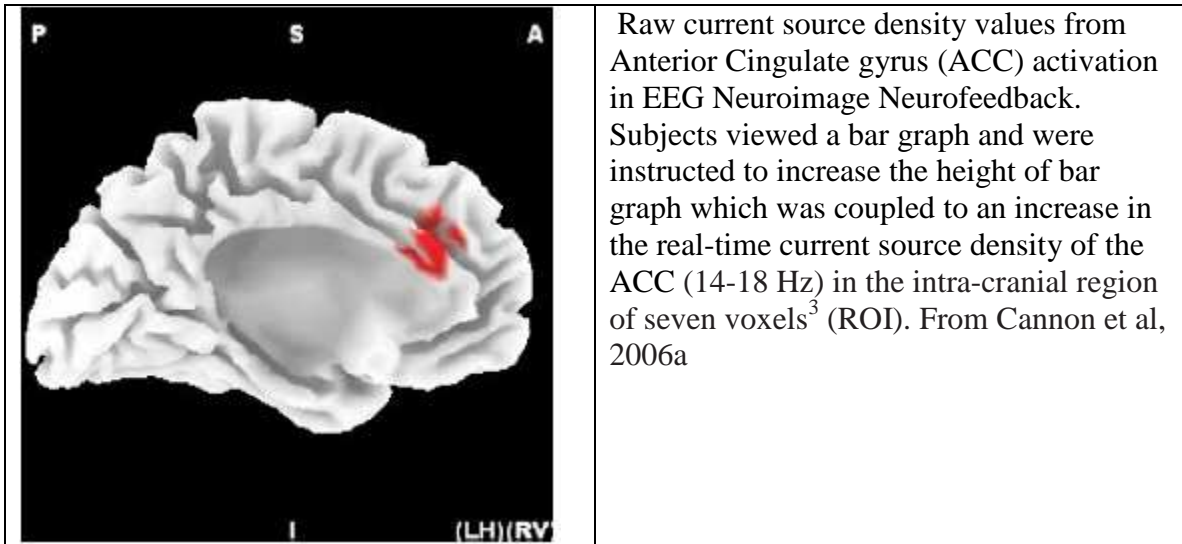
Information from individual spatial points can be segregated into multiple anatomically defined three-dimensional regions of interest. Here the activation levels (represented as colours) of three brain regions are rendered on a translucent 'glass brain' view. **(d)** - Activation in these regions can either be plotted second-by-second in real time or can be presented to subjects in more abstract forms, such as this virtual-reality video display of a beach bonfire, in which each of the three elements of the flickering fire corresponds to activation in a particular brain region. Brain activation can control arbitrarily complex elements of computer-generated scenarios. (From de Charms, 2008).

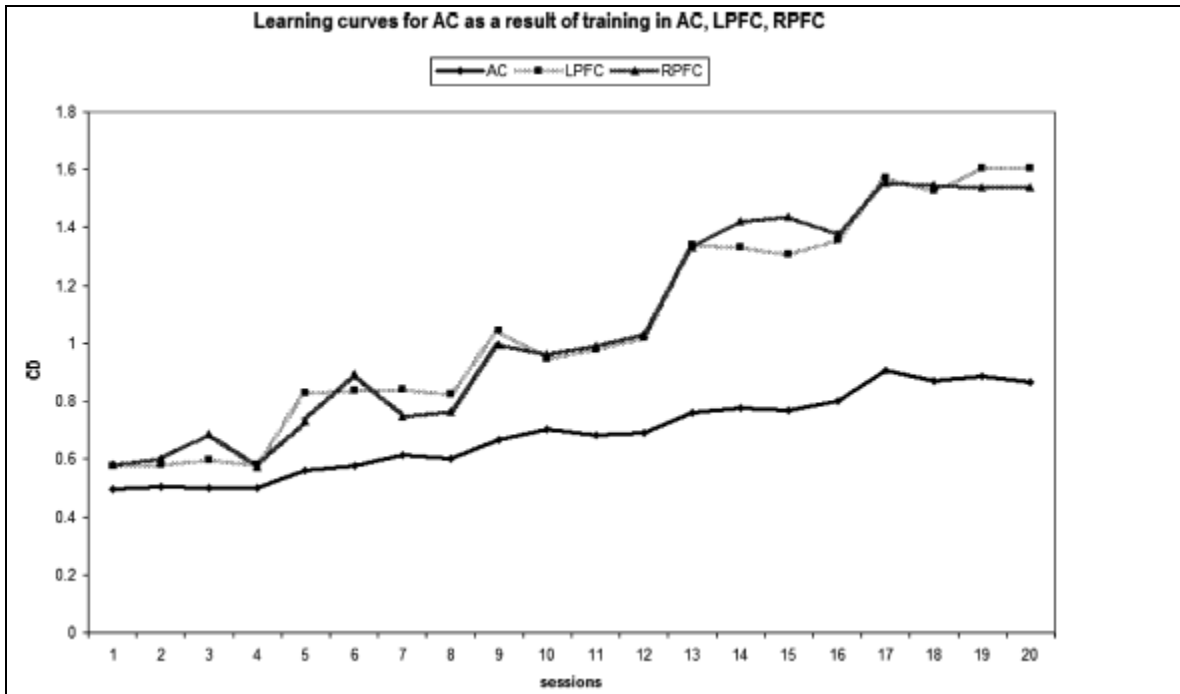
However, fMRI biofeedback also referred to as Neuroimaging Therapy has several significant limitations in comparison to LORETA 3-dimensional EEG biofeedback⁵: 1- A long time delay between a change in localized brain activity and the feedback signal, e.g., 20 seconds to minutes for fMRI while LORETA EEG biofeedback signals involve millisecond delays; 2- fMRI only provides indirect measures of neural activity because blood flow changes are delayed and secondary to changes in neural activity whereas EEG biofeedback is a direct measure of neural electrical activity and, 3- Expense in which fMRI costs 3 million dollars for the MRI machine plus \$30,000 per month for liquid helium whereas EEG biofeedback equipment and maintenance costs are less than \$10,000. The spatial resolution of LORETA source localization is approximately 7 mm^3 which is comparable to the spatial resolution of fMRI.⁶ fMRI, however, offers the

⁵ LORETA means "Low Resolution Electromagnetic Tomography" (Pascual-Marqui et al, 1994). Since the inception of this method in 1994 there have been over 500 peer reviewed publications (see <http://www.uzh.ch/keyinst/NewLORETA/QuoteLORETA/PapersThatQuoteLORETA05.htm> for a partial listing of this literature).

⁶ The voxel resolution of LORETA is 7 mm^3 which is adequate spatial resolution because the Brodmann areas are much greater in volume than 7 mm^3 . Also, the biological resolution of functional MRI may be worse than LORETA because it depends on the vascular architecture of the brain. For example, Ozcan et al (2005) showed that maximal fMRI spatial resolution is $> 12 \text{ mm}^3$.

advantage of imaging of non-cortical structures such as the striatum, thalamus, cerebellum and other brain regions where as QEEG is limited to imaging of cortical dipoles produced by pyramidal cells. Nonetheless, even with this limitation several studies have proven that biofeedback using LORETA real-time 3-dimensional sources is feasible and results in positive clinical outcomes (Lubar et al, 2003; Cannon et al, 2005; 2006a; 2006b; 2007; 2008). The next two figures shows examples of LORETA EEG biofeedback of the anterior cingulate gyrus and corresponding increases in current density as a function of biofeedback sessions.





Increase in current density (14–18 Hz) from three different ROIs, resulting from training of the Anterior Cingulate gyrus (AC). LPFC = left pre-frontal cortex; RPF = right pre-frontal cortex. The AC appears to influence increases in the LPFC & RPF higher than the increase for itself although all three ROIs increased current density as a function of training. Corresponding improvements in working memory and attention were also measured. From Cannon et al, 2009.

21 – Coherence, Phase and Circular Statistics

Phase angle has an intrinsic discontinuity, for example consider the linear and circular distributions of 360 equidistant points. In the linear distribution 0 and 360 are at opposite ends while in the circular distribution $0^0 = 360^0$ (Jammalamadaka and SenGupta, 2001). To evaluate phase angles it is necessary to use vector algebra and compute a mean vector with magnitude or length r , and a direction Θ and to calculate the average x and y components of the mean vector:

$$\text{Eq. 21 - } \bar{x} = \frac{1}{n} \sum_{i=1}^n [\sin(\alpha_1) + \sin(\alpha_2) + \sin(\alpha_3) + \dots \sin(\alpha_n)]$$

$$\text{Eq. 22 - } \bar{y} = \frac{1}{n} \sum_{i=1}^n [\cos(\alpha_1) + \cos(\alpha_2) + \cos(\alpha_3) + \dots \cos(\alpha_n)]$$

where n is the number of observations and α_i is the i th observation.

The length or magnitude of the mean vector is:

$$\text{Eq. 23 - } r = \sqrt{\bar{x}^2 + \bar{y}^2}$$

And the vector mean direction is:

$$\text{Eq. 24 - } \bar{\Theta} = \arctan(\bar{x} / \bar{y})$$

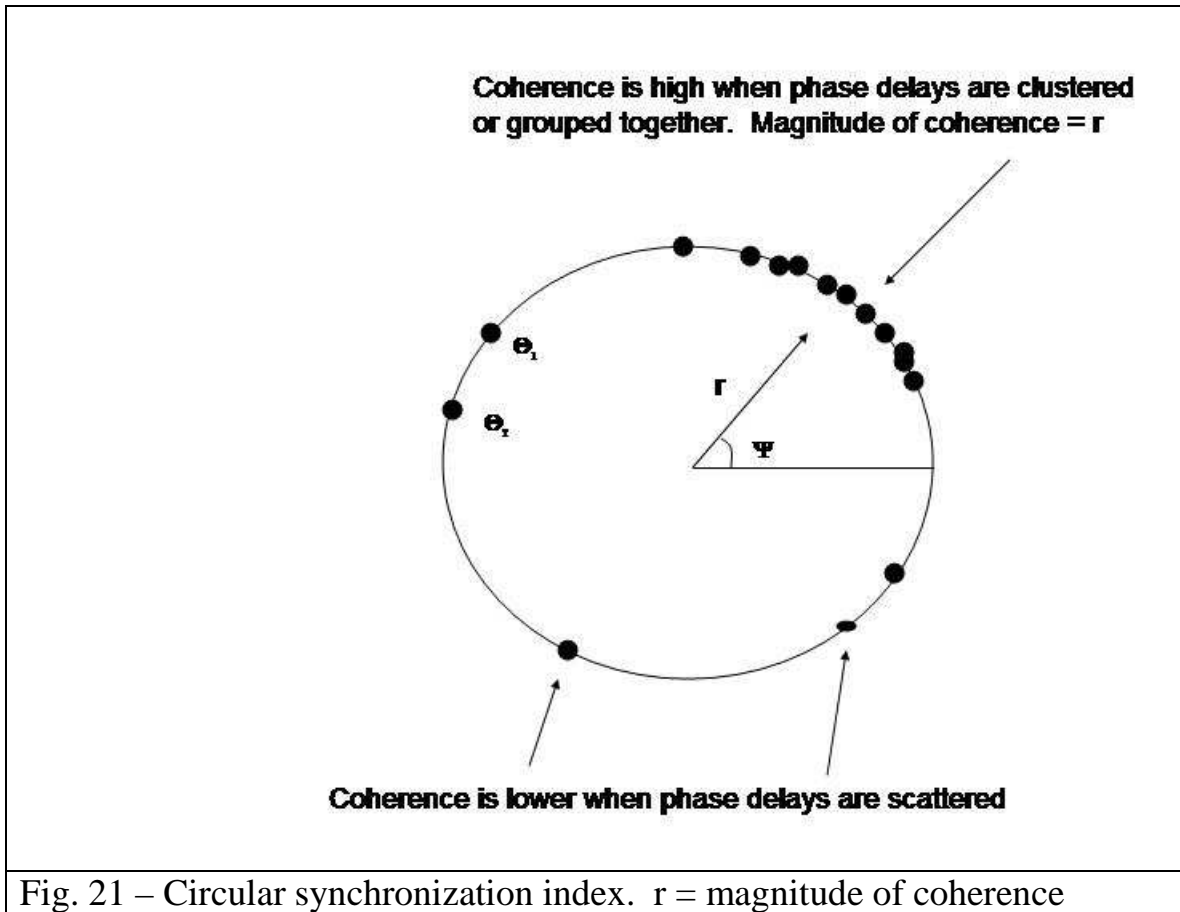
The magnitude of the mean vector gives an indication of the relative dispersion or coherence of the observations. The range of r is 0.0 to 1.0. If the phase angles or differences are clustered or clumped together in one direction then r will approximate 1. If the phase differences are random over the interval, then r will be small and approximate 0. The statistical computation of the cross-spectral “atoms” provides a complete description of the EEG phase locking, synchrony and phase angles (also phase resetting if differences or derivatives as a function of time are used).

$$\text{Eq. 25 - } \text{Angular variance: } s^2 = 2(1-r)$$

This is equivalent to variance in linear statistics.

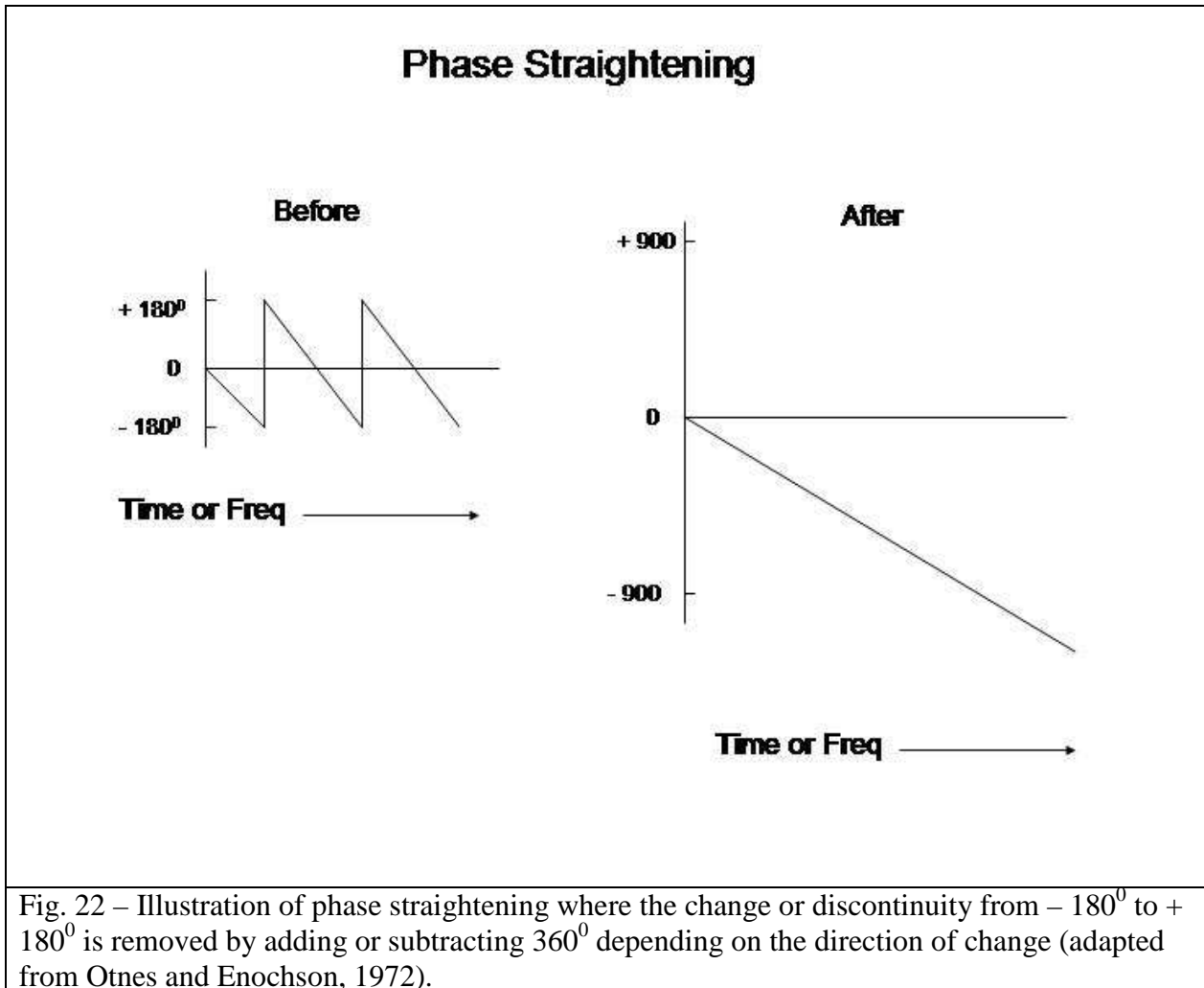
$$\text{Eq. 26 - } \text{Angular deviation: } s = 2(1-r)^{1/2}$$

This is equivalent to standard deviation in linear statistics.



22 – Phase straightening

As mentioned previously phase angle has an intrinsic discontinuity, where 0 and 360 are at opposite ends while in the circular distribution $0^0 = 360^0$ (Jammalamadaka and SenGupta, 2001). A method to remove discontinuities due to the mathematical limit of the arctangent is a procedure called “phase straightening” by Otnes and Enochson (1972, p. 238). The procedure involves checking for a large jump which happens when the phase goes from $+180^0$ to -180^0 and then adding or subtracting 360^0 depending on the direction of sign change. For example, $\Delta\theta = (180 - \varepsilon)^0 + (180 - \varepsilon)^0 = 360^0 - 2\varepsilon$ which is the same as 2ε since $-(180 - \varepsilon)^0 = 180 + \varepsilon$. This procedure results in phase being a smooth function of time or frequency and removes the discontinuities. The programmer needs only to keep track of the number of winds around the circle also called the “winding number” if absolute phase differences are needed.



Phase straightening is important when computing the first and second derivatives of the time series of phase differences because the discontinuity between -180° to $+180^{\circ}$ can produce artifacts. All of the derivatives and phase reset measures in this paper were computed after phase straightening in order to avoid possible artifact.

23 – EEG Spindles and Burst Activity

The human Electroencephalogram is characterized by electrical events that have a specific shape and physiological origin called “spindles” or “burst activity”. A spindle is defined as a rhythmic and sequential build up of EEG amplitudes that wax and wane and appears as an “envelope” structure. Spindles are also referred to as augmenting and recruiting responses (Steriade, 1995). Spindles are especially prevalent during late drowsiness and sleep, however, spindles also occur during waking and focused attention. In animal studies spindle like responses referred to as

“augmenting responses” can be produced by thalamic stimulation and involve activation of the upper layers of the cortex and are typically negative in polarity as the first event in the sequential build up of voltages.

“Recruiting responses” also have a spindle like structure but the first wave is positive in polarity at the scalp surface and involves activation of the lower layers of the cortex (Steriade, 1995). Both augmenting and recruiting responses exhibit the same spindle like “envelope” shape but have different initial polarities and are not easy to distinguish in the human EEG record. For this reason, Steriade (1995) recommends that one refer to all spindles as “augmenting responses”.

There are several methods that are used to quantify “spindle” or augmenting response structure such as the inter-spindle interval, spindle peak amplitude and spindle duration. Figure 23 shows an example of how NeuroGuide quantifies spindle activity using JTFA and the time series of instantaneous spectral measures (go to www.appliedneuroscience.com download the free demo).

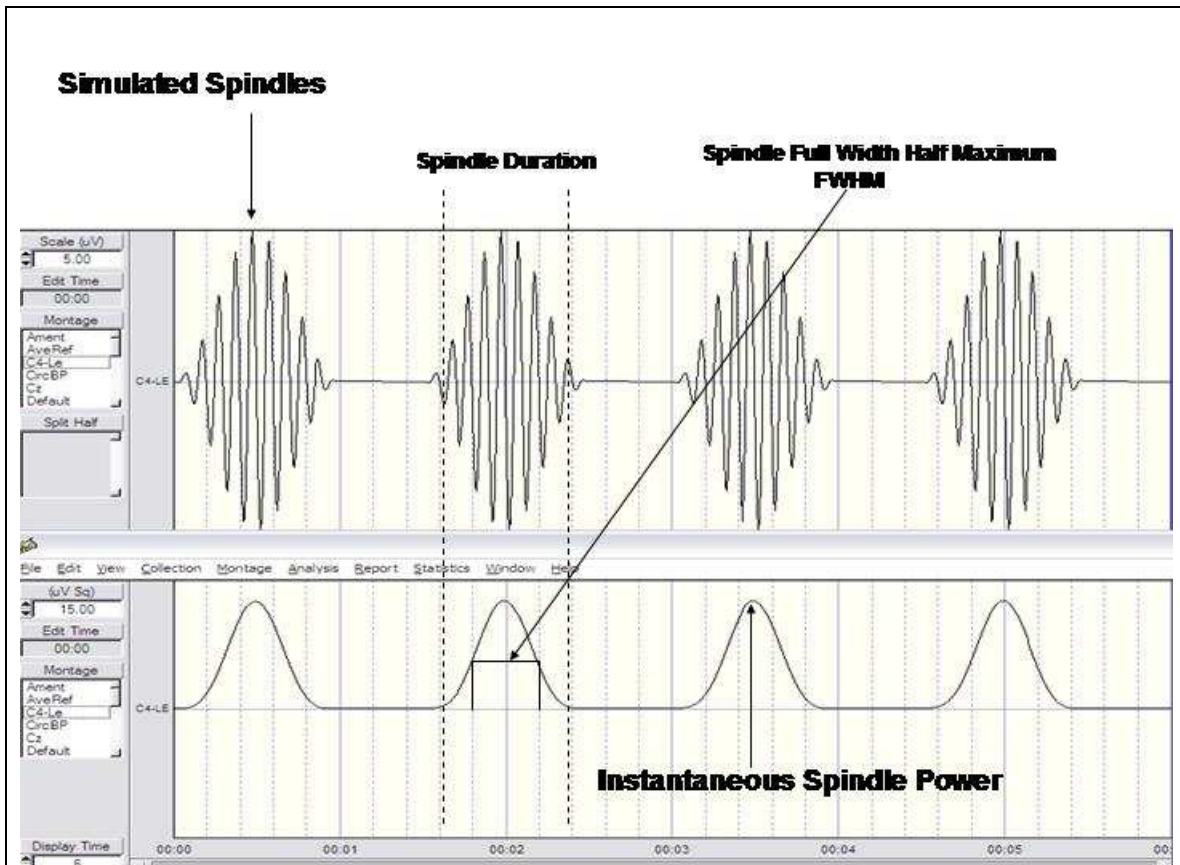


Fig. 23 – Top are simulated spindles and bottom is the time series of the instantaneous power of the spindles. Quantitative measures of spindle duration, intensity and average inter-spindle intervals are computed. The Full Width Half Maximum (FWHM) is a

measure of the area under the curve and is also a measure of the duration of the spindle or “burst” activity. Example produced using NeuroGuide demo software from www.appliedneuroscience.com.

24 – The Bi-Spectrum and Bi-Coherence and Bi-Phase Difference

Another method to quantify spindle activity and brain connectivity as it relates to spindles is the Bi-Spectrum which is divided into auto-channel cross-frequency (single channels different frequencies) and cross-channel cross-frequency (different frequencies in different channels). There are several different definitions of the Bi-Spectrum. One is by Hasselman et al, (1963) as the 3rd moment statistical property called “skewness” which was used to detect nonlinear interacting ocean waves. Brillinger and Rosenblatt (1967) elaborated and described the computation of the tri-spectrum as the 4th power statistical moment or “kurtosis”. The application of this definition of bi-spectra is purely statistical and it is primarily used to detect non-linearities. The second definition of bi-spectra is by Bendat and Piersol (1980) in which bi-spectra are produced by partial-coherence analyses in order to isolate the covariances between different frequencies and locations. The bi-spectrum using partial-coherence is a measure of the association between different frequencies and different inputs, for example, a measure of the phase consistency and the phase difference between theta and beta frequencies (Helbig et al, 2006). Witte et al (1997) and Helbig et al (2006) provide detailed time-series analysis and mathematics of the bi-spectrum, bi-amplitude, bi-coherence and phase bi-coherence. In the present paper we use the Bendat and Piersol (1980) approach to bi-spectra and bi-coherence to develop measures of coherence and phase differences between different frequencies within a single channel (auto bi-coherence and bi-phase) and the correlation between frequencies in different EEG channels or sensors (cross bi-coherence and cross bi-phase).

To calculate bi-coherence, it is necessary to multiply two complex domain transforms of the digital time series to obtain a 3rd order transform and because of the linearity of the transforms and the need for real-time computations we transform each instant of time for X_t to the complex domain by multiplying a time series by a sine and cosine sine wave at a specific center frequency and band width followed by low-pass filtering. This well established signal processing method is called “complex demodulation” (Otnes and Enochson, 1972) and is equivalent to a Hilbert transform that refer to it as a complex demodulation transform or “CDF” where each time point is represented as a point on the unit circle 0 to 2π .

This is an instantaneous cosine and sine representation of a time series from which the time series of the “cospectrum” and “quadspectrum” are computed from the cross-spectrum (see Appendix B for the mathematical details of complex demodulation). As described in section 9 the results of the CDF is the creation of a new real valued time series. The CDF real valued time series is then used as the input to spectral analyses for the computation of bi-coherence and bi-phase.

25- What is the physiological meaning of EEG Auto-Frequency Coherence (AFC) and Auto-Frequency Phase (AFP)?

Cross-channel Auto-Frequency Coherence and Auto-frequency phase measure the spatial and temporal relations between EEG “spindles” or “burst activity” and “rhythmic episodes” as well as the frequency structure of EEG bursts between two channels but at the same frequency (i.e., auto-frequency). Complex demodulation of a EEG time series at a given center frequency measures the instantaneous power (μV^2) of activity at each instant of time in a frequency band, similar to a filter except that the time series is represented in the complex domain. The frequency spectrum of “spindle activity” at a given frequency measures spindle duration and inter-spindle intervals or how common spindles are within a record and auto bi-coherence shows the phase synchrony of spindle activity at different frequencies within a channel. Cross bi-coherence measures the phase synchrony of spindle or burst activity at the same or different frequency in different channels.

The FFT of the complex demodulation time series (x'_t) computes the inter-burst frequency and average burst duration and burst rise times because x'_t is the envelope of the spindle structure of EEG events. For example, long duration bursts result in high power in the lower frequencies of the FFT spectrum. Short inter-burst intervals result in high power at higher frequencies of the FFT spectrum.

FFT of the JTFA Time Series shows high power at low frequencies when burst durations are long and high power at high frequencies when inter burst intervals are short

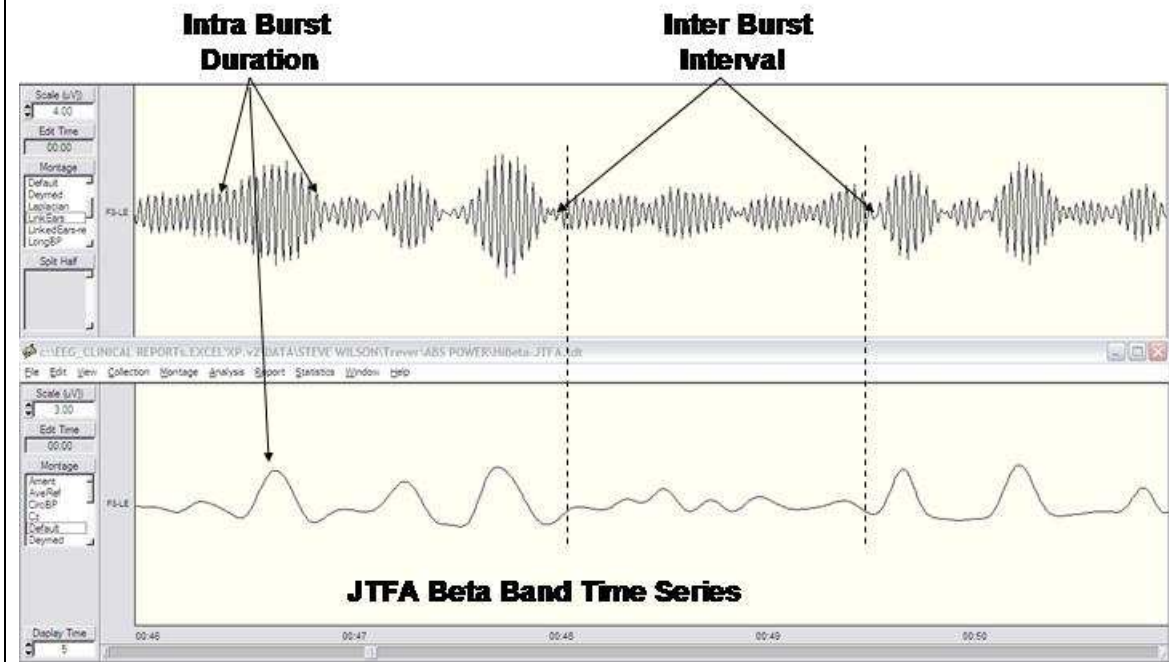


Fig. 24 – Top is filtered EEG at 25 – 30 Hz from F8 and reveals the burst structure of the EEG. Bottom is the complex demodulation (JTFA) time series of instantaneous power at 25 – 30 Hz (x'_t) and represents the integral or envelope of burst activity in the hi-beta frequency band. Long duration bursts result in high spectral power in the lower frequencies and short inter-burst intervals result in high spectral power in the higher frequencies of the spectrum. Analyses were produced using the NeuroGuide Lexicor demo from the download at www.appliedneuroscience.com

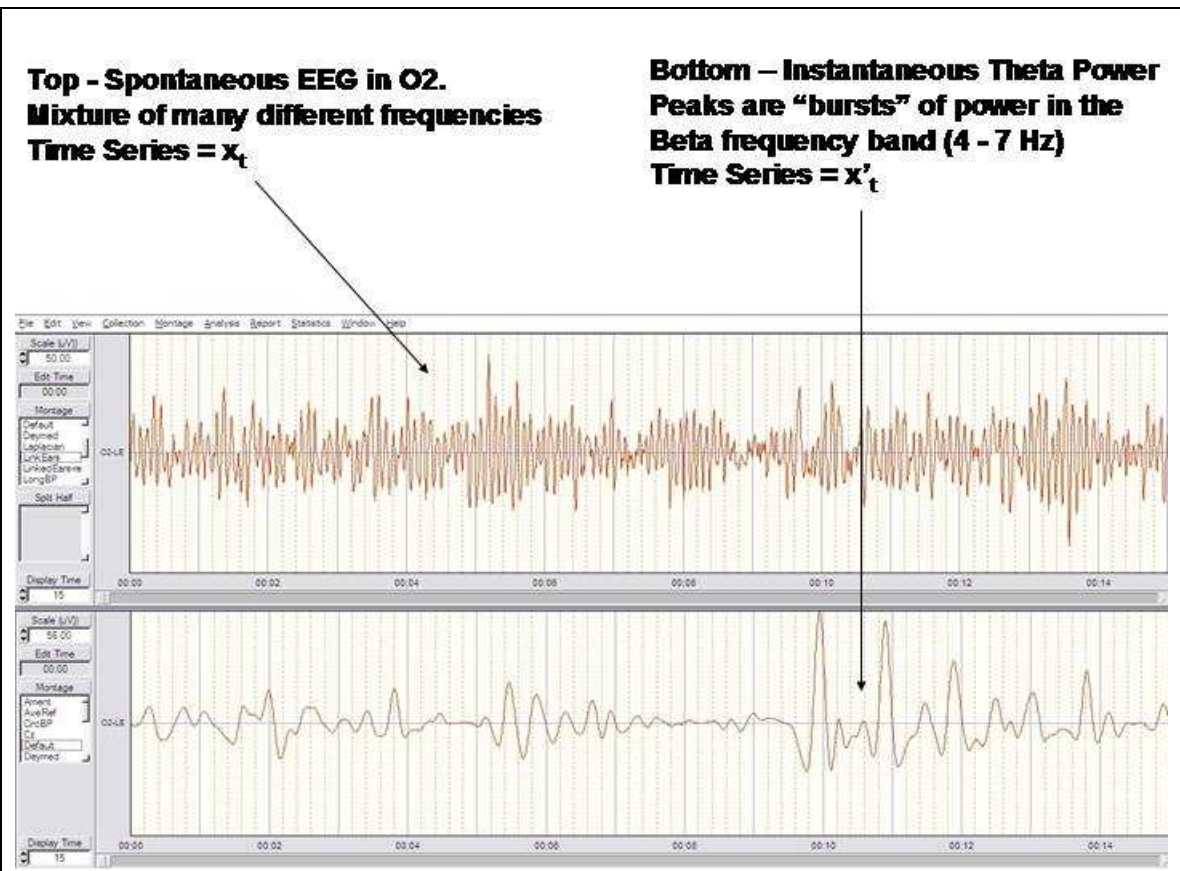


Fig. 25 - Top is the spontaneous EEG from O2. Bottom is the complex demodulation (JTFA) time series (x'_t) of the instantaneous power between 4 – 7 Hz. Peaks in the JTFA time series represent integrations or the instantaneous envelope of burst activity in the theta frequency band. Analyses were produced using the NeuroGuide Lexicor demo from the download at www.appliedneuroscience.com

Top - Spontaneous EEG in O2.
Mixture of many different frequencies
Time Series = x_t

Bottom - Instantaneous Beta Power
Peaks are “bursts” of power in the
Beta frequency band (25 – 30 Hz)
Time Series = x'_t

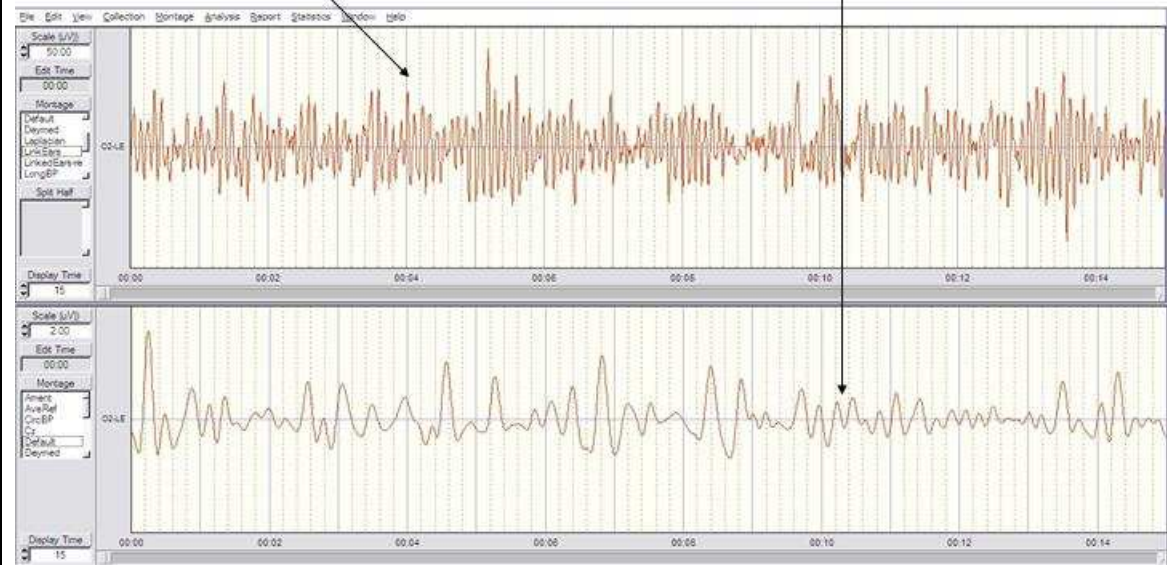
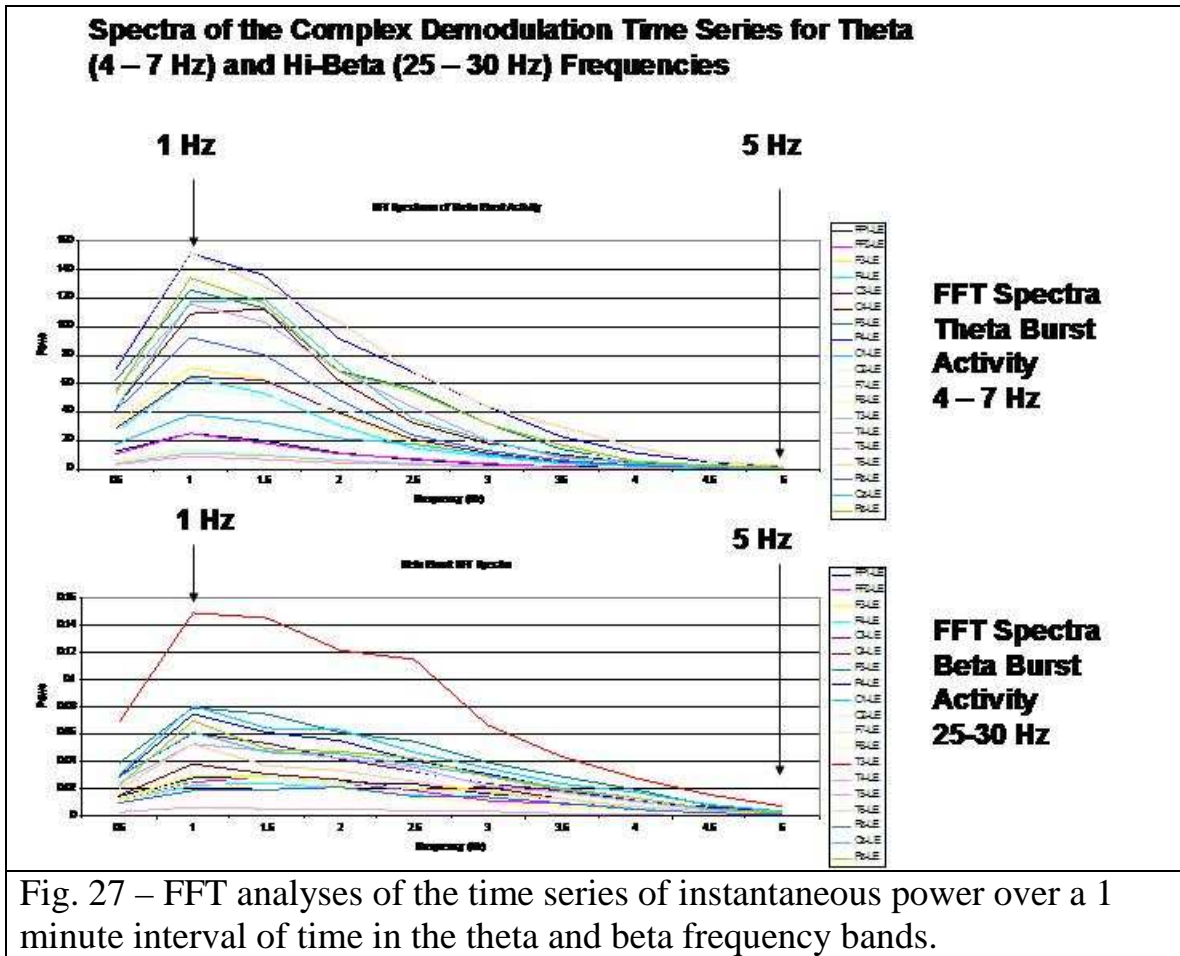


Fig. 26 - Top is the spontaneous EEG from O2. Bottom is the complex demodulation (JTFA) time series (x'_t) of the instantaneous power between 25 - 30 Hz. Peaks in the JTFA time series represent integrations or the instantaneous envelope of burst activity in the hi-beta frequency band. Bi-coherence between the two JTFA time series in fig. 20 and fig. 21 measure the phase synchrony of burst activity in the theta and beta frequency bands. Bi-phase measures the average time differences between theta and beta burst activity. Analyses were produced using the NeuroGuide Lexicor demo from the download at www.appliedneuroscience.com



26- How to compute the Bi-Spectral Amplitude or Cross-Frequency Correlation

The simplest of the Bi-Spectral measures is the correlation or covariance of amplitude or power over time between different frequencies. For example, the covariance or correlation between amplitudes at 6 Hz (theta) and 15 Hz (beta) over time. One simply computes the correlation coefficient in a matrix of $m \times n$ dimension where m = channels and n = frequency. The diagonal of the matrix = 1 where the correlation is between the same channel and the same frequency. In NeuroGuide the matrix is computed from 1 to 50 Hz at 1 Hz resolution and thus the matrix is $50 \times 50 \times 171$ electrode combinations (actually $171 + 19$ [diagonal] = 190). The equation for this computation is the same as equation 2 used in the spectral correlation coefficient but expanded to include correlations between different frequencies.

27- How to compute Auto-channel Cross-Frequency Coherence (ACC) (same channel different frequencies)

The procedure is:

- 1- Transform the digital value of the EEG time series x_t in channel X to a new time series x'_t by multiplying each time point by a sine wave at frequency 1 and a cosine wave at frequency 1. Then, low pass filter and compute the square root of the sum of squares of the cospectrum and quadspectrum at each point of time to produce the new time series x'_t (see section 9).
- 2- Transform the digital value of the EEG time series x_t in channel X to a new time series x''_t by multiplying each time point by a sine wave at frequency 2 and a cosine wave at frequency 2. Then low pass filter and then compute the square root of the sum of squares of the cospectrum and quadspectrum at each point of time to produce the new time series x''_t (see section 9).
- 3- Compute the coherence of the two time series x'_t and x''_t from the same channel for the two frequencies 1 and 2 for each instant of time.

28- How to compute Cross-Channel Cross-Frequency Coherence (CCC) (different channels different frequencies).

The procedure is:

- 4- Transform the digital value of the EEG time series x_t in channel X to a new time series x'_t by multiplying each time point by a sine wave at frequency 1 and a cosine wave at frequency 1. Then, low pass filter and compute the square root of the sum of squares of the cospectrum and quadspectrum at each point of time to produce the new time series x'_t .
- 5- Transform the digital value of the EEG time series y_t in channel Y to a new time series y'_t by multiplying each time point by a sine wave at frequency 2 and a cosine wave at frequency 2. Then low pass filter and then compute the square root of the sum of squares of the cospectrum and quadspectrum at each point of time to produce the new time series y'_t .

Auto-Channel Cross-Frequency Phase (ACFP) and Cross-Channel Cross-Frequency Phase (CCFP) are computed in the same manner as in previous sections by computing the arctangent of the ratio of the quadspectrum to the cospectrum at each moment of time for the two transformed phase difference time series.

In summary, there are four categories of the bi-spectrum for the purposes of relating different frequencies: 1- Auto-Channel Auto-Frequency (AA), 2- Cross-Channel Auto-Frequency (CA), 3- Auto-Channel Cross-Frequency (AC) and 4- Cross-Channel Cross-Frequency (CC).

29- Auto Channel Cross-Frequency Coherence (ACC) is defined as the square of the ratio of the cross-spectra within a single channel at two different frequencies divided by the product of the auto-spectra. For example, the auto bi-spectrum between the EEG theta frequency (4 - 7 Hz) and the beta frequency band (25 – 30 Hz) as recorded from electrode location F3. To compute auto channel cross-frequency coherence one first transforms each time point to the complex domain using complex demodulation and then one computes the Fourier transform of the complex domain time series.

Eq. 27:

Auto Cross-Frequency Coherence (ACC) (f_1, f_2) after complex demodulation (x', y') is defined as

$$ACC = \frac{(\sum_N (a(x' f_1)u(x'' f_2) + b(x' f_1)v(x'' f_2)))^2 + (\sum_N (a(x' f_1)v(x'' f_2) - b(x' f_1)u(x'' f_2)))^2}{\sum_N (a(x' f_1)^2 + b(x' f_2)^2) \sum_N (u(x'' f_2)^2 + v(x'' f_2)^2)}$$

Where x = frequency activity recorded from a single channel and x' = frequency 1 and x'' = frequency two recorded from the same channel. N and the summation sign represents averaging over frequencies in the raw spectrogram or averaging replications of a given frequency or both. The numerator and denominator of bi-coherence always refers to smoothed or averaged values, and, when there are N replications or N frequencies then each bi-coherence value has $2N$ degrees of freedom.

30- Cross-Channel Cross-Frequency Coherence (CCC) is a measure of the phase consistency between two different frequencies recorded from two different locations. For example, the phase consistency between theta (4-7 Hz) and High Beta (20 – 40 Hz) EEG signals in two spatially separated channels F3 and F4 of the 10/20 system of EEG electrode location.

Mathematically, the Cross-Channel Cross-Frequency Coherence (CCC) is defined as the ratio of the auto-spectra and cross-spectra for two channels, X and Y and two frequencies f_1 and f_2 . We again refer to the definitions of the cospectrum and the quad spectrum (see section 9) and then we define the cross bi-spectral coherence:

Eq. = 28

$$CCC = \frac{(\sum_N (a(x' f_1)u(y' f_2) + b(x' f_1)v(y' f_2)))^2 + (\sum_N (a(x' f_1)v(y' f_2) - b(x' f_1)u(y' f_2)))^2}{\sum_N (a(x' f_1)^2 + b(x' f_2)^2) \sum_N (u(y' f_2)^2 + v(y' f_2)^2)}$$

Where x' = channel 1 and y' = channel 2, f_1 = frequency 1 in channel 1 and f_2 = frequency 2 in channel 2. N and the summation sign represents averaging over frequencies in the raw spectrogram or averaging replications of a given frequency or both. The numerator and denominator of bi-coherence always refers to smoothed or averaged values, and, when there are N replications or N frequencies then each bi-coherence value has $2N$ degrees of freedom.

31- Bi-Spectral Phase

Bi-spectral phase difference is generically defined as:

Eq. 29 –

$$\text{Phase difference } (f_1, f_2) = \text{Arctan} \frac{(\text{Smoothed quad spectrum}(f_1, f_2))}{(\text{Smoothed cospectrum}(f_1, f_2))}$$

Like bi-coherence there are two subdivisions of bi-spectral phase: 1- Auto Bi-spectral phase and 2- Cross Bi-spectral phase.

32- Auto-Channel Cross-Frequency Phase Difference (ACP) is a measure of the phase difference between two phase difference time series at two frequencies recorded from one location. Phase difference between two time series and two frequencies is defined as a point on the unit circle and is represented in degrees or radians and is “normalized” with respect to frequency (i.e., independent of frequency because $r = 1$). For example, a phase difference of 45^0 is the same for the standard EEG frequency bands of delta, theta, alpha, beta, gamma, etc. Because of this fact and because of the physics of superposition of waves the bi-spectral phase measure is a useful measure of local generator signals that are coupled at different frequencies and exhibit bi-frequency phase locking. The first and second derivatives of bi-frequency phase coupling are similar to the inter-coupling measures and are useful measures of “transition states” or bifurcation points and stability measures of homeostatic systems measured from a single location and given superposition of waves from many different locations.

The equation for use with a hand calculator to compute Auto Bi-Spectral Phase (f_1, f_2) **or ACP** is:

Eq. 30

$$ACP = \text{Arc tan} \frac{\sum_N (a(x' f_1)v(x'' f_2) - b(x' f_1)u(x'' f_2))}{\sum_N (a(x' f_1)u(x'' f_2) + b(x' f_1)v(x'' f_2))}$$

Where $x' =$ frequency 1 and $x'' =$ frequency two recorded from the same channel and $N =$ number of time samples (for cospectrum and quadspectrum calculation see section 9).

33- Cross-Channel Cross-Frequency Phase Difference (CCP) is a measure of the phase difference between two real valued phase difference time series at two frequencies recorded from two different locations. This is an important measure of network dynamics and communication at different frequencies across space. Because instantaneous phase is a scalar and a real number then the commutation properties of algebra hold and the use of the Fourier transform is valid to compute the arctangent of the quadspectrum and cospectrum. Phase difference between two locations and two frequencies is defined as a point on the unit circle and is represented in

degrees or radians and is “normalized” with respect to frequency (i.e., independent of frequency because $r = 1$). For example, a phase difference of 45° is the same for the standard EEG frequency bands of delta, theta, alpha, beta, gamma, etc. Because of this fact and because of the physics of superposition of waves the bi-spectral phase measure is a useful measure of local and distant coupling by frequency and phase locking. The first and second derivatives of bi-phase coupling are useful measures of “transition states” or bifurcation points and stability measures of homeostatic systems (similar to their application to phase reset described in section 9).

The equation for use with a hand calculator to compute Cross Bi-Spectral Phase or **CCP** is:

Eq. 31-

$$CCP = \text{Arc tan} \frac{\sum_N ((a(x' f_1)v(y' f_2) - b(x' f_1)u(y' f_2)))}{\sum_N ((a(x' f_1)u(y' f_2) + b(x' f_1)v(y' f_2)))}$$

34- Coherence of Coherence

Defined as the average Coherence between two time series of instantaneous coherence for a pair of electrodes with a common reference. The importance of a common reference is because algebraic subtraction occurs only by virtue of a common reference whereas an average reference or a Laplacian reference mixes signals from all leads into each of the remaining leads thus eliminating valid and meaningful algebra. A view of all pair wise combinations of “Coherence of Coherence” for 19 leads = 171 combinations using Cz as the reference electrode is in Figure 28.

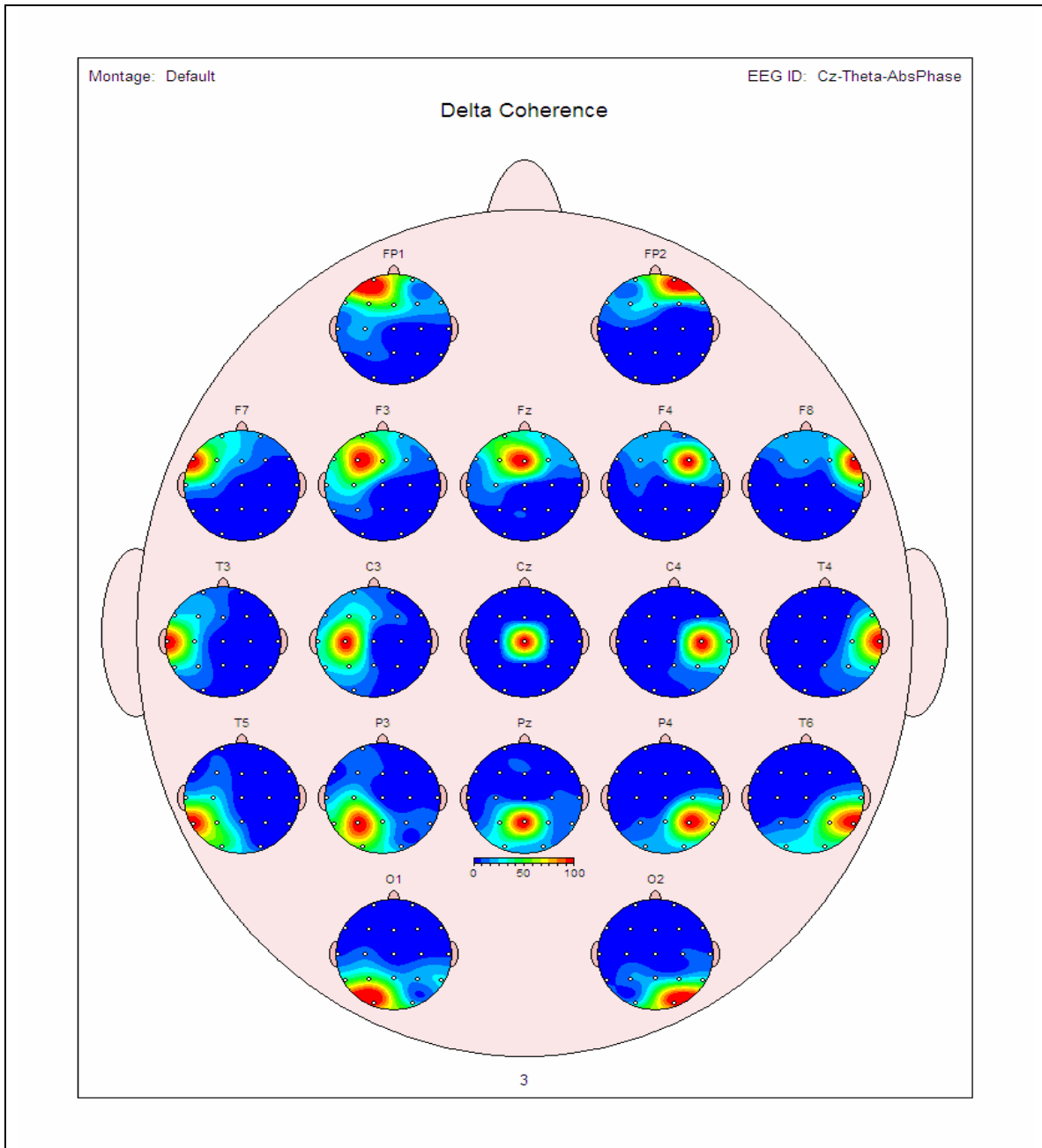
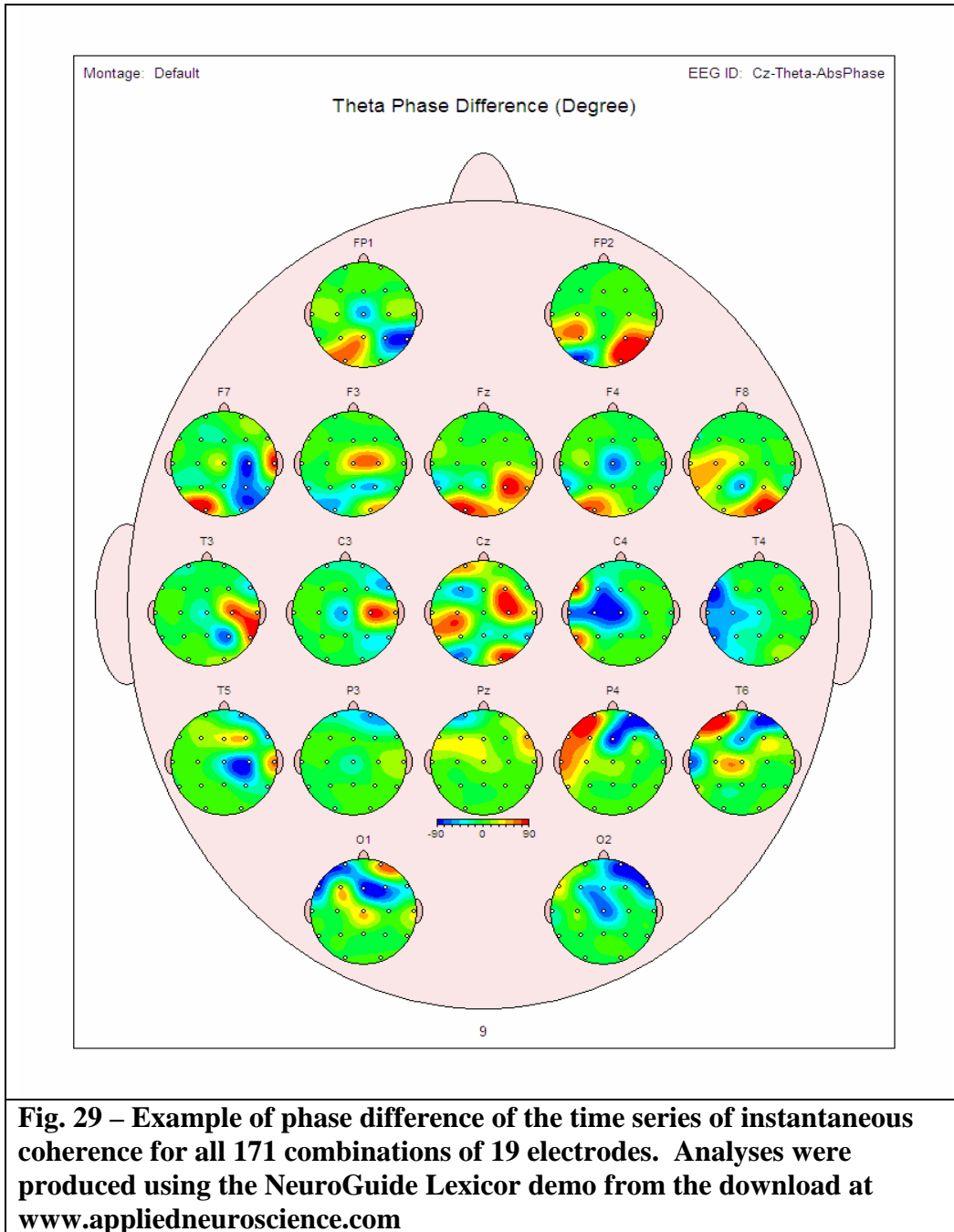


Fig. 28 – Example of coherence of coherence for all 171 combinations of 19 electrodes. Analyses were produced using the NeuroGuide Lexicor demo from the download at www.appliedneuroscience.com

35 – Phase Difference of Coherence

Defined as the average Phase difference of the time series of instantaneous coherence between any pair of electrodes with respect to a common electrode. For example, the two time series of instantaneous coherence between Cz-P3 and Cz-P4 are the input to the phase analysis in which the average phase difference between the two time series of coherence

exhibits statistically significant phase stability over time (i.e., significant coherence values). An example of 19 leads = 171 combinations is in Figure 29.



36 – Coherence of Phase Differences

Defined as the average Coherence of the time series of instantaneous phase differences between any pair of electrodes with respect to a common

electrode. For example, the two time series's of instantaneous phase difference between Cz-P3 and Cz-P4 are the input of the coherence analysis in which coherence between the two time series of phase difference exhibits statistically significant phase stability over time (i.e., significant coherence values). An example of 19 leads = 171 combinations is in Figure 30.

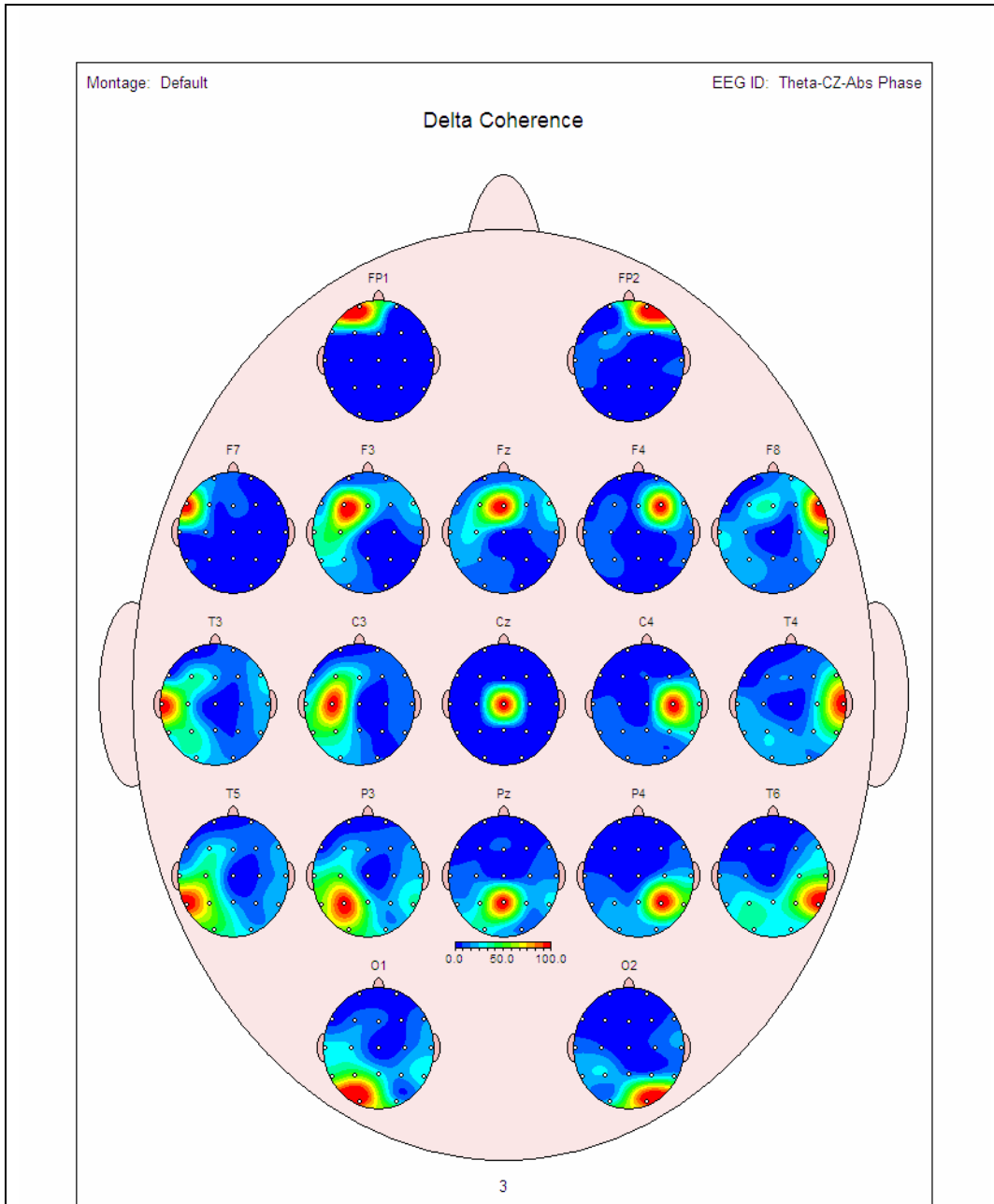


Fig. 31 – Example of coherence of the time series of instantaneous phase differences for all 171 combinations of 19 electrodes. Analyses were produced using the NeuroGuide Lexicor demo from the download at

37 – Coherence Between Two Time Series of Phase Resets

Defined as the average Coherence of the First Derivative of the Time Series of Instantaneous Phase Differences (i.e., “Phase Reset”) between any pair of electrodes with respect to a common electrode. For example, the two time series of phase resets for Cz-P3 and Cz-P4 are the input to the coherence analysis in which there is significant phase stability between the two time series of phase reset. See section 15 for an explanation of phase reset. An example of 19 leads = 171 combinations is in Figure 31.

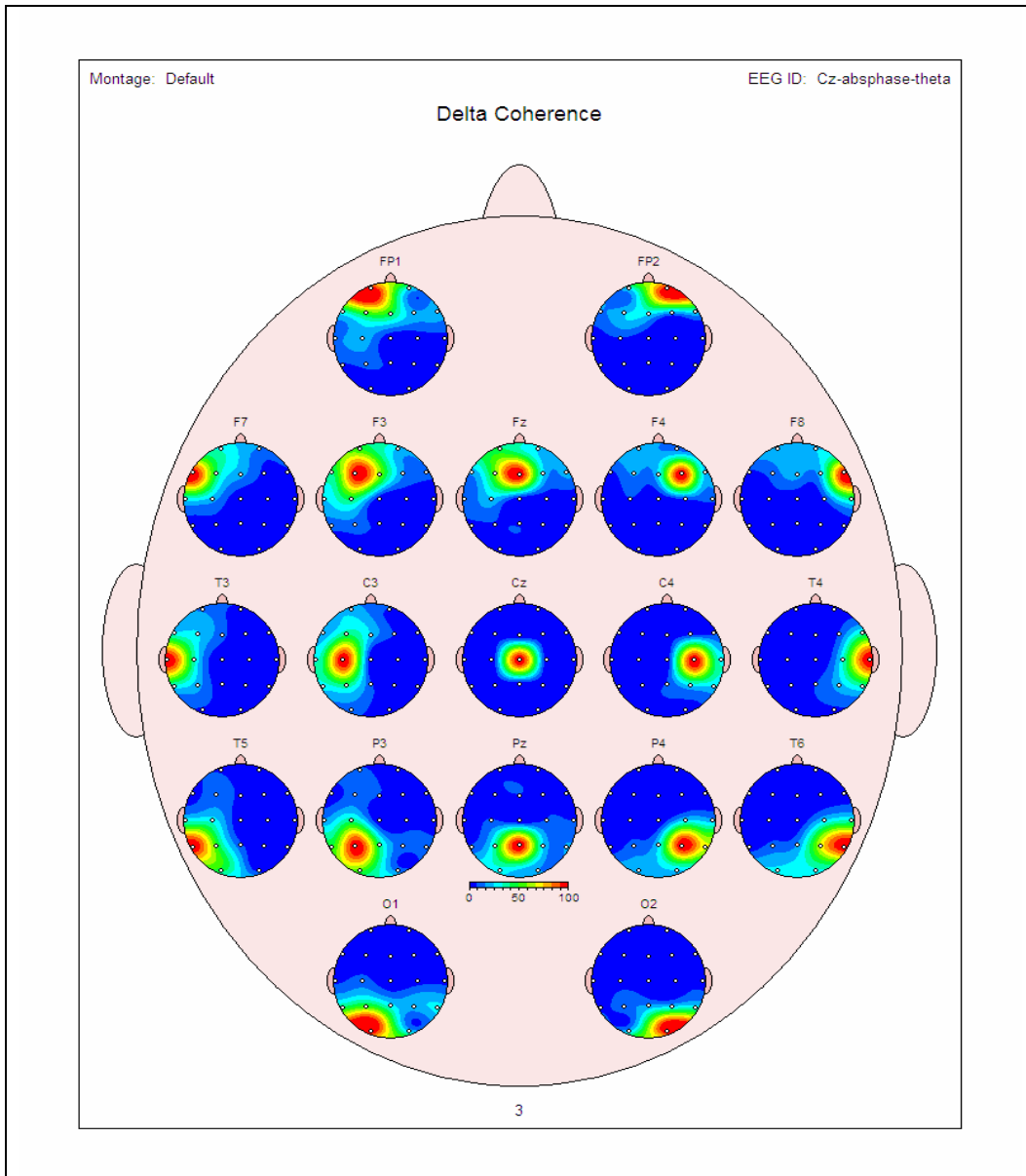
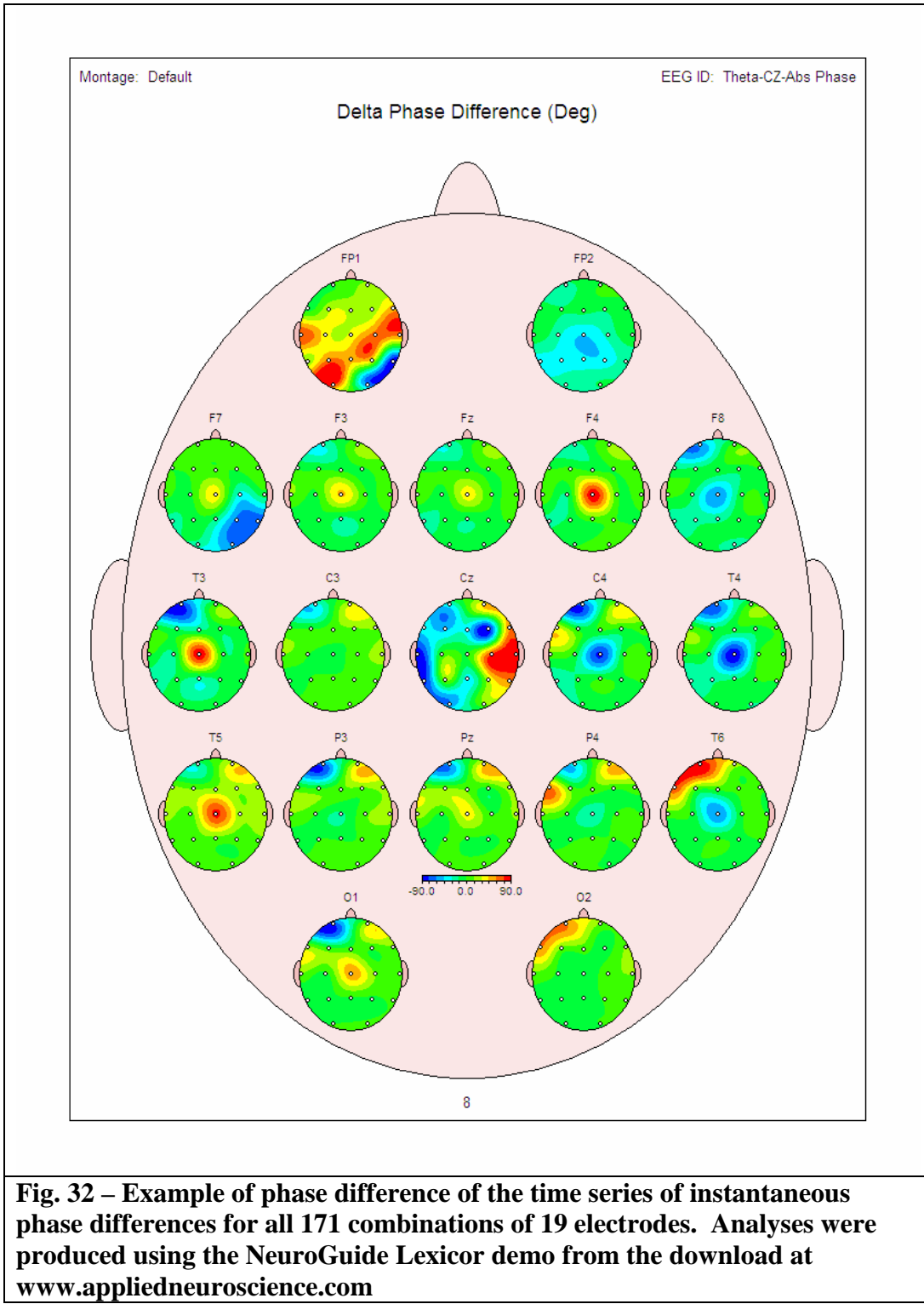


Fig. 31 – Example of coherence of the time series of instantaneous phase re-set for all 171 combinations of 19 electrodes. Analyses were produced using the NeuroGuide Lexicor demo from the download at www.appliedneuroscience.com

38 – Phase Difference Between Two Phase Difference Time Series

Defined as the average Phase difference of the Time Series of Instantaneous Phase Differences between two channels with respect to a common reference. A map of all pair wise combinations (19 leads = 171 combinations with respect to Cz) is useful to visualize the full manifold of

relationships as defined by the phase difference of the time series of phase differences. An example of 19 leads = 171 combinations is in Figure 32.



39 – Phase Difference of Phase Reset

Defined as the average phase difference of the First Derivative of the Time Series of Instantaneous Phase Differences (i.e., Phase Reset) between two electrode combinations referenced to a common reference as explained in section 34. See section 15 for an explanation of phase reset. An example of 19 leads = 171 combinations is in Figure 33.

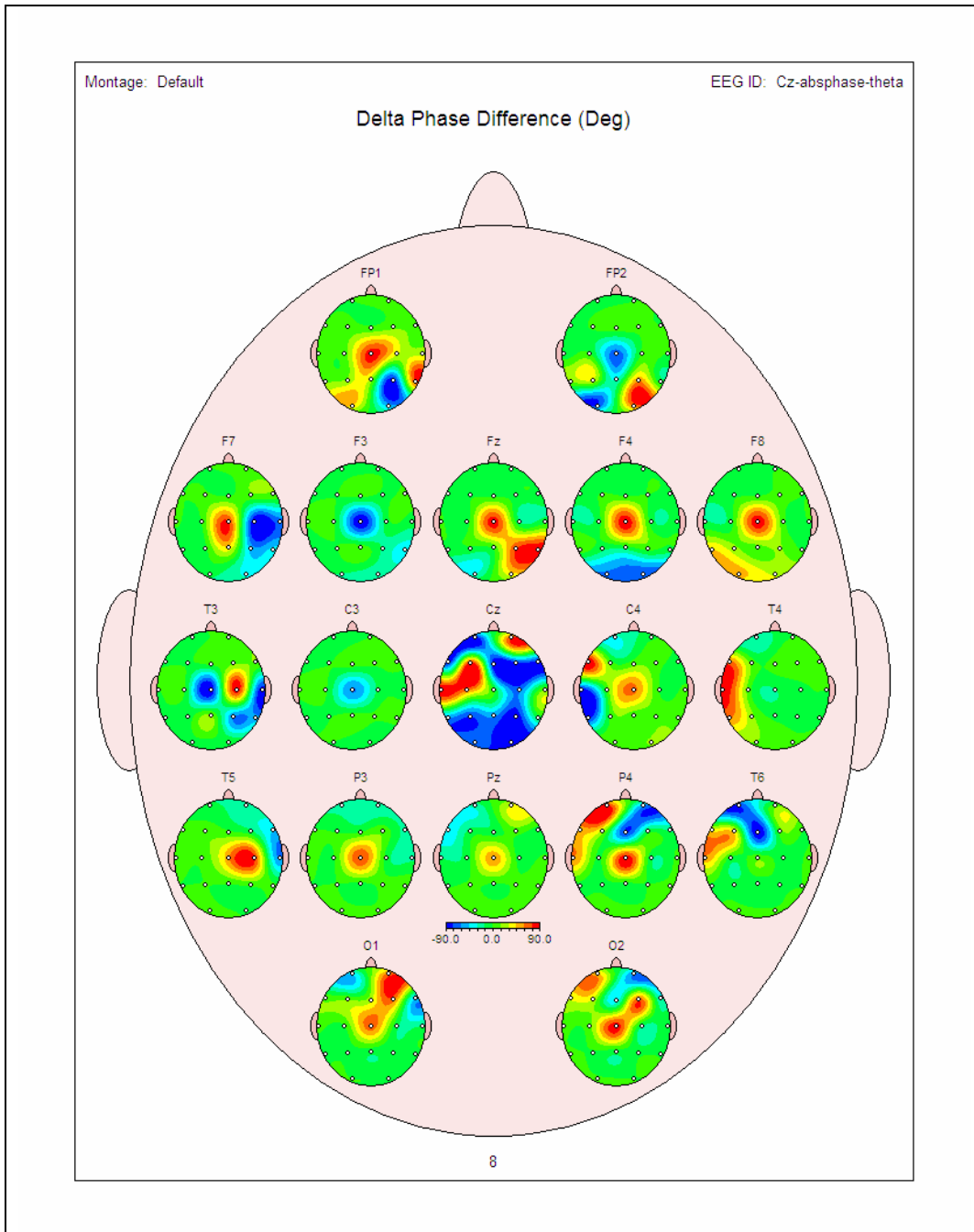


Fig. 33 – Example of phase differences of the time series of instantaneous phase re-set for all 171 combinations of 19 electrodes. Analyses were produced using the NeuroGuide Lexicor demo from the download at www.appliedneuroscience.com

40 – Bi-Spectral Cross-Frequency Power Correlations

A common method of evaluating bi-spectral relations is to compute the cross-frequency power correlation (Linas et al, 2005). The method involves computing the covariance of power at each frequency bin with respect to all other frequency bins. An example is shown for the cross-frequency power correlations from 1 to 50 Hz in wakefulness, drowsiness and sleep in the same subject as shown in

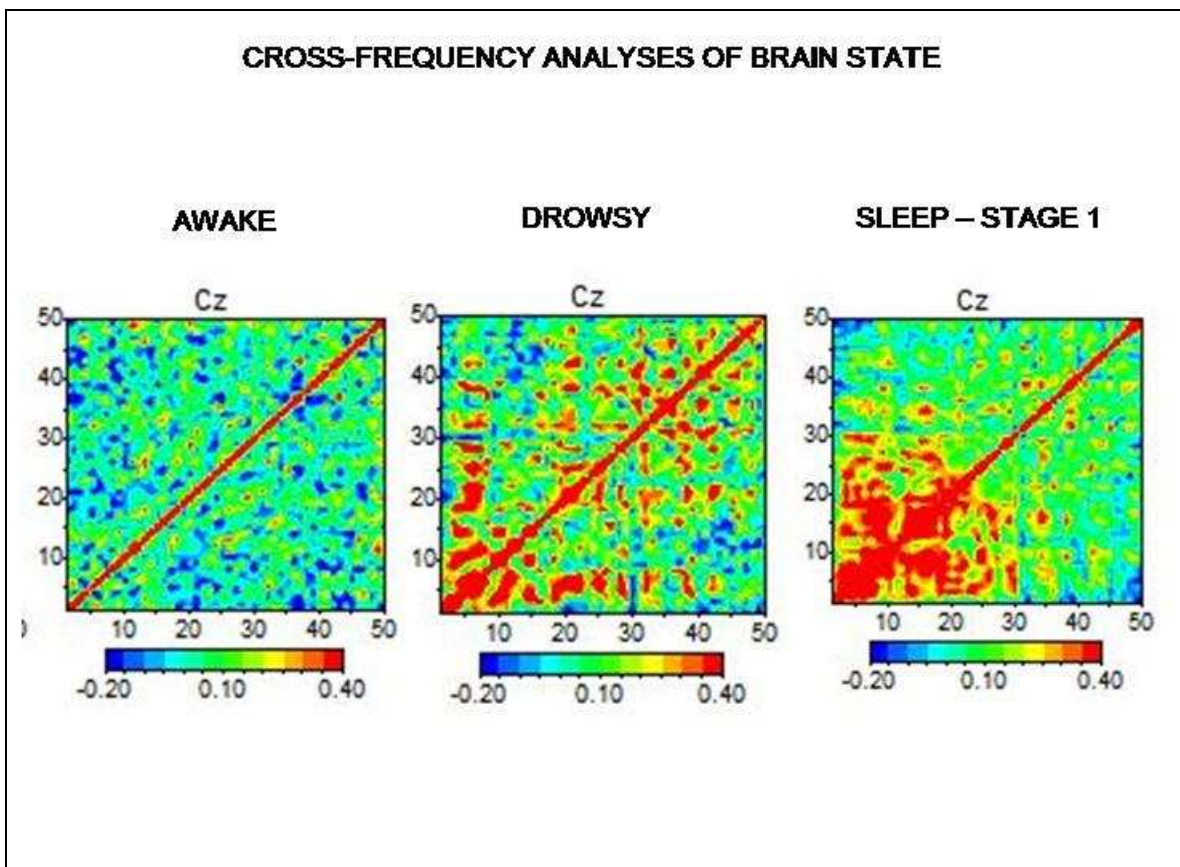


Fig. 34 – Example of bi-spectrum of cross-frequency power correlations from 1 to 50 Hz from Cz in the same subject but at different brain states, i.e., wakefulness, drowsy and sleep.

41- Cross-Frequency Phase Synchrony or m:n Phase Synchronization

Cross-frequency phase synchrony is also called m:n phase synchronization (Schack et al, 2002; 2005). **Phase synchronization** is the process by which two or more cyclic signals tend to oscillate with a repeating sequence of relative phase angles. Phase synchronisation is usually applied to two waveforms of the same frequency with identical phase angles with each cycle. However it can be applied if there is an integer relationship of frequency, such that the cyclic signals share a repeating sequence of phase angles over consecutive cycles. These integer relationships are the so called Arnold Tongues which follow from bifurcation of the circle map” (www.wikipedia.org; Pikovsky et al, 2003).

We mathematically define cross-frequency phase synchrony as the average Second Derivative of the instantaneous phase difference between different frequencies. Different frequencies, e.g., 4 Hz vs. 7 Hz results in a continuum of changing phase differences and in beat frequencies (frequency mixing). However, when the two frequencies are coupled and do not change over time (i.e., phase synchrony), then the first derivative of the phase difference between two different frequencies is constant. That is, if two different frequencies are coupled over time then the 1st derivative is constant, although different depending on the difference in phase angle. In order to measure phase synchrony across frequencies it is necessary to compute the 2nd derivative of the phase differences which = zero when there is phase synchrony. That is, a constant first derivative results in a zero 2nd derivative. Thus, the average 2nd derivative is a direct measure of cross-frequency phase synchrony, because the lower the average 2nd derivative then the greater is phase synchrony across frequencies. Figures 35 to 39 illustrate the measure of cross-frequency phase synchrony and Figures 40 and 41 are examples of cross-frequency phase shift duration and cross-frequency phase lock duration.

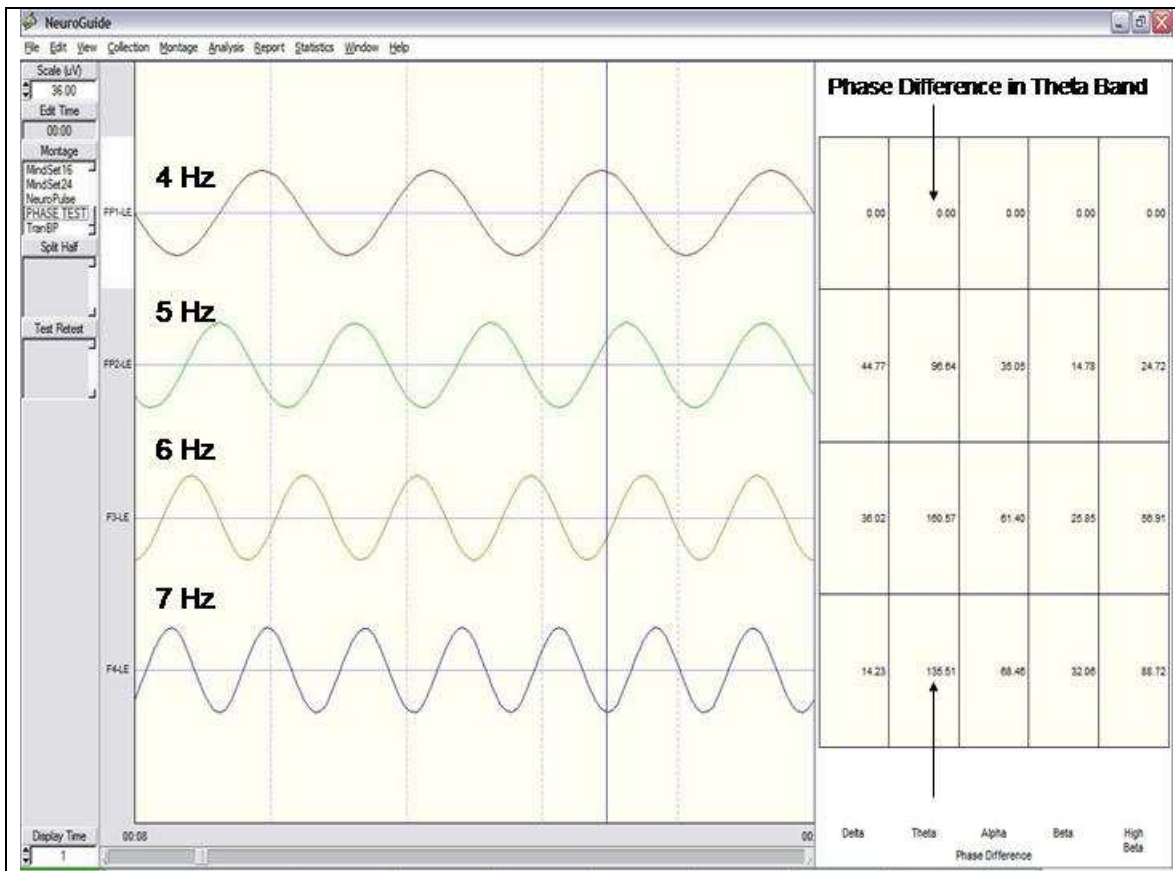


Fig. 35 – Example of 4 different frequencies and their phase relations. Instantaneous phase differences change at each moment of time.

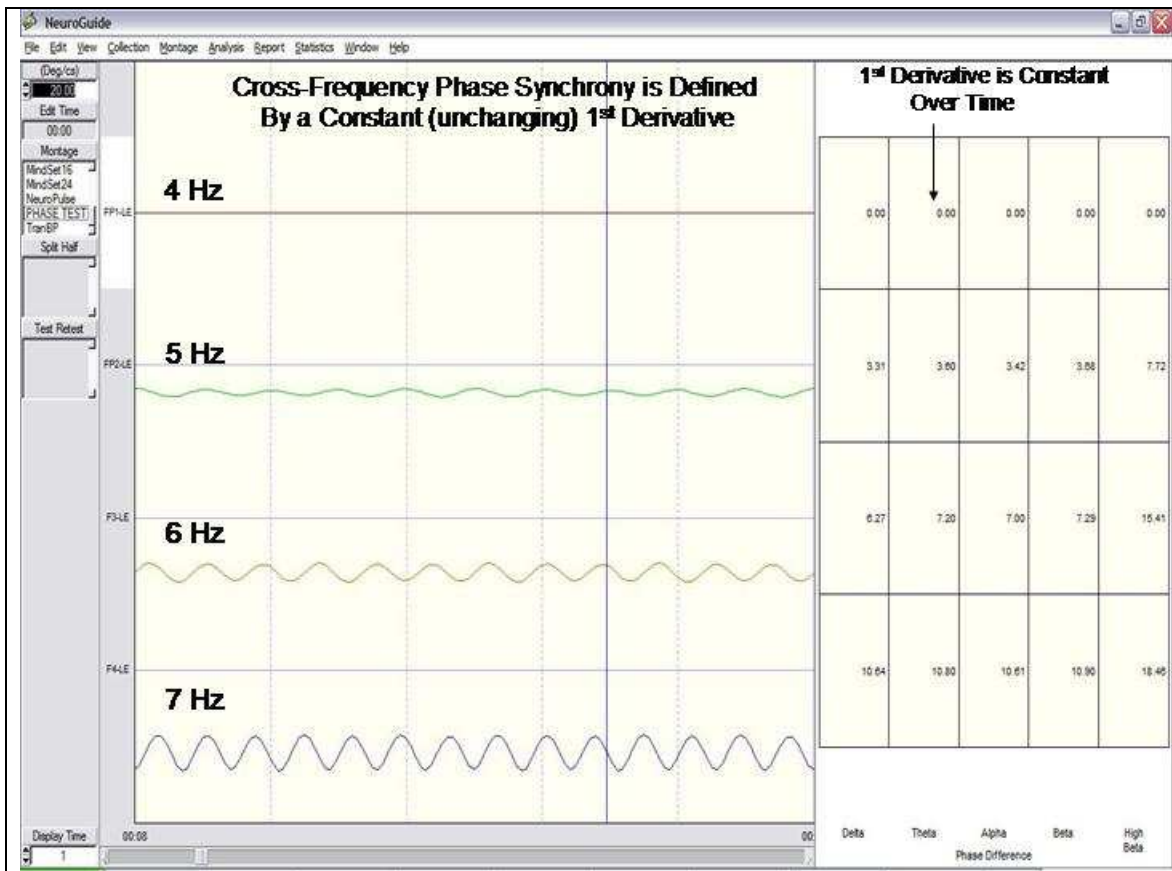


Fig. 36 – Example of a constant 1st derivative when different frequencies do not change their phase relationship over time.

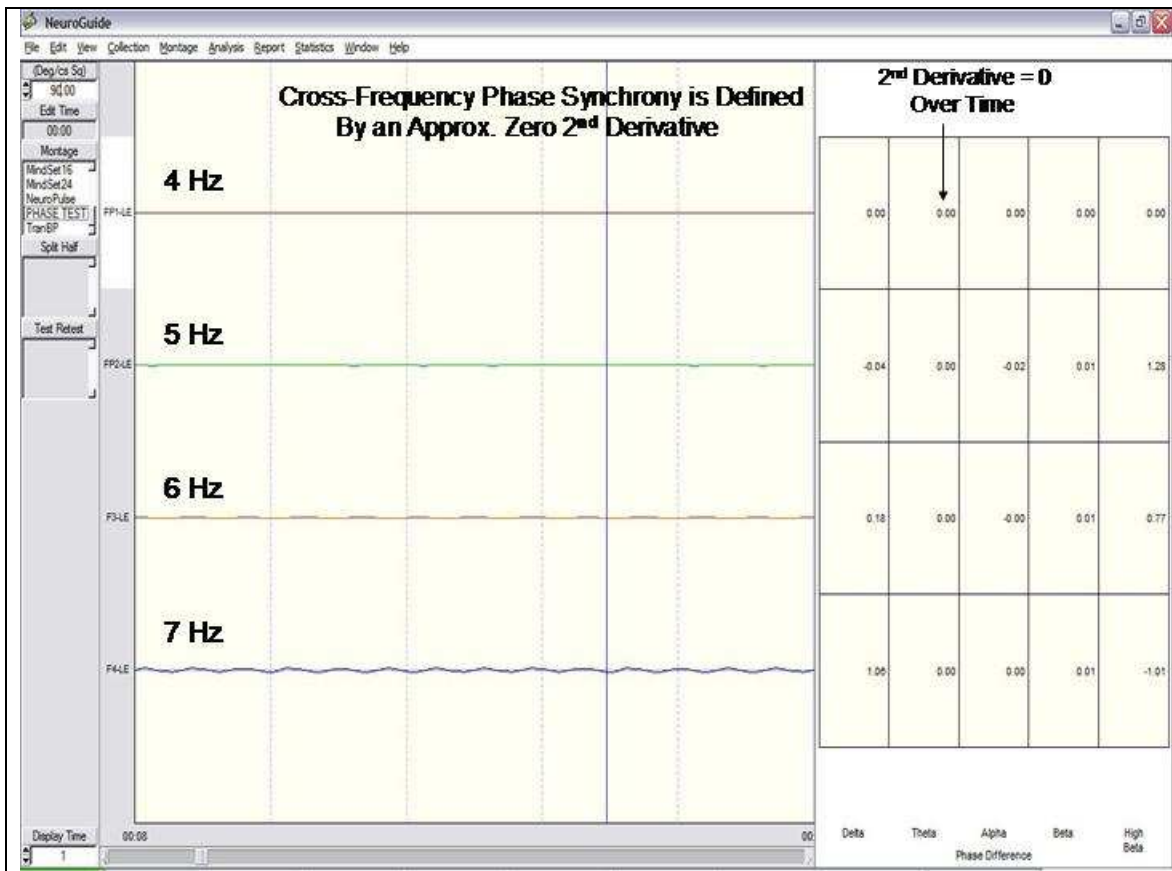


Fig. 37 – Example of a measure of cross-frequency phase synchrony which is defined as maximal when the 2nd derivative of the phase difference time series = 0 or the average 2nd derivative approximates zero. The lower the average 2nd derivative then the greater is cross-frequency phase synchrony or n:m phase synchrony.

Figure 38 summarizes the important relationship between cross-frequency phase locking and the constant phase differences and the 2nd derivative = 0.

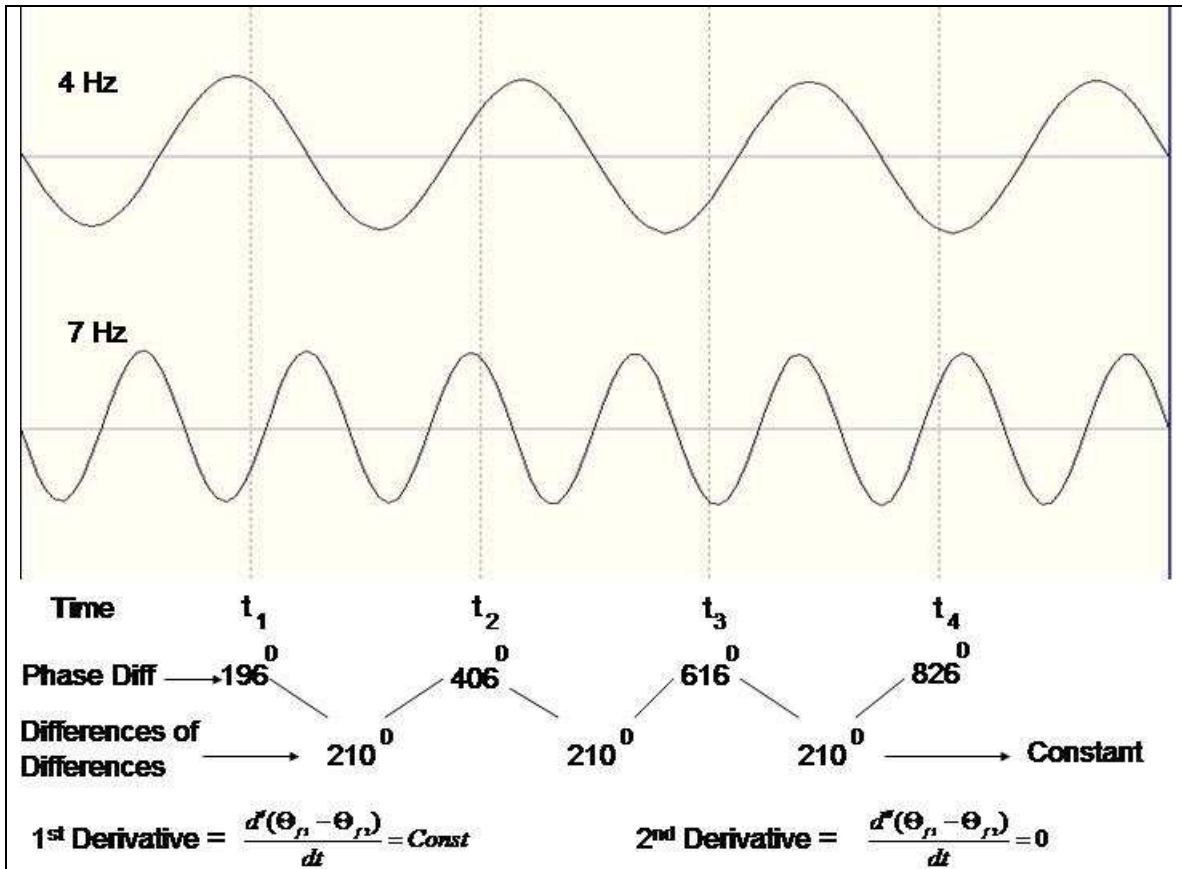


Fig. 38 – Illustrates the constant phase differences as a function of time when two different frequencies are phase locked. Cross-frequency phase locking and cross-frequency phase shift are measured by the 2nd derivative of instantaneous cross-frequency phase differences which = 0 when there is phase locking and is > 0 when there is a cross-frequency phase shift.

Figure 39 illustrates the measures that are computed in order to quantify cross-frequency phase lock duration and cross-frequency phase shift duration in milliseconds. The average magnitude of phase locking is directly related to the average magnitude of the 2nd derivative during the phase lock periods.

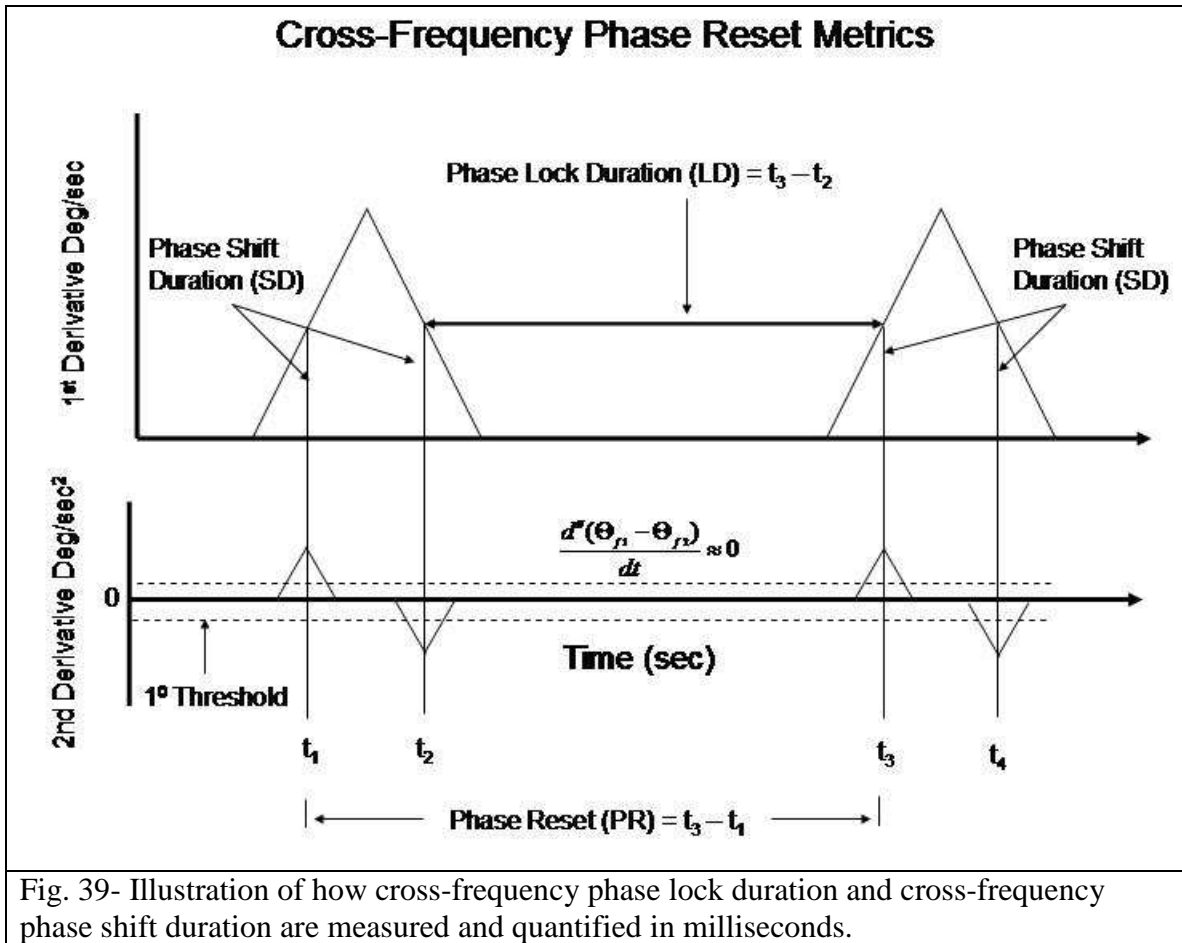


Fig. 39- Illustration of how cross-frequency phase lock duration and cross-frequency phase shift duration are measured and quantified in milliseconds.

Figure 40 shows an example of cross-frequency phase shift duration and figure 41 shows an example of cross-frequency phase lock duration in milliseconds for each cross-frequency coupling.

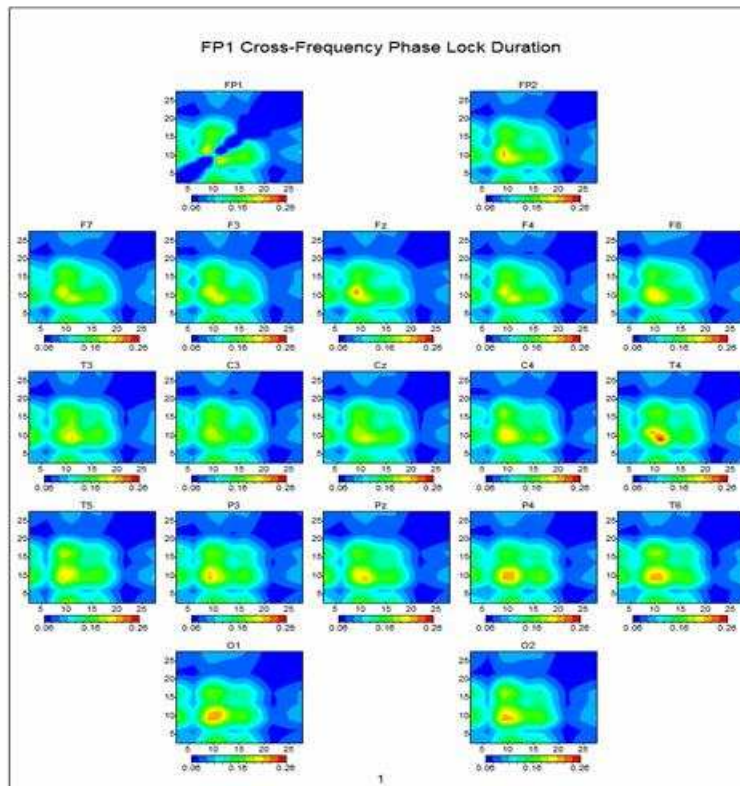


Fig. 40- Example of cross-frequency phase lock duration (msec) of the EEG recorded from Fp1 with respect to the 18 remaining scalp electrodes. This figure can be generated using the free NeuroGuide demo that can be downloaded at www.appliedneuroscience.com

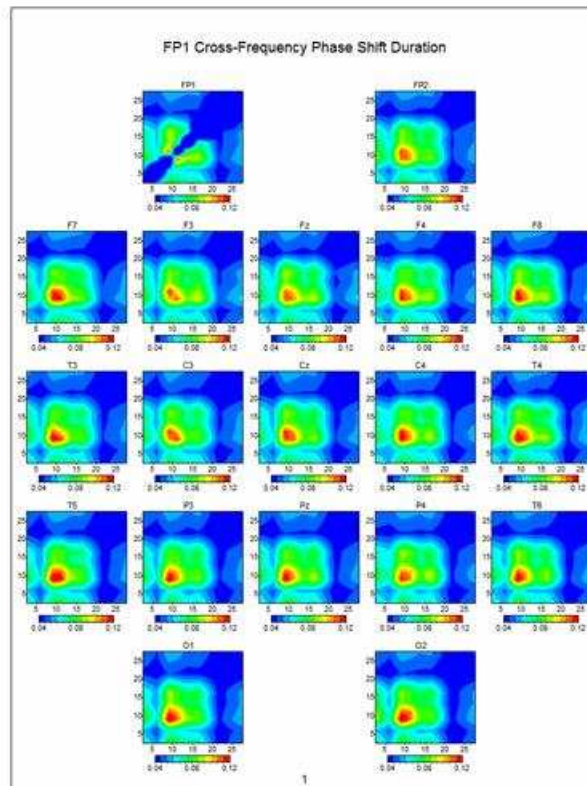


Fig. 41- Example of cross-frequency phase shift duration (msec) of the EEG recorded from Fp1 with respect to the 18 remaining scalp electrodes. This figure can be generated using the free NeuroGuide demo that can be downloaded at www.appliedneuroscience.com

42- References

Adey, W.R., Walter, D.O. and Hendrix, C.E. Computer techniques in correlation and spectral analyses of cerebral slow waves during discriminative behavior. *Exp Neurol.* 1961, 3:501-24.

Barth, D.S. Submillisecond synchronization of fast electrical oscillations in neocortex. *J Neurosci.* (2003), 23(6):2502-2510.

Bendat, J. S. & Piersol, A. G. (1980). *Engineering applications of correlation and spectral analysis.* New York: John Wiley & Sons.

Benignus, V.A. Estimation of the coherence spectrum and its confidence interval using the Fast Fourier Transform. *IEEE Transactions on Audio and Electroacoustics*, 1969a, 17: 145-150.

Benignus, V.A. Estimation of the coherence spectrum of non-Gaussian time series populations. *IEEE Transactions on Audio and Electroacoustics*, 1969b, 17: 109-201.

Bloomfield, P. *Fourier Analysis of Time Series: An Introduction*, John Wiley & Sons, New York, 2000.

Braitenberg, V. Cortical architectonics: general and areal. In: *Architectonics of the cerebral cortex*, edited by M.A.B. Brazier and H. Petsche, New York, Raven Press, 1978, pp. 443-465.

Collura, T. F. Making the connection – Connectivity-based EEG training made simple. 14th Annual ISNR Conference, September 9, 2006, Atlanta, GA.

Cooper R, Winter AL, Crow HJ and Walter WG. Comparison of subcortical, cortical and scalp activity using chronically indwelling electrodes in man. *Electroencephalogr Clin Neurophysiol* 1965; 18:217-22

Dixon, W.J. *Biomedical computer programs*. Los Angeles: University of California Press, 1970.

Dixon, W.J. *Biomedical computer programs. X-series supplement*. Los Angeles: University of California Press, 1970.

Ekhorn, R., Bauer, R., Jordan, W., Brosch, M, Kruse, W., Munk, M. and Reitboeck, H.J. Coherent oscillations: A mechanism of feature linking in the visual cortex? *Biol. Cybernetics* 60: 121-130, 1988.

Gomez, J. and Thatcher, R.W. Frequency domain equivalence between potentials and currents using LORETA. *Int. J. of Neuroscience*, 107: 161-171, 2001.

Granger, C.W.J. and Hatanka, M. *Spectral Analysis of Economic Time Series*, Princeton University Press, New Jersey, 1964.

Gray, C.M., Konig, P., Engle, A.K. and Singer, W. Oscillatory responses in cat visual cortex exhibit inter-columnar synchronization which reflects global stimulus properties. *Nature*, 338: 334- 337, 1989.

Haier, R.J., Siegel, B., Tang, C., Abes, I and Buchsbaum, M.S. (1992): Intelligence and changes in regional cerebral glucose metabolic rate following learning. *Intelligence*, 16: 415-426.

Haier, R.J. and Benbow, C.P. (1995): Sex difference and lateralization in temporal lobe glucose metabolism during mathematical reasoning. *Dev. Neuropsychol.* 4: 405-414.

Helbig, M., Schwab, K., Leistritz, L., Eiselt, M and Witte, H. (2006). Analysis of time-variant quadratic phase couplings in the tracé alternant EEG by recursive estimation of 3rd-order time-frequency distributions. *J. Neurosci. Methods*, 157:168-177.

Herscovitch, P. (1994): Radiotracer techniques for functional neuroimaging with positron emission tomography. In: Functional Neuroimaging: Technical Foundations. Thatcher, R.W., Hallett, M., Zeffiro, T., John, E.R. and Huerta, M (Eds.). Academic Press, San Diego, CA.

Izhikevich, E. and Kuramoto, Y. Weakly coupled oscillators, *Encyclopedia of Mathematics*, 2005).

Jammalamadaka, R.S. and SenGupta, A. *Topics in Circular Statistics*, World Scientific, New Jersey, 2001.

Jausovec N. and Jausovec K. (2003): Spatiotemporal brain activity related to intelligence: a low resolution brain electromagnetic tomography study. *Brain Res Cogn Brain Res.* 16(2):267-72.

Jenkins, G.M. and Watts, D.G. *Spectral analysis and its applications*. San Francisco, Holden-Day, 1969.

Jindra, R.H. Electroencephalogram spectral analysis by the direct and indirect methods: a comparison. *Neuroscience*. 1976, 1(6):515-7.

John, E.R. From synchronous neural discharges to subjective awareness? *Progress in Brain Research*, Vol. 150, 2005.

Kazantsev, V.B., Nekorkin, V.I., Makarenko, V.I. and Linas, R. Self-referential phase reset based on inferior olive oscillator dynamics. *Proceedings of the Nat. Acad. Of Sciences*, 101(52): 18183-18188, 2004.

Korzeniewska, A., Mańczak, M., Kamiński, M., Blinowska, K. and Kasicki, S. Determination of information flow direction between brain structures by a modified Directed Transfer Function method (dDTF). *Journal of Neuroscience Methods* **125**, 195-207, 2003.

Rodolfo Llinás, Francisco J. Urbano, Elena Leznik, Rey R. Ramírez and Hein J.F. van Marle (2005). Rhythmic and dysrhythmic thalamocortical dynamics: GABA systems and the edge effect. *Trends in Neurosciences*, 28(6): 325-333.

Lopes Da Silva, F.H. (1995) Dynamic of Electrical Activity of the Brain, Networks, and Modulating Systems. In: P. Nunez, ed., *Neocortical Dynamics and Human EEG Rhythms*, 249-271.

Nolte, G., Bai, O., Wheaton, L., Mari, Z., Vorbach, S. and Hallett, M. (2004). Identifying true brain interaction from EEG data using the imaginary part of coherency. *Clin. Neurophysiol.*, 115: 2292-2307.

Nunez, P. 1981. *Electrical Fields of the Brain*. Oxford University Press, New York.

Nunez, P. 1994. *Neocortical Dynamics and Human EEG Rhythms*, Oxford University Press, New York.

Nunez, P. L. EEG coherency I: statistics, reference electrode, volume conduction, Laplacians, cortical imaging, and interpretation of multiple scales. *EEG and Clin. Neurophysiol.*, 1997, 103: 499-515.

Paigacheva, I.V. and Korinevskii, A.V. Investigation of the functional role of the septum. *Neurosci Behav Physiol.* 1977, 8(3):222-229.

Pascual-Marqui RD. Review of Methods for Solving the EEG Inverse Problem. *International Journal of Bioelectromagnetism* 1999, 1:75-86.

Pascual-Marqui, R.D., Koukkou, M., Lehmann, D. and Kochi, K. Functional

localization and functional connectivity with LORETA comparison of normal controls and first episode drug naïve schizophrenics. 2001, *J. of Neurotherapy*, 4(4): 35-37.

Pascual-Marqui, R.D. (2007) Coherence and phase synchronization: generalization to pairs of multivariate time series, and removal of zero-lag contributions. arXiv:0706.1776v3 [stat.ME] 12 July 2007. (<http://arxiv.org/pdf/0706.1776>).

Pikovsky, A., Rosenblum, M. and Kurths, J. “Synchronization: A universal concept in nonlinear sciences”, Cambridge University Press, Cambridge, UK, 2003.

Orr, W.C. and Naitoh, P. The coherence spectrum: An extension of correlation analysis with applications to chronobiology. *Internat. J. of Chronobiology*, 1976, 3: 171-192.

Otnes, R. K. & Enochson, L. (1972). *Digital time series analysis*. New York: John Wiley and Sons.

Press, W. H., Teukolsky, S. A., Vetterling, W. T. & Flannery, B. P. (1994). *Numerical recipes in C*, Cambridge Univ. Press.

Rappelsberger and Petsche, 1988

Rogers, R.L. Magnetoencephalographic imaging of cognitive processes. In: R. Thatcher, M. Hallett, T. Zeffiro, E. John and M. Huerta (Eds.), Functional Neuroimaging: Technical Foundations, Academic Press: New York, 1994.

Savitzky, A. and Golay, M.J.E. Smoothing and differentiation of data by simplified least squares procedures, vol. 36, No. 8, 1964.

Schack, B., Vath, N., Petsche, H., Geissler, H.G. and Moller, E. Phase-coupling of theta-gamma EEG rhythms during short-term memory processing. *Inst. J. Psychophysiol.*, 44:143-163, 2002.

Schack, B., Klimesch, W. and Sauseng, P. Phase synchronization between theta and upper alpha oscillations in a working memory task. *Int. J. Psychophysiol.*, 57: 105-114, 2005.

Schulz, A. and Braintenberg, V. The human cortical white matter: Quantitative aspects of cortico-cortical long-range connectivity. In: *Cortical Areas: Unity and Diversity*, edited by A. Schultz and R. Miller, Conceptual Advances in Brain Research, London, 2002, pp. 377-386.

Steriade, M. "Cellular substrates of Brain Rhythms" in: *Electroencephalography*", ed. Niedermeyer and Lopes da Silva, Williams and Wilkins, Baltimore, 1995.

Serman, M. and Kaiser, D. Comodulation: A new QEEG analysis metric for assessment of structural and functional disorders of the central nervous system. (2001), *J. Neurotherapy*, 4(3): 73-83.

Thatcher, R.W. and John, E.R. *Functional Neuroscience: Foundations of Cognitive Processes*, Erlbaum, N.J., 1977.

Thatcher, R., Wang, B., Toro, C. and Hallett, M. Human Neural Network Dynamics Using Multimodal Registration of EEG, PET and MRI. In: R. Thatcher, M. Hallett, T. Zeffiro, E. John and M. Huerta (Eds.), Functional Neuroimaging: Technical Foundations, Academic Press: New York, 1994.

Thatcher, R.W., Biver, C.J. and North, D.N. EEG coherence and phase differences: Comparison of the common reference, average reference and the Laplacian reference, (in preparation, 2004 download at www.appliedneuroscience.com and click on Articles).

Thatcher, R.W., Biver, C. J., and North, D. LORETA current source correlations and intelligence, *Human Brain Mapping*, May 25, 2006.

Thatcher, R.W., North, D., and Biver, C. EEG inverse solutions and parametric vs. non-parametric statistics of Low Resolution Electromagnetic Tomography (LORETA). *Clin. EEG and Neuroscience*, *Clin. EEG and Neuroscience*, 36(1), 1 – 9, 2005a.

Thatcher, R.W., North, D., and Biver, C. Evaluation and Validity of a LORETA normative EEG database. *Clin. EEG and Neuroscience*, 2005b, 36(2): 116-122.

Thatcher, R.W., Biver, C. J., and North, D. LORETA current source correlations and cortical connectivity, *Clin. EEG and Neuroscience*, 38(1):

35 – 48, 2007.

Thatcher, R.W., Biver, C. J., and North, D. LORETA current source correlations and intelligence, *Human Brain Mapping*, 2007, 28(2): 118 – 133.

Thatcher, R.W., North, D., and Biver, C. Development of cortical connectivity as measured by EEG coherence and phase. *Human Brain Mapp.*, Oct. 23, 2007.

Thatcher, R.W., North, D., and Biver, C. Self organized criticality and the development of EEG phase reset. *Human Brain Mapp.*, Jan 24, 2008a.

Thatcher, R.W., North, D., and Biver, C. Intelligence and EEG phase reset: A two-compartmental model of phase shift and lock, *NeuroImage* (in press, 2008b).

Tick, L.J. Estimation of coherence. B. Harris (Ed.), Inc: *Spectral analysis of time series*. New York: John Wiley & Sons, 133-152, 1967.

Tryer, L. (1988). *Biochemistry*. W.H. Freeman and Company, New York.

Walter, D.O. Spectral analysis for electroencephalograms: mathematical determination of neurophysiological relations from records of limited duration. *Experimental Neurology*, 1963, 8: 155-181.

Walter, D.O. A posteriori “Wiener filtering” of averaged evoked responses. D.O. Walter and M.A.B Brazier (Eds.). In: *Advances in EEG analysis. Electroencephalography and Clinical Neurophysiol.*, 1969, Supplement No. 27, 61-70.

Witte H, Putsche P, Eiselt M, Hoffmann K, Schack B, Arnold M, et al. (1997). Analysis of the interrelations between a low-frequency and a high-frequency signal component in human neonatal EEG during quiet sleep. *Neurosci Lett.*, 236:175–179.

19 Channel EEG Biofeedback References:

Adey, W.R., Walter, D.O. and Hendrix, C.E. (1961). Computer techniques in correlation and spectral analyses of cerebral slow waves during discriminative behavior. *Exp Neurol.*, 3:501-524.

Apkarian, A. V. Functional magnetic resonance imaging of pain consciousness: cortical networks of pain critically depend on what is implied by “pain”. *Curr. Rev. Pain* 3, 308–315 (1999).

Berger, H. Über das Electrenkephalogramm des Menschen. Neunte Mitteilungj. *Archiv. Fur. Psychiatrie und Neverkrankheiten*, 102: 538-557, 1934.

Bray, S., Shimojo, S. & O’Doherty, J. P. Direct instrumental conditioning of neural activity using functional magnetic resonance imaging-derived reward feedback. *J. neurosci.* 27, 7498–7507 (2007).

Buzsaki, G. (2006). *Rhythms of the Brain*, Oxford Univ. Press, New York.

Cannon, R., Congredo, M., Lubar, J., and Hutchens, T. (2009). Differentiating a network of executive attention: LORETA neurofeedback in anterior cingulate and dorsolateral prefrontal cortices. *Int J Neurosci.* 119(3):404-441.

Cannon, R., Lubar, J., Gerke, A., Thornton, K., Hutchens, T and McCammon, V. (2006a). EEG Spectral-Power and Coherence: LORETA Neurofeedback Training in the Anterior Cingulate Gyrus. *J. Neurotherapy*, 10(1): 5 – 31.

Cannon, R., Lubar, J. F., Congedo, M., Gerke, A., Thornton, K., Kelsay, B., et al. (2006b). The effects of neurofeedback training in the cognitive division of the anterior cingulate gyrus. *International Journal of Science* (in press).

Cannon, R., Lubar, J., Thornton, K., Wilson, S., & Congedo, M. (2005) Limbic beta activation and LORETA: Can hippocampal and related limbic activity be recorded and changes visualized using LORETA in an affective memory condition? *Journal of Neurotherapy*, 8 (4), 5-24.

Cannon, R., & Lubar, J. (2007). EEG spectral power and coherence: Differentiating effects of Spatial–Specific Neuro–Operant Learning (SSNOL) utilizing LORETA Neurofeedback training in the anterior cingulate and bilateral dorsolateral prefrontal cortices. *Journal of Neurotherapy*, 11(3): 25-44.

Cannon, R., Lubar, J., Sokhadze, E. and Baldwin, D. (2008). LORETA Neurofeedback for Addiction and the Possible Neurophysiology of Psychological Processes Influenced: A Case Study and Region of Interest Analysis of LORETA Neurofeedback in Right Anterior Cingulate Cortex. *Journal of Neurotherapy*, 12 (4), 227 - 241.

Caria, A. *et al.* Regulation of anterior insular cortex activity using real-time fMRI. *neuroimage* 35, 1238–1246 (2007).

Chen, Z.J., He, Y., Rosa-Neto, P., Germann, J. and Evans, A.C. (2008). Revealing Modular Architecture of Human Brain Structural Networks by Using Cortical Thickness from MRI. *Cerebral Cortex*, 18:2374-2381.

Collura, T.F, Thatcher, R.W., Smith, M.L., Lambos, W.A. and Stark, C.R. EEG biofeedback training using live Z-scores and a normative database. In: Introduction to QEEG and Neurofeedback: Advanced Theory and Applications, T. Budzinsky, H. Budzinsky, J. Evans and A. Abarbanel (eds)., Academic Press, San Diego, CA, 2008.

Cooper, R., Osselton, J.W. and Shaw, J.G. “EEG Technology”, Butterworth & Co, London, 1974.

deCharms, R. C. *et al.* Learned regulation of spatially localized brain activation using real-time fMRI. *neuroimage* 21, 436–443 (2004).

deCharms, R. C. (2008). Applications of real-time fMRI *Nature Neuroscience*, 9: 720-729.

Fox, S.S. Rudell, A.P. Operant controlled neural event: formal and systematic approach to electrical coding of behavior in brain. *Science*, 162, 1299-1302, 1968.

Freeman W.J. and Rogers, L.J. (2002). Fine temporal resolution of analytic phase reveals epistemic synchronization by state transitions in gamma EEGs. *J. Neurophysiol*, 87(2): 937-945.

Freeman, W.J., Burke, B.C. and Homes, M.D. (2003). Aperiodic phase re-setting in scalp EEG of beta-gamma oscillations by state transitions at alpha-theta rates. *Hum Brain Mapp*. 19(4):248-272.

Gomez, J. and Thatcher, R.W. Frequency domain equivalence between potentials and currents using LORETA. Int. J. of Neuroscience, 107: 161-171, 2001.

Hagmann, P., Cammoun, L., Gigandet, X., Meuli, R., Honey, C.J., Wedeen, V.J., and Sporns, O. (2008). Mapping the Structural Core of Human Cerebral Cortex. PLoS Biol 6(7): e159. doi:10.1371/journal.pbio.0060159

He, Y., Wang, J., Wang, L., Zhang, C.J., Yan, C., Yang, H., Tang, H., Zhul, C, Gong, O, Zang, Y and Evans, A.C. (2009). Uncovering Intrinsic Modular Organization of Spontaneous Brain Activity in Humans. PLoS ONE 4(4):e5226. doi:10.1371/journal.pone.0005226

Hughes, JR, John ER Conventional and quantitative electroencephalography in psychiatry. Neuropsychiatry 1999, 11(2): 190-208.

John, E.R. Functional Neuroscience, Vol. II: Neurometrics: Quantitative Electrophysiological Analyses. E.R. John and R.W. Thatcher, Editors. L. Erlbaum Assoc., N.J., 1977.

John, E.R. Karmel, B., Corning, W. Easton, P., Brown, D., Ahn, H., John, M., Harmony, T., Prichep, L., Toro, A., Gerson, I., Bartlett, F., Thatcher, R., Kaye, H., Valdes, P., Schwartz, E. (1977). Neurometrics: Numerical taxonomy identifies different profiles of brain functions within groups of behaviorally similar people. Science, 196, :1393-1410.

John, E. R., Prichep, L. S. & Easton, P. (1987). Normative data banks and neurometrics: Basic concepts, methods and results of norm construction. In A. Remond (Ed.), *Handbook of electroencephalography and clinical neurophysiology: Vol. III. Computer analysis of the EEG and other neurophysiological signals* (pp. 449-495). Amsterdam: Elsevier.

John, E. R., Prichep, L. S., Fridman, J. & Easton, P. (1988). Neurometrics: Computer assisted differential diagnosis of brain dysfunctions. Science, 293, 162-169.

Kamiya, J. (1971). Biofeedback Training in Voluntary Control of EEG Alpha Rhythms. Calif. Med., 115(3): 44-49.

- Lubar, J., Congedo, M. and Askew, J.H. (2003). Low-resolution electromagnetic tomography (LORETA) of cerebral activity in chronic depressive disorder. *Int J Psychophysiol.* 49(3):175-185.
- Luria, A. The Working Brain. Penguin Press, London ISBN 0 14 080654 7
- Matousek, M. & Petersen, I. (1973). Automatic evaluation of background activity by means of age-dependent EEG quotients. *EEG & Clin. Neurophysiol.*, 35: 603-612.
- Niedermeyer, E. and Ds Silva, F.L. *Electroencephalography: Basic principles, clinical applications and related fields*. Baltimore: Williams & Wilkins, 1995.
- Pascual-Marqui, RD, Michel, CM and Lehmann, D. Low resolution electromagnetic tomography: A new method for localizing electrical activity in the brain. *Internat. J. of Psychophysiol.*, 18, 49-65, 1994.
- Sauseng, P, and Klimesch, W. (2008). What does phase information of oscillatory brain activity tell us about cognitive processes? *Neuroscience and Biobehavioral Reviews*, 32(5):1001-1013.
- Sterman, M.B. (1973). Neurophysiologic and clinical studies of sensorimotor EEG biofeedback training: some effects on epilepsy. *Semin. Psychiatry*, 5(4): 507-525.
- Teuber, H. (1968). Disorders of memory following penetrating missile wounds of the brain. *Neurology*. 18(3):287-298.
- Thatcher, R.W. EEG normative databases and EEG biofeedback (1998). *Journal of Neurotherapy*, 2(4): 8-39.
- Thatcher, R.W. EEG database guided neurotherapy (1999a). In: J.R. Evans and A. Abarbanel Editors, *Introduction to Quantitative EEG and Neurofeedback*, Academic Press, San Diego.
- Thatcher, R.W. (2000a). EEG Operant Conditioning (Biofeedback) and Traumatic Brain Injury. . *Clinical EEG*, 31(1): 38-44.
- Thatcher, R.W. (2000b) "An EEG Least Action Model of Biofeedback" 8th Annual ISNR conference, St. Paul, MN, September.

Thatcher, R.W., Walker, R.A., Biver, C., North, D., Curtin, R., (2003). Quantitative EEG Normative databases: Validation and Clinical Correlation, *J. Neurotherapy*, 7 (No. 3/4): 87 – 122.

Thatcher, R.W., North, D., and Biver, C. Evaluation and Validity of a LORETA normative EEG database. *Clin. EEG and Neuroscience*, 2005b, 36(2): 116-122.

Thatcher, R.W. and Collura, T. Z Score Biofeedback and New Technology. International Society of Neuronal Regulation Annual Meeting, Atlanta, GA, September 16-21, 2006.

Thatcher, R.W., North, D., and Biver, C. Self organized criticality and the development of EEG phase reset. *Human Brain Mapp.*, Jan 24, 2008a.

Thatcher, R.W., North, D., and Biver, C. Intelligence and EEG phase reset: A two-compartmental model of phase shift and lock, *NeuroImage*, 42(4): 1639-1653, 2008b.

Thatcher, R.W. and Lubar, J.F. History of the scientific standards of QEEG normative databases. In: *Introduction to QEEG and Neurofeedback: Advanced Theory and Applications*, T. Budzinsky, H. Budzinsky, J. Evans and A. Abarbanel (eds.), Academic Press, San Diego, CA, 2008.

Thatcher, R.W., North, D., Neurbrander, J., Biver, C.J., Cutler, S. and DeFina, P. Autism and EEG phase reset: Deficient GABA mediated inhibition in thalamo-cortical circuits. *Dev. Neuropsych.* (In press, 2009).

Weiskopf, N. *et al.* Physiological self-regulation of regional brain activity using real-time functional magnetic resonance imaging (fMRI): methodology and exemplary data. *neuroimage* 19, 577–586 (2003).

Woody, R.H. (1966) Intra-judge Reliability in Clinical EEG. *J. Clin. Psychol.*, 22: 150-159.

Woody, R.H. (1968). Inter-judge Reliability in Clinical EEG. *J. Clin. Psychol.*, 24: 251-261,

Yoo, S. S. *et al.* Increasing cortical activity in auditory areas through neurofeedback functional magnetic resonance imaging. *neuroreport* 17, 1273–1278 (2006).

43- Appendix - A

A.1 – Minimization of RMS Error

Time series are sequences, discrete or continuous, of quantitative data of specific moments in time. They may be simple such as a single numerical observation at each moment of time and studied with respect to their distribution in time, or multiple in which case they consist of a number of separate quantities tabulated according to a common time base (e.g., a mixture of sine waves beginning at time = 0).

The statistics of a time series is the science of predicting an immediate or long time future sequence based on a sample of past sequential quantitative data. In general, the longer the sample of past quantitative moments of time then the greater the accuracy of predicting future sequence(s).

The fine details of accuracy of prediction of the future based upon past samples is generally governed by the relationship of $1 / \text{sq rt. of } N$. To understand why this is the case let us define a statistic of a time series based on the “signal” or “message” that is transmitted and the “noise” or randomness that the signal is embedded in. This relationship was described by the Nobel laureate Normbet Wiener (N. Wiener, *Time Series*, MIT Press, Cambridge, Mass., 1949) in which a time series is a combination of a signal + noise or the signal $f(t)$ and the message $g(t)$ + noise, where noise is defined as $f(t) - g(t)$. In other words noise is defined as the difference between the “message” and the measured quantitative values or $f(t) - g(t)$. For example, noise = 0 when $f(t) - g(t) = 0$.

Let us consider the output of an electrical circuit with input $f(t)$. If the circuit has the response $A(t)$ to a unit-step function, then the output is given by:

$$F(t) = \int_0^{+\infty} A'(\tau) f(t - \tau) d\tau + A(0) f(t)$$

The goal is to have $F(t)$ approximate as closely as possible the message $g(f)$. That is, we want to minimize $[F(t) - g(t)]$. As a criterion

The Ergotic goal of time series statistics is to minimize the difference between the measured values $f(t)$ and the “signal” $g(t)$.

The time series can be divided into two general categories: 1- the statistics of short-time biological data and other short-time interval events such as economic, sociological, etc. and 2- long time span events such as astronomical, meteorological, geologic and geophysical data – to be continued

44- Appendix – B

Instantaneous Coherence and Phase Difference

Complex demodulation was used to compute instantaneous coherence and phase-differences (Granger and Hatanaka, 1964; Otnes and Enochson, 1972; Bloomfield, 2000). This method first multiplies a time series by the complex function of a sine and cosine at a particular frequency followed by a low pass filter which removes all but very low frequencies and transforms the time series into instantaneous amplitude and phase and an “instantaneous” spectrum (Bloomfield, 2000). We place quotations around the term “instantaneous” to emphasize that there is always a trade-off between time resolution and frequency resolution. The broader the band width the higher the time resolution but the lower the frequency resolution and vice versa (Bloomfield, 2000). For example, if we multiply a time series $\{x_t, t = 1, \dots, n\}$ by $\sin \omega_0 t$ and $\cos \omega_0 t$ and then apply a low pass filter F, we have

$$Z'_t = F(x_t \sin \omega_0 t)$$

$$Z''_t = F(x_t \cos \omega_0 t)$$

and $2[(Z'_t)^2 + (Z''_t)^2]^{1/2}$ is an estimate of the “instantaneous” amplitude of the frequency ω_0 at time t and $\tan^{-1} \frac{Z'_t}{Z''_t}$ is an estimate of the “instantaneous” phase at time t.

The instantaneous cross-spectrum is computed when there are two time series $\{y_t, t = 1, \dots, n\}$ and $\{y'_t, t = 1, \dots, n\}$ and if F [] is a filter passing only frequencies near zero, then, as above

$R_t^2 = F[y_t \sin \omega_0 t]^2 + F[y_t \cos \omega_0 t]^2 = |F[y_t e^{i\omega_0 t}]|^2$ is the estimate of the amplitude of frequency ω_0 at time t and

$$\varphi_t = \tan^{-1} \left(\frac{F[y_t \sin \omega_0 t]}{F[y_t \cos \omega_0 t]} \right)$$

is an estimate of the phase of frequency ω_0 at time t and since

$$F[y_t e^{i\omega_0 t}] = R_t e^{i\varphi_t},$$

and likewise,

$$F[y'_t e^{i\omega_0 t}] = R'_t e^{i\varphi'_t}$$

the instantaneous cross-spectrum is

$$\begin{aligned} V_t &= F[y_t e^{i\omega_0 t}] F[y'_t e^{-i\omega_0 t}] \\ &= R_t R'_t e^{i[\varphi_t - \varphi'_t]} \end{aligned}$$

and the instantaneous coherence is

$$\frac{|V_t|}{R_t^2 R'^2_t} \equiv 1$$

however coherence is computed as the average of the sine and cosine functions over an interval of time or

$$\bar{C}(t, \omega) = \frac{|\bar{V}_t|}{R_t^2 R'^2_t}$$

The instantaneous phase-difference is $\varphi_t - \varphi'_t$ which is also the arctan of the imaginary part of V_t divided by the real part (or the quadspectrum divided by the cospectrum).

Computation of the First Derivatives of the Time Series of Coherence and Phase Angles

The first derivative of the time series of phase-differences between all pair wise combinations of two channels was computed in order to detect advancements and reset of phase-differences. The Savitzky-Golay procedure was used to compute the first derivatives of the time series using a window length of 3 time points and the polynomial degree of 2 (Press et al, 1994). The units of the 1st derivative are in degrees/point which is normalized to degrees/second and degrees/millisecond in the case of EEG. The second derivative was computed using a window length of 5 and a polynomial degree of 3 and is in units of degrees/second² or degrees/millisecond² in the case of EEG. For simplicity, in NeuroGuide the units of the first derivative of a phase time series is degrees per centiseconds (i.e., degrees/cs² = degrees/10 msec.²).

Listing of the Relevant Connectivity Equations. All of the equations below can be evaluated using a hand calculator and the equations can be easily programmed by a competent programmer. See the sections above for details. The goal is to help develop standardization and simplification for the implementation of EEG connectivity measures:

1- Pearson Product Correlation Coefficient

$$r = \frac{N \sum XY - \sum X \sum Y}{\sqrt{[N \sum X^2 - (\sum X)^2][N \sum Y^2 - (\sum Y)^2]}}$$

2- The cospectrum and quadspectrum (see section 9):

$a(xf_1)$ = cosine coefficient for the frequency (f_1) for channel X

$b(xf_1)$ = sine coefficient for the frequency (f_1) for channel X

$u(yf_2)$ = cosine coefficient for the frequency (f_2) for channel Y

$v(yf_2)$ = sine coefficient for the frequency (f_2) for channel Y

The cospectrum and quadspectrum are algebraically defined as:

$$\text{Cospectrum } (f_1, f_2) = a(xf_1) u(yf_2) + b(xf_1) v(yf_2)$$

$$\text{Quadspectrum } (f_1, f_2) = a(xf_1) v(yf_2) - b(xf_1) u(yf_2)$$

3- Auto-spectrum

$$F(x) = (a^2(x) + b^2(x))$$

4- The cross-spectrum amplitude:

$$= \sqrt{((a(x)u(y) + b(x)v(y))^2 + (a(x)v(y) - b(x)u(y))^2)}$$

5- Coherence

$$\text{Coh } (f) = \frac{(\sum_N (a(x)u(y) + b(x)v(y)))^2 + (\sum_N (a(x)v(y) - b(x)u(y)))^2}{\sum_N (a(x)^2 + b(x)^2) \sum_N u(y)^2 + v(y)^2}$$

6- Phase Delay or phase difference

$$\text{Phase difference (f)} = \text{Arctan} \frac{\sum_N (a(x)v(y) - b(x)u(y))}{\sum_N (a(x)u(y) + b(x)v(y))}$$

7- Auto Channel Cross-Frequency Coherence (f_1, f_2) (ACC) after complex demodulation:

$$\text{ACC} = \frac{(\sum_N (a(x' f_1)u(x'' f_2) + b(x' f_1)v(x'' f_2)))^2 + (\sum_N (a(x' f_1)v(x'' f_2) - b(x' f_1)u(x'' f_2)))^2}{\sum_N (a(x' f_1)^2 + b(x' f_2)^2) \sum_N (u(x'' f_2)^2 + v(x'' f_2)^2)}$$

8- Cross Channel Cross-Frequency Coherence (f_1, f_2) (CCC) for channels X and Y after complex demodulation

$$\text{CCC} = \frac{(\sum_N (a(x' f_1)u(y' f_2) + b(x' f_1)v(y' f_2)))^2 + (\sum_N (a(x' f_1)v(y' f_2) - b(x' f_1)u(y' f_2)))^2}{\sum_N (a(x' f_1)^2 + b(x' f_2)^2) \sum_N (u(y' f_2)^2 + v(y' f_2)^2)}$$

9- Auto Channel Cross-Frequency phase difference (f_1, f_2) (ACP) after complex demodulation

$$\text{ACP} = \text{Arc tan} \frac{\sum_N (a(x' f_1)v(x'' f_2) - b(x' f_1)u(x'' f_2))}{\sum_N (a(x' f_1)u(x'' f_2) + b(x' f_1)v(x'' f_2))}$$

10- Cross-Channel Cross-Frequency Phase Difference (f_1, f_2) (CCP) after complex demodulation

$$\text{CCP} = \text{Arc tan} \frac{\sum_N ((a(x' f_1)v(y' f_2) - b(x' f_1)u(y' f_2)))}{\sum_N ((a(x' f_1)u(y' f_2) + b(x' f_1)v(y' f_2)))}$$

Equations for sections 31 to 36 will be added in a future update.